Journal of MOLECULAR BIOLOGY

UNIVERSITY OF HAWAII LIBRARY
MAR 23 '60

EDITOR-IN-CHIEF: J. C. KENDREW

Volume I, Number 3, September 1959

ACADEMIC PRESS LTD., LONDON
ACADEMIC PRESS INC., NEW YORK

JOURNAL OF MOLECULAR BIOLOGY

EDITOR-IN-CHIEF

J. C. KENDREW, Peterhouse, Cambridge, England

EDITORIAL BOARD

P. DOTY, Department of Chemistry, Harvard University, Cambridge, Mass., U.S.A.
A. F. HUXLEY, Physiological Laboratory, University of Cambridge, England.
R. L. SINSHEIMER, Division of Biology, California Institute of Technology, Pasadena, Cal., U.S.A.
J. D. WATSON, Biological Laboratories, Harvard University, Cambridge, Mass., U.S.A.
M. H. F. WILKINS, Physics Department, King's College, London, England.

ADVISORY BOARD

S. BENZER, Purdue University, U.S.A.
M. CALVIN, University of California, Berkeley, U.S.A.
F. H. C. CRICK, University of Cambridge, England.
J. F. DANIELLI, King's College, London, England.
A. ENGSTRÖM, Karolinska Institutet, Stockholm, Sweden.
A. D. HERSHEY, Carnegie Institute, Cold Spring Harbor, U.S.A.
F. JACOB, Pasteur Institute, Paris, France.
A. KORNBERG, Stanford University, Stanford, California, U.S.A.
C. LEVINTHAL, Massachusetts Institute of Technology, Cambridge, Mass., U.S.A.
S. E. LURIA, Massachusetts Institute of Technology, Cambridge, Mass., U.S.A.
D. MAZIA, University of California, Berkeley, U.S.A.
P. B. MEDAWAR, University College, London, England.
L. E. ORGEL, University of Cambridge, England.
M. F. PERUTZ, University of Cambridge, England.
R. D. PRESTON, University of Leeds, England.
G. N. RAMACHANDRAN, University of Madras, India.
A. RICH, Massachusetts Institute of Technology, Cambridge, Mass., U.S.A.
G. SCHRAMM, Max-Planck Institut, Tübingen, Germany.
F. S. SJØSTRAND, Karolinska Institutet, Stockholm, Sweden.
I. WATANABE, University of Tokyo, Japan.
R. C. WILLIAMS, University of California, Berkeley, U.S.A.

Published by Academic Press Inc. (London) Limited

Volume I, 1959: 100*s*. ($14.00)

Subscription orders should be sent to Academic Press Inc. (London) Limited, 17 Old Queen Street, London, S.W.1, with the exception of those originating in the U.S.A., Canada, Central America, and South America; these should be sent to Academic Press Inc., 111 Fifth Avenue, New York 3, N.Y.

Copyright © 1959, by Academic Press Inc. (London) Limited

J. Mol. Biol. (1959), **1**, 195-203

Studies on Deoxyribonucleic Acid after Exposure to Tritium Gas†

Ellen Borenfreund, Herbert S. Rosenkranz‡ and Aaron Bendich

Sloan-Kettering Division, Cornell University Medical College, New York 21, N.Y., U.S.A.

(*Received 11 March 1959*)

Deoxyribonucleic acid (DNA) from human leukocytes was exposed to 0·39 atm of tritium (2·4 curies) for 14 days at room temperature, and approximately 0·1 % replacement of hydrogen by tritium was effected. The molar ratios of tritium in the bases was adenine 1·0, thymine 9·8, guanine 1·4 and cytosine 2·4. The treatment caused a drop in average molecular weight from 5·2 to $1·3 \times 10^6$ as estimated from sedimentation data and there was a concomitant alteration in the anion exchange chromatographic behavior. Evidence was also obtained for some aggregation in addition to the degradation. These macromolecular changes did not appear to be accompanied by significant denaturation (i.e., twin-strand separation).

1. Introduction

The great recent interest in the use of tritium in tracer studies stems from its ready availability at high specific activity and relatively low cost, and the versatility of its applications to a variety of biological problems. Complex molecules such as enzymes (Steinberg, Vaughan, Anfinsen & Gorry, 1957) and insulin (Holt & Holt, 1958) can be directly labeled by mere exposure to tritium gas (the Wilzbach procedure (Wilzbach, 1957)), with retention of biological activity. This has made it possible to pursue a variety of biochemical studies which could be approached previously only with the greatest difficulty. The Wilzbach method has been applied to a specimen of deoxyribonucleic acid (DNA) and a product was obtained in which about one out of a thousand hydrogen atoms had been replaced by tritium.

This paper deals with the effects of this replacement on a number of the properties of the DNA and includes an evaluation of the suitability of this type of labeling for biological investigation.

2. Experimental

(a) *Material*

The DNA was isolated according to the method of Kay, Simmons & Dounce (1952) from the white cells of a patient with chronic granulocytic (myeloid) leukemia. (We are grateful to Dr. G. di Mayorca for a gift of this preparation.) Some of the properties of this specimen of DNA, referred to as 3LD, have been presented previously (Bendich, Pahl, Korngold, Rosenkranz & Fresco, 1958). A sample was labeled with tritium according to the Wilzbach method (Wilzbach, 1957). (This procedure was carried out by the New England Nuclear Corp., 575 Albany Street, Boston 18, Mass.) After exposure of 85 mg of the nucleic acid to 2·4 curies of tritium at a pressure of 0·39 atm at 27°C for 2 weeks, the tritiated sample showed a specific activity of 0·86 mc/mg.

†This investigation was supported by funds from the American Cancer Society, National Cancer Institute, National Institutes of Health, Public Health Service (Grant No. CY-3190), and from the Atomic Energy Commission (Contract No. AT (30–1) 910).

‡Postdoctoral Research Fellow.

(b) *Methods*

(i) Radioactivity measurements were carried out with an internal Geiger-Müller flow-counter using helium-isobutane gas. Infinitely thin films were plated on 10 cm^2 aluminum planchets and triplicate determinations for radioactivity were made. The standard counting error was less than 5%. Coincidence corrections were low enough to be disregarded.

(ii) *Column Chromatography.* A comparison was made of the chromatographic elution patterns of samples of 3LD before and after triation (Bendich, Pahl, Korngold, Rosenkranz & Fresco, 1958). A solution of 1 mg/ml. tritiated DNA in 0·001 M-NaCl was dialyzed for 3 weeks in the cold against frequent changes of 0·001 M-NaCl (saturated with chloroform) in order to remove labile tritium.

About one-fifth of the initial radioactivity was lost in the course of dialysis. Unless otherwise noted, all experiments with tritiated 3LD refer to the dialyzed sample.

Solutions (3 ml.) of 3LD or tritiated 3LD (1 mg/ml. 0·001 M-NaCl) were applied to columns of the anion exchanger ECTEOLA-SF1 which were then extensively washed with 0·01 M-phosphate buffer, pH 7. Fractionation was carried out by the gradient elution method with two mixing chambers, as described elsewhere. Elution was achieved at a flow rate of about 6 ml./hr and eluates were collected at 2 hr intervals with an automatic fraction collector. Absorbancies at 240, 250, 260, 280 and 290 mμ were measured in a Beckman DU Spectrophotometer.

The following solvent systems were used for the column chromatography.

Region I: elution with NaCl solutions of increasing concentration to a limit molarity of 0·5 (in 0·01 M-phosphate) at pH 7·0. The gradient elution was affected by employing two mixing chambers each of which contained 125 ml. of 0·01 M-phosphate buffer, pH 7·0, and an upper dropping funnel containing 0·5 M-NaCl (Bendich, Pahl, Korngold, Rosenkranz & Fresco, 1958). Region II: discontinuous elution with a solution of 0·1 M-NH_3/2·0 M-NaCl in 0·01 M-phosphate. Region III: gradient elution with two mixing chambers each containing 125 ml. 0·1 M-NH_3/2·0 M-phosphate. The upper dropping funnel contained a solution of 1 M-NH_3/2·0 M-NaCl/0·01 M-phosphate. An increase in pH at a constant salt concentration was thus effected. The final fraction (Region IV), which constituted less than 8% of the total DNA, was eluted with 0·5 N-NaOH. Recovery of DNA ranged between 96% and 104% in these experiments.

Absorbancies, in optical density units (optical density at 260 mμ multiplied by the volume of the collection in ml.), were plotted against tube numbers to obtain the chromatographic profiles which are shown in Fig. 1.

The contents of each collection tube were dialyzed for two days against large volumes of 0·001 M-NaCl. This removed the excess salts which were present in the solvents and prevented their interference with the radioactivity determinations.

(iii) *Ultracentrifugal analysis.* The effect of tritiation of 3LD on its sedimentation behavior was investigated. Solutions containing 0·003% DNA in 0·20 M-NaCl were analyzed at 59,780 rev/min (259,700 *g*) in 12 mm cells in a Spinco Model E ultracentrifuge equipped with ultraviolet optics (Shooter & Butler, 1956; Schumaker & Schachman, 1957). The integral distributions of sedimentation coefficients, corrected to 20°C and water, were calculated by an adaptation (Rosenkranz, 1959) of the method of Schumaker & Schachman (1957) and are reproduced in Fig. 2. The average sedimentation coefficients, $S_{50\%}$, were estimated from the 0·5 intercepts of the sedimentation distribution curves. (The reproducibility of the method was found to be within $\pm$ 0·3 S (Rosenkranz & Bendich, 1959)).

(iv) *Hyperchromic effect.* Since the increases in the absorbancy of DNA at 260 mμ upon alkalinization (Hotchkiss, 1957) and acidification (Cavalieri, Rosoff & Rosenberg, 1956) are considered to be criteria for native character, the hyperchromic effects exhibited by 3LD and tritiated 3LD before and after dialysis were studied. The absorption increment due to alkalinization at 260 mμ was measured by adding 0·04 ml. of 19 N-NaOH to 2·0 ml. of a solution containing 0·01 mg/ml. in 0·001 M-NaCl which raised the pH to about 13·5. The hyperchromic effect due to acidification was measured by gradually adding a small volume of 1 N-HCl with a microburette to 2·0 ml. of 0·01 mg/ml. DNA in 0·001 M-NaCl until no further increase in absorbancy at 260 mμ was observed (pH 3·0).

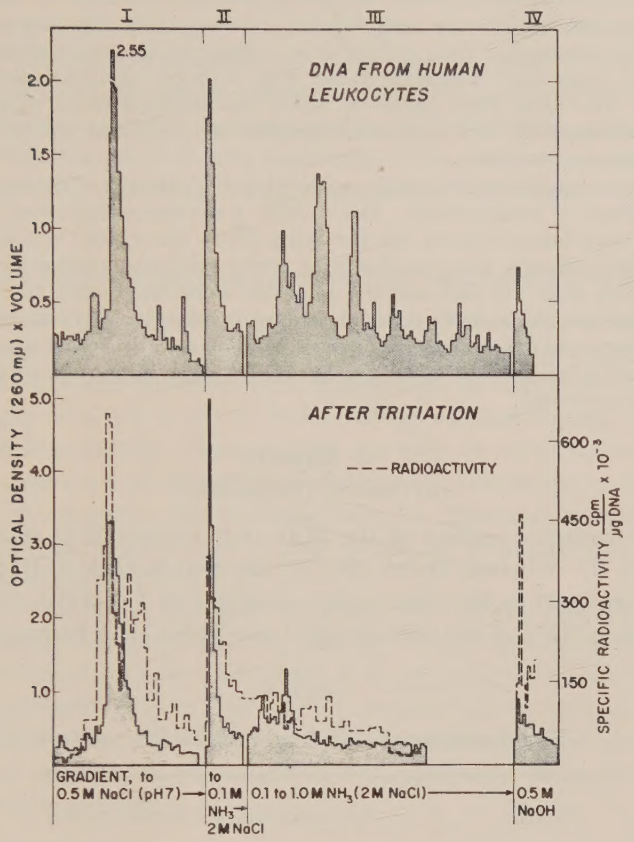

FIG. 1. Chromatography on a column of ECTEOLA (0·8 × 5·6 cm; 0·20 m-equiv/g; flow-rate about 6 ml./hr) of 3 mg of DNA isolated from human leucocytes. Upper profile: original DNA; lower profile: after tritiation. The Roman numerals above the upper profile refer to the four major chromatographic regions.

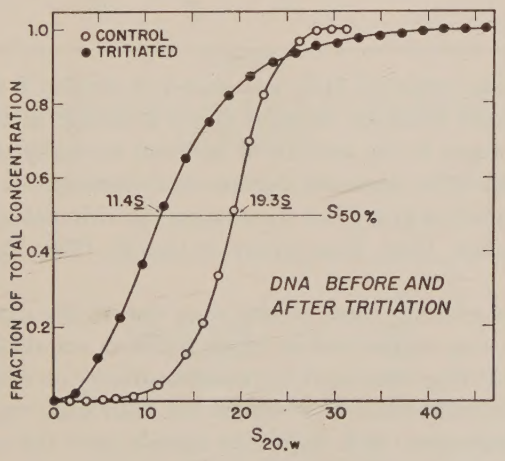

FIG. 2. Distribution of sedimentation coefficients of DNA (from human leukocytes) before and after tritiation.

(v) *Base analysis and determination of specific activities.* Samples of 3LD and tritiated 3LD were hydrolyzed with formic acid (Wyatt & Cohen, 1953), aliquots were removed for phosphorus determinations (Fiske & Subbarow, 1925) and the rest was spotted on Whatman No. 1 filter paper and chromatographed with *iso*propyl alcohol as the solvent system (Wyatt, 1951). The dried filter paper on which the tritiated bases were separated was scanned for radioactivity with a chromatographic strip counter equipped with a rectilinear galvanometric recorder.

The bases were eluted from the paper with 0·1 N-HCl, subjected to analysis and plated for determinations of radioactivity. For further purification solutions of the bases of tritiated 3LD were made slightly alkaline with dilute NaOH and absorbed on columns of Dowex-1. The columns were washed with water until the eluates were neutral. The bases were eluted with 1 N-HCl and the solutions were evaporated to dryness *in vacuo* over phosphorus pentoxide and pellets of sodium hydroxide. The samples were freed of excess HCl by repeated evaporation to dryness. Ultraviolet absorption measurements were made on aqueous solutions and, after appropriate dilution, aliquots were plated for determination of radioactivity.

3. Results

(a) *Column fractionation*

The chromatographic profiles of the 3LD and tritiated 3LD specimens differed markedly (Fig. 1). Whereas about 50% of the non-labeled 3LD applied to the column was recovered in the third region (gradient to 1 M-NH_3), this same region yielded only about 15% of the tritiated 3LD (see Table 1). A correspondingly larger

TABLE 1

Chromatography of DNA on ECTEOLA columns

Sample	Per cent recovered in each region			
	I	II	III	IV
3LD	45	6	41	8
	50	26	18	6
Tritiated 3LD †	46	39	11	4
	51	27	17	5

percentage of the total tritiated 3LD was eluted in Region I and Region II. It is therefore seen that the tritiation brought about a change in the DNA which was manifested by a decrease in the amount of material normally eluted in Region III. Previous studies with DNA from calf thymus have revealed a correlation between molecular size and position of a DNA fraction on the chromatogram (Rosenkranz & Bendich, 1959; Bendich, Pahl, Rosenkranz & Rosoff, 1958; Rosoff, di Mayorca & Bendich, 1957).

In order to decide whether these results were due to the extensive dialysis, two control experiments were carried out in which tritiated non-dialyzed 3LD and non-tritiated dialyzed 3LD were examined by chromatography on columns of ECTEOLA-SF1. The amounts of nucleic acid recovered in the individual regions were calculated (Table 1). In both instances, each respective sample gave the same elution pattern before as after dialysis.

† Three independent fractionations on the same material.

The radioactivities of the dialyzed fractions of the tritiated DNA increased with increasing absorption at 260 mμ thus giving a pattern comparable to the chromatographic profile obtained by plotting O.D. units (optical density $\times$ ml.) against tube numbers. A calculation of specific activity (counts/min/μg DNA) also yielded a plot which gradually increased and decreased within a given elution peak (Fig. 1). This type of radioactivity-optical density relationship was observed previously (Bendich, Pahl & Brown, 1957) with DNA which contained [2-^{14}C]5-bromouracil.

(b) *Ultracentrifugation of tritiated and non-tritiated samples*

(i) The effect of exposure to tritium gas on the sedimentation behavior of DNA is shown in Fig. 2. A decrease in number average sedimentation coefficient S_n ($S_{50\%}$) from 19·3 to 11·4 S was observed. This corresponds to a drop in number average molecular weight from $5{\cdot}2 \times 10^6$ to $1{\cdot}29 \times 10^6$ as calculated using the formula of Doty, McGill & Rice (1958).† Together with this shift to lower values of sedimentation coefficient, there is a considerable broadening of the distribution of sedimentation coefficients. This increased heterogeneity can be expressed numerically by the M_w/M_n ratio where M_w is the weight average molecular weight and M_n is the number average molecular weight (Doty, 1957).

This ratio is 2·20 for the untreated DNA and 11·4 for the tritiated sample when calculated (Rosenkranz, 1959) from S_n and S_w (weight average sedimentation coefficient) by the formula of Doty *et al.* (1958). A M_w/M_n ratio of 11·4 is very far removed from the most probable ratio of 2·00 which is assumed (Doty, 1957) for DNA. These data tend to indicate that the exposure of DNA to tritium gas has resulted both in a degradation and aggregation, the degree of the aggregation being far less extensive than that of the degradation.

(c) *Hyperchromic effect*

A study of the hyperchromic effect obtained by exposing non-tritiated and tritiated 3LD to acid and alkali showed essentially no difference in the reactivity of the two samples (Table 2). By these criteria, no significant denaturation had attended the tritiation.

TABLE 2

Hyperchromic effect of non-tritiated and tritiated DNA following acidification and alkalinization

Sample	Condition	pH 13·5	pH 3·0
		%	%
3LD	non-dialyzed	39	21·0
3LD	dialyzed	36	24·8
Trit. 3LD	non-dialyzed	34	23·5
Trit. 3LD	dialyzed	30	20·0

†The intrinsic viscosity dropped from 38 to 8 after tritiation and the molecular weights calculated from these data (according to Doty *et al.*, 1958) were found to be the same as those estimated from the sedimentation coefficients.

(d) *Base analysis and determination of specific activities*

A comparison of the base ratios of 3LD before and after tritiation indicated that no significant change in base composition has taken place (Table 3). A 95% recovery of bases was calculated from phosphorus determinations.

TABLE 3

Ratios of bases in DNA before and after tritiation
(*adenine* = 1·00)

Sample	3LD	Tritiated 3LD
Adenine	1·00	1·00
Thymine	0·97	1·00
Guanine	0·65	0·61
Cytosine	0·68	0·70

The first indication of variation in the specific activity of the individual bases came from an examination of a paper chromatogram of a formic acid hydrolysate of tritiated 3LD with the chromatographic paper strip counter. Distinct radioactive peaks were recorded in the region of each base. The thymine peak was markedly more radioactive than the remaining bases. When a photographic film was exposed to the paper chromatogram for 10 days, only the thymine spot was recorded on the radioautogram. After a 4-week exposure, all four bases gave distinct spots, although the thymine spot was the most pronounced.

To determine specific radioactivities, the eluted bases were plated and assayed for radioactivity. Assigning an arbitrary value of 1·0 to adenine, the thymine proved to be eight times as active (see Table 4). This ratio is considerably larger than might

TABLE 4

Bases from tritiated DNA

Base	Stable H † / Total H	Radioactivity: Eluted from paper chromatograms counts/min/μM	Ratio	Further purified on Dowex-1 counts/min/μM	Ratio ‡	Theoretical ratio ‡
Adenine	2/4	$1{\cdot}53 \times 10^6$	1·0	$1{\cdot}22 \times 10^6$	1·0	1·0
Thymine	4/5	$12{\cdot}00 \times 10^6$	7·9	$12{\cdot}00 \times 10^6$	9·8	1·6
Guanine	1/4	$2{\cdot}09 \times 10^6$	1·3	$1{\cdot}76 \times 10^6$	1·4	0·5
Cytosine	2/4	$3{\cdot}01 \times 10^6$	2·0	$2{\cdot}89 \times 10^6$	2·4	1·0

possibly have been expected on the basis of the number of stably-bound H-atoms in these heterocycles. Since the ratio of the radioactivities of guanine to cytosine appeared to be about as expected, the value for adenine seems to be somewhat low.

† Stable H refers only to those hydrogen atoms bound to carbon when in nucleotide linkage.
‡ Based on Adenine = 1·0.

Further purification of the bases was achieved by adsorption onto, and desorption from, a column of Dowex 1. Analysis of radioactivity showed that essentially no change in the ratios was obtained other than a further change in the adenine : thymine ratio (Table 4). The position of attachment of tritium at the carbon atoms of the bases is under investigation.

4. Discussion

The exposure of many organic substances to tritium leads to chemical alterations as well as replacement of hydrogen atoms (Steinberg, Vaughan, Anfinsen & Gorry, 1957; Jellinck & Smyth, 1958; Riesz & Wilzbach, 1958). It was therefore expected that it would also cause a change in the DNA molecule. DNA is quite sensitive to a variety of physical and chemical treatments (for reviews and references see Beaven, Holiday & Johnson, 1955; Bendich, Pahl, Rosenkranz & Rosoff, 1958; Chargaff, 1955; Zamenhof, 1957) and even exposure to as ostensibly a mild environment as salt-free water gives rise to irreversible changes.

A number of physical alterations could have followed the subjection of the DNA to the Wilzbach procedure. The two most obvious are degradation (main-chain scission with decrease in molecular weight) and denaturation (separation of the twin helical strands (Crick & Watson, 1954; Wilkins, 1956) of the DNA), both of which accompany the treatment of DNA with ionizing radiation (Shooter, Pain & Butler, 1956; Cox & Peacocke, 1957; Butler, Pain, Robins & Rotblat, 1958; Rosoff & Baturay, in press). The hyperchromic shifts of the tritiated DNA indicated that no extensive denaturation had taken place. Ultracentrifugal analysis, however, revealed a considerable degradation, resulting in an estimated four-fold decrease in average molecular weight. There also was an increase in ultracentrifugal heterogeneity as seen in the spread of sedimentation coefficients and in the occurrence of some aggregation (Fig. 2).

These alterations can be correlated (Rosenkranz & Bendich, 1959; Bendich, Pahl, Rosenkranz & Rosoff, 1958) with the changes which are seen in the anion exchange chromatographic profiles (Fig. 1). The degradations were probably caused by the type of double-chain scission which results, for example, from sonication (Doty *et al.*, 1958; Rosenkranz & Bendich, 1958).

It is possible that radiation-induced random breaks in one of the chains of the twin helix were responsible for the aggregations, or else the formation of even a few tritium (in place of hydrogen) bonds might lead to a deformity involving bridging at new, and more stable, points between two polynucleotide strands. As the carbon-tritium bond is stronger than the carbon-hydrogen bond (Kamen, 1951), it can be expected that there might be a similar difference in the strength of the tritium bonds which hold the double polynucleotide strands of the DNA together. This might possibly bring about a reorientation of some of the partner single strands which make up the double helices, especially if there were discontinuities in the single strands, as for instance in the interrupted-strand double helical model proposed by Dekker & Schachman (1954). This could lead, in addition, to two-chain structures other than the Watson-Crick type (see Donohue, 1956).

Studies are under way to help decide whether nucleic acids, labeled in this manner by exposure to tritium, can be of value as a tracer in biological problems. In preliminary explorations using autoradiography, the tritiated DNA and chromatographic fractions thereof have been observed to penetrate human cells (HeLa) grown in

tissue culture and to localize largely in the nuclear region. The tritiation is also being applied to a pneumococcal transforming DNA to determine if the biological activity has been affected.†

It has been difficult to obtain nucleic acids of such high specific radioactivity by biosynthetic or other means. The desirability of having suitably labeled polynucleotides has been underscored by the fact that *free* nucleic acids exert important biological effects when placed in contact with appropriate cells or tissues. Thus, nucleic acids have been found to cause genetic transformations in bacteria (Hotchkiss, 1955), and to induce viral infections (for references see Alexander, Koch, Mountain & Van Damme, 1958) or multiple tumors in mice (Latarjet, Rebeyrotte & Moustacchi, 1958). Very little, if anything, is known of the metabolic fate of such nucleic acids.

Since the various DNA fractions in the present investigation were unequally altered by the tritiation (Figs. 1 and 2), it should be possible by anion exchange chromatography to select fractions of desired size or average sedimentation coefficient (see Rosenkranz & Bendich, 1959) for further study.

The authors would like to express their appreciation to Drs. George B. Brown and M. Earl Balis and to Mrs. Grace C. Korngold for valuable discussions, advice and assistance.

REFERENCES

Alexander, H. E., Koch, G., Mountain, I. M. & Van Damme, O. (1958). *J. Exp. Med.* **108**, 493.

Beaven, G. H., Holiday, E. R. & Johnson, E. A. (1955). *The Nucleic Acids*, Vol. I, ed. by E. Chargaff & J. N. Davidson, p. 493. New York: Academic Press.

Bendich, A., Pahl, H. B. & Brown, G. B. (1957). *The Chemical Basis of Heredity*, ed. by W. D. McElroy & B. Glass, p. 378. Baltimore: Johns Hopkins Press.

Bendich, A., Pahl, H. B., Korngold, G. C., Rosenkranz, H. S. & Fresco, J. R. (1958). *J. Amer. Chem. Soc.* **80**, 3949.

Bendich, A., Pahl, H. B., Rosenkranz, H. S. & Rosoff, M. (1958). *Symp. Soc. Exp. Biol.* **12**, 31.

Butler, J. A. V., Pain, R. H., Robins, A. B. & Rotblat, J. (1958). *Proc. Roy. Soc.* B **149**, 12.

Cavalieri, L. F., Rosoff, M. & Rosenberg, B. H. (1956). *J. Amer. Chem. Soc.* **78**, 5239.

Chargaff, E. (1955). *The Nucleic Acids*, Vol. I, ed. by E. Chargaff & J. N. Davidson, p. 307. New York: Academic Press.

Cox, R. A. & Peacocke, A. R. (1957). *J. Polym. Sci.* **23**, 765.

Crick, F. H. C. & Watson, J. D. (1954). *Proc. Roy. Soc.* A. **223**, 80.

Dekker, C. A. & Schachman, H. K. (1954). *Proc. Nat. Acad. Sci., Wash.* **40**, 894.

Donohue, J. (1956). *Proc. Nat. Acad. Sci., Wash.* **42**, 60.

Doty, P. (1957). *J. Cell. Comp. Physiol.* **49**, Suppl. 1, 27.

Doty, P., McGill, B. B. & Rice, S. A. (1958). *Proc. Nat. Acad. Sci., Wash.* **44**, 432.

Fiske, C. H. & Subbarow, Y. (1925). *J. Biol. Chem.* **66**, 375.

Holt, C. V. & Holt, L. V. (1958). *Naturwissenschaften*, **45**, 289.

Hotchkiss, R. D. (1955). *The Nucleic Acids*, Vol. II, ed. by E. Chargaff & J. N. Davidson p. 435. New York: Academic Press.

Hotchkiss, R. D. (1957). *Methods in Enzymology*, Vol. III, p. 708. New York: Academic Press.

Jellinck, P. H. & Smyth, D. G. (1958). *Nature*, **182**, 46.

Kamen, M. D. (1951). *Radioactive Tracers in Biology*, 2nd edn, p. 209. New York: Academic Press.

Kay, E. R. M., Simmons, N. S. & Dounce, A. L. (1952). *J. Amer. Chem. Soc.* **74**, 1724.

Latarjet, R., Rebeyrotte, N. & Moustacchi, E. (1958). *C.R. Acad. Sci., Paris*, **246**, 853.

† Pneumococcal transforming DNA, exposed to 2 curies of tritium gas for 1 day, retained transforming activity. Details will be reported elsewhere.

Riesz, P. & Wilzbach, K. E. (1958). *J. Phys. Chem.* **62**, 6.
Rosenkranz, H. S. (1959). Ph.D. Thesis, Graduate School of Medical Sciences, Cornell University, N.Y.
Rosenkranz, H. S. & Bendich, A. (1958). *J. Biophys. Biochem. Cytol.* **4**, 663.
Rosenkranz, H. S. & Bendich, A. (1959). *J. Amer. Chem. Soc.* **81**, 902.
Rosoff, M., di Mayorca, G. & Bendich, A. (1957). *Nature*, **180**, 1355.
Schumaker, V. N. & Schachman, H. K. (1957). *Biochim. biophys. Acta*, **23**, 628.
Shooter, K. V. & Butler, J. A. V. (1956). *Trans. Faraday Soc.* **401**, 734.
Shooter, K. V., Pain, R. H. & Butler, J. A. V. (1956). *Biochim. biophys. Acta*, **20**, 497.
Steinberg, D., Vaughan, M., Anfinsen, C. B. & Gorry, J. (1957). *Science*, **126**, 447.
Wilkins, M. H. F. (1956). *Cold. Spr. Harb. Symp. Quant. Biol.* **21**, 75.
Wilzbach, K. E. (1957). *J. Amer. Chem. Soc.* **79**, 1013.
Wyatt, G. R. (1951). *Biochem. J.* **48**, 584.
Wyatt, G. R. & Cohen, S. S. (1953). *Biochem. J.* **55**, 774.
Zamenhof, S. (1957). *The Chemical Basis of Heredity*, ed. by W. D. McElroy & B. Glass, p. 351. Baltimore: Johns Hopkins Press.

J. Mol. Biol. (1959), **1**, 204-217

Ribonucleoprotein Particles within Chloromycetin-Inhibited *Escherichia Coli*

Masayasu Nomura † and J. D. Watson

The Biological Laboratories, Harvard University, Cambridge, Mass., U.S.A.

(*Received 17 April 1959*)

Cell free extracts of *E. coli* cells exposed to chloromycetin were examined in the analytical ultracentrifuge and compared to control cell extracts. A large new peak (15 *S*) was observed in the chloromycetin cells. It is highly sensitive to ribonuclease, contains 75% ribonucleic acid and 25% protein, and in free electrophoresis has a greater negative charge than normal *E. coli* ribonucleoprotein particles. 70% of the total ribonucleic acid in the chloromycetin-treated cells may be in the 15 *S* form. Isotopic experiments indicate that about 75% of the ribonucleic acid of the 15 *S* component is derived from phosphorus assimilated after chloromycetin addition. The remaining 25% of the 15 *S* phosphorus is present in the bacteria before chloromycetin addition and may be derived from normal ribonucleoprotein particles, the majority of which break down following addition of chloromycetin.

1. Introduction

Chloromycetin (CM) acts in a very interesting way. Immediately after its introduction to sensitive bacteria, protein synthesis stops while both deoxyribonucleic acid (DNA) and ribonucleic acid (RNA) synthesis continue (Gale & Folkes, 1953; Wisseman, Smadel, Hahn & Hopps, 1954). The amount of nucleic acid synthesized in the absence of concomitant protein synthesis (CM nucleic acid) is substantial, often representing a 60 to 100% increase over the pre-inhibition level. Recently Tomizawa (1958) has shown that CM DNA synthesized in T2-infected bacteria serves as a precurser for T2 DNA. CM DNA is thus similar if not identical to the normal free DNA intermediate observed in bacteriophage-infected cells.

The position of CM RNA is less clear. Though its base composition (Pardee & Prestidge, 1956) is identical to normal bacterial RNA, several experiments suggest a possible abnormal role. Firstly, Neidhardt & Gros (1957) have shown that following removal of CM much CM RNA may be broken down and released from the bacteria. Secondly, an experiment of Pardee, Paigen & Prestidge (1957) hinted that the CM RNA exists largely in a molecular form not observable in normal bacteria. Neither experiment, however, is conclusive and the possibility remains open that CM RNA is similar to a RNA intermediate normally present in only trace amounts.

In this paper we report some experiments designed to reveal the molecular form of CM RNA. Our observations parallel many of Pardee's and in general confirm his experiments. We differ, however, in one major respect. Most CM RNA does not exist in low molecular weight form. Instead it is present as relatively large units which for convenience we call CM particles. These CM particles do not exist as major components of normal *Escherichia coli* cells and their differentiation from normal bacterial ribonucleoprotein particles is the main object of this paper.

† Fellow of The Rockefeller Foundation; on leave from the Institute of Applied Microbiology, University of Tokyo, Tokyo.

2. Materials and Methods

(a) *Cultures and cell free extracts*

E. coli B/1/5 was grown in L broth, at 37°C, under forced aeration. The composition of L broth is as follows: bacto tryptone 1%, NaCl 1%, yeast extract 0·5%, glucose 0·1%, pH 7·0 adjusted with NaOH.

When ^{32}P incorporation experiments were performed, a low phosphate medium (P medium) of the following composition was used: glycerol 0·2%, casamino acids 0·1%, NH_4Cl 0·1%, phosphate 10^{-3} M, tris-(hydroxymethyl)-amino methane buffer 10^{-2} M, pH adjusted to 7·2 with NaOH.

The bacteria were grown to a density of about 4×10^8/ml. and divided into two parts. One part was harvested, washed with tris buffer (10^{-2} M, pH 7·2) and served as *control cells*. Another part received chloromycetin, usually at the concentration of 200 μg/ml., and was incubated for 1 hr at 37°C under aeration. During this CM treatment, the total protein content of the culture remained constant while both the RNA and the DNA content increased by about 50%. After this incubation, the cells were harvested, washed with tris buffer (10^{-2} M, pH 7·2) containing CM (20 μg/ml.) and served as the *CM cells*. Both normal and CM cells were ground with 2·5 parts of alumina powder in the cold, and extracted with 6 volumes of cold tris buffer (usually 10^{-3} M, pH 7·2) containing both CM (20 μg/ml.) and various amounts of Mg^{++} acetate. Addition of CM to the normal extract does not change the sedimentation pattern. The final pH was about 7·0 in both control and CM extracts. Usually deoxyribonuclease (2 μg/ml.) was added to the extracts. The alumina and cellular fragments and debris were removed by two low speed centrifugations (9,000 rev/min for 15 min) and the supernatant used as the cell free extract. (The extract of cells treated with CM will be called " CM extract " in this paper.)

(b) *Sedimentation analysis*

The ultracentrifuge analyses were carried out in a Spinco Model E ultracentrifuge equipped with a Philpot-Svenson optical system. The sedimentation constants were corrected to 20°C and expressed in Svedberg units (*S*). Many measurements were performed on crude extracts, and in such instances, the sedimentation constant of particles in normal extracts showed a lower value than those obtained on purified particles. This was due to the relatively high viscosity of the crude extracts. The ratio of the sedimentation constant of the 50 *S* particles observed in the crude extract to that of the zero concentration value was used as a correction factor for the other particles observed in the extract of CM cells.

(c) *Electrophoresis*

Electrophoresis was performed with a Spinco Model H electrophoresis-diffusion apparatus at 0·96°C under the constant current supply of 5·0 mA. Crude extracts or isolated particle preparations were first dialyzed against 100 volumes of tris-Mg^{++} buffer (tris 0·02 M, pH 7·2, Mg^{++} usually 5×10^{-4} M). The outer solution of dialysis was used as a buffer. Because of the instability of ribonucleoprotein particles in solutions of moderate ionic strength, buffer solutions of relatively low ionic strength were used. Accordingly the deviation from the ideal case of electrophoresis was large and exact calculation of mobilities was not performed.

(d) *Chemical and isotopic analyses*

The various samples were acidified in the cold with $HClO_4$ to a final concentration of 0·25 N. The precipitates were collected by centrifugation, and washed once with cold 0·25 N-$HClO_4$. The nucleic acid was then extracted with 0·5 N-$HClO_4$ at 70°C for 50 min. The remaining pellets were dissolved in 2 N-NaOH (protein fraction). Chemical analyses were then performed on each fraction. DNA was determined by a modification (Burton, 1956) of the Dische diphenylamine reaction, RNA was determined by the orcinol reaction (Schneider, 1945) and protein by the biuret reaction (Zamenhof, 1957) using crystalline chymotrypsin as a standard.

In the ^{32}P experiments, a modified Schmidt-Thanhauser fractionation method similar to that of Hershey (1953) was used to isolate the RNA fraction. Radioactivity was measured on an aliquot of this fraction.

3. Results

We must first briefly summarize previous observations on ribonucleoprotein particles in normal *E. coli* cells. A logarithmically growing *E. coli* cell contains about 25 to 30% of RNA on a dry weight basis (Tissières & Watson, 1958). Of this amount about 10 to 20% is present in low molecular weight form (Berg & Ofengand, 1958), and may be homologous to the "soluble RNA" (Hoagland, Zamecnik & Stephenson, 1957) of higher organisms. The remaining 80 to 90% of bacterial RNA is combined with protein as high molecular weight ribonucleoprotein particles. In the presence of divalent salts (in our experiments always magnesium), these particles are stable and can be easily extracted from bacterial cells in highly purified form.

There exist four main varieties of *E. coli* ribonucleoprotein particles (Tissières & Watson, 1958; Bolton, Hoyer & Ritter, 1958). They differ in size and shape and are classified by their sedimentation constants of 30 *S*, 50 *S*, 70 *S*, and 100 *S*. Each class contains 63% RNA and 37% protein. Their relation to each other is expressed by the following equation (Tissières & Watson, 1958).

$$2(30\,S) + 2(50\,S) \rightleftarrows 2(70\,S) \rightleftarrows 100\,S.$$

The molecular weight of the 30 *S* component is about $0{\cdot}75 \times 10^6$ while that of the 50 *S* component is $1{\cdot}8 \times 10^6$ (Tissières & Watson, 1958). Each 70 *S* particle contains one 30 *S* unit and one 50 *S* unit. It thus has a molecular weight of about $2{\cdot}6 \times 10^6$. The 100 *S* particle is a dimer formed from two 70 *S* particles. The equilibrium position is strongly influenced by the divalent ion concentration. At low concentrations the 30 *S* and 50 *S* components predominate, while at higher levels first the 70 *S* and then the 100 *S* particles are more common. A larger amount of Mg^{++} must be added to crude bacterial extracts than to purified particle preparations. For instance in a crude extract to which 10^{-3} M-Mg^{++} has been added only 30 *S* and 50 *S* particles are observed. On the contrary, this Mg^{++} concentration added to a purified preparation results in a predominantly 70 *S* preparation. We believe these results reflect the binding of free Mg^{++} by soluble protein and RNA of the crude extract. Similarly we note that the ribonucleoprotein particles themselves bind Mg^{++} and can appreciably reduce the free Mg^{++} concentration.

Divalent ions not only govern the above equilibrium transitions but are also necessary for the stability of the isolated 30 *S* and 50 *S* particles (Tissières & Watson, 1958). At Mg^{++} concentrations less than 10^{-4}M both 30 *S* and 50 *S* particles break down.

(a) *RNA partition within chloromycetin-inhibited cells*

Chloromycetin (200 μg/ml.) was added to vigorously aerated logarithmically growing *E. coli* cells. The inhibited cells were incubated for one hour, broken open by alumina grinding and a cell-free extract prepared in 10^{-3}M-tris buffer containing 10^{-3} M-Mg^{++}. The extract was then examined in the ultracentrifuge and compared with a control extract (Figs. 1 and 2). Two striking facts became obvious:

(i) There is a marked breakdown of ribonucleoprotein particles during CM inhibition. The control extract contains 30 *S* and 50 *S* particles. In contrast virtually no 30 *S*

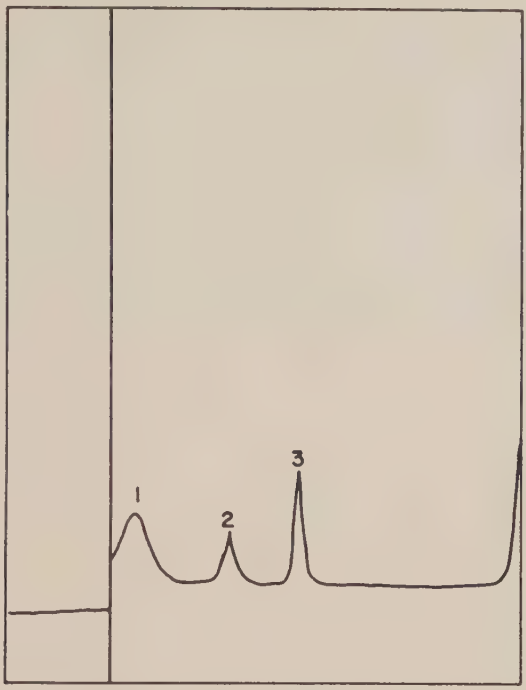

FIG. 1. Ultracentrifuge pattern of control extract prepared using buffer containing 10^{-3} M-Mg^{++}. Photograph taken 14 min after reaching 50,740 rev/min. 1, Soluble component (5 *S*); 2, 30 *S*; 3, 50 *S*.

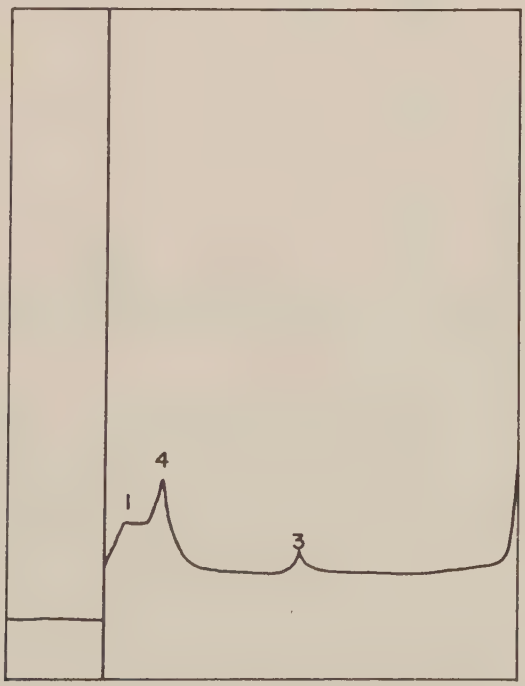

FIG. 2. Ultracentrifuge pattern of extract of CM-inhibited cells. Photograph taken 14 min after reaching 50,740 rev/min. 1, Soluble component (5 *S*); 3, 50 *S*; 4, 15 *S*.

particles and a greatly reduced amount of 50 *S* particles are seen in the CM extract. There is also a reduction in the amount of the 5 *S* soluble fraction which contains most of the bacterial soluble protein. A disappearance of 30 *S* particles was previously observed by Pardee *et al.* (1957).

(ii) A new peak (15 *S*) is observed in the CM extract. No significant trace of this component is seen in the control extract. Its initial sharpness suggested that it might represent DNA which for some reason was resistant to deoxyribonuclease. This hypothesis was disproved by the following observations: (i) the 15 *S* peak is extremely sensitive to ribonuclease (1 μg/ml. acting for several minutes at room temperature); in contrast it is not reduced by deoxyribonuclease acting at 10 μg/ml. for 1 hr: (ii) deletion of deoxyribonuclease from the extract resulted in the appearance of two sharp

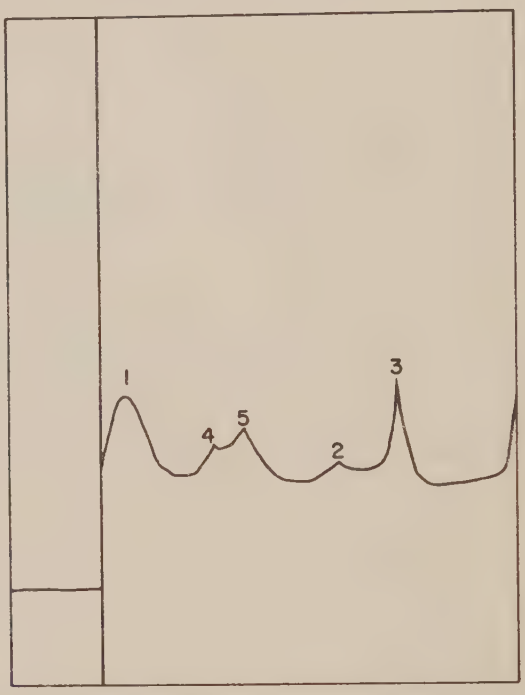

FIG. 3. Ultracentrifuge pattern of extract of CM-inhibited cells prepared using buffer containing 10^{-2}M-Mg^{++}. Photograph taken at 6 min after reaching 50,740 rev/min. 1, Soluble component (5 *S*); 2, 50 *S*; 3, 70 *S*; 4 and 5, " CM particles " (24 *S* and 31 *S*).

peaks (10 *S* and 15 *S*). The 10 *S* peak is completely destroyed by traces of deoxyribonuclease. It was thus clear the 15 *S* peak contained RNA and its large area suggested that a significant fraction of the RNA synthesized in the presence of CM was located here. The 15 *S* component is relatively stable in cell free extracts and may be stored virtually unchanged for several days at 4°C. This indicates that very little, if any, free bacterial ribonuclease is present. Elson (1958) has first shown that *E. coli* ribonucleoprotein particles contain a bound ribonuclease which is inactive under conditions of particle stability. The experiments of Pardee *et al.* (1957) were done before the divalent ion requirement for particle stability was established. Hence it is possible that some particle breakdown occurred in their extracts and accounted for their failure to observe the 15 *S* schlieren peak.

Since the 15 *S* component appears at a time when virtually no new protein synthesis occurs we wondered whether it might not represent free RNA. Attempts were made to isolate the 15 *S* fraction free from the various other fractions. In doing so, several preliminary experiments were carried out in which varying amounts of Mg^{++} were added to our extract. It was our hope to aggregate the normal ribonucleoprotein particles and thus effect a more efficient preparative centrifugal separation. In doing so two unexpected observations emerged.

(i) The ultracentrifugal pattern (Fig. 3) of a CM extract prepared in 10^{-2} M-Mg^{++} did not show any 15 *S* peak. Instead a large less homogenous double peak (24 *S* and 31 *S*) is seen. These peaks like the 15 *S* are highly sensitive to ribonuclease action in

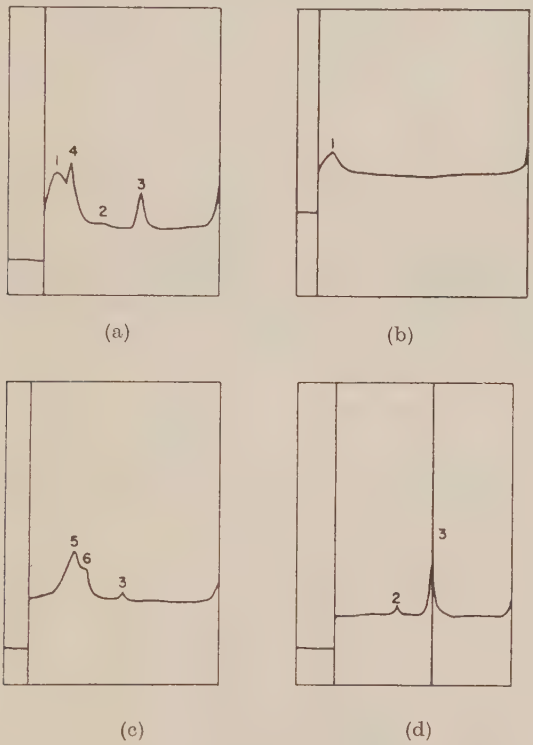

FIG. 4. Fractionation of the extract of CM treated cells. (a) original extract prepared using 10^{-3} M-Mg^{++}, (b) SS fraction, (c) SP fraction (in 10^{-3} M-Mg^{++}), (d) P fraction (in 10^{-3} M-Mg^{++}). Pictures were taken 10 min after reaching 50,740 rev/min. The concentration of particles and the bar angle used are not the same in each fraction. 1, Soluble component (5 *S*); 2, 30 *S*; 3, 50 *S*; 4, 15 *S*; 5 and 6, (24 *S* and 31 *S*).

contrast to normal particles. The 31 *S* CM peak thus should not be confused with normal 30 *S* particles. They are seen either when the extract is initially prepared in 10^{-2} M-Mg^{++} or when the high Mg^{++} level is reached subsequent to initial preparations in 10^{-3} M-Mg^{++}. These observations indicate that a major portion of the 15 *S* component upon exposure to increased Mg^{++} levels is converted to the (24 *S* and 31 *S*) fraction.

(ii) Increased Mg^{++} levels also lead to the appearance of 70 *S* particles, often in amounts exceeding the pre-existing 50 *S* component. We recall that 70 *S* particles form from the union of 30 *S* and 50 *S* particles in the presence of high Mg^{++} levels. Their presence is anticipated in control extracts prepared in 10^{-2} M-Mg^{++}. Their appearance,

however, in the 10^{-2} M-Mg^{++} CM extract was surprising since in 10^{-3} M-Mg^{++} extracts the 30 *S* component is effectively absent. The identification of the CM 70 *S* particle was therefore checked by centrifugal isolation and resuspension in low ($2{\cdot}5 \times 10^{-4}$M) Mg^{++} tris buffer. When this was done a mixture of 30 *S* and 50 *S* particles emerged. The addition of further Mg^{++} to low level Mg^{++} CM extracts thus induced the formation of 30 *S* particles from components present in the CM extract.

(b) *Isolation and some properties of chloromycetin particles*

We call both the 15 *S* and (24 *S* and 31 *S*) fractions chloromycetin particles. The CM cell-free extract prepared in 10^{-3} M-Mg^{++} was centrifuged at 100,000 *g* (average) for 120 min in the 40 rotor of the Spinco Model L ultracentrifuge. The major part of the supernatant solution was carefully withdrawn by suction (S1 fraction), leaving less than 1 ml. of solution surrounding the pellet. This remaining liquid was then decanted off and saved (S2 fraction). The pellet was resuspended in 10^{-2} M-tris buffer to which 10^{-3} M-Mg^{++} was added (P fraction). The S1 fraction was then made 10^{-2} M with regard to Mg^{++} and then centrifuged at 100,000 *g* for 120 min. Its supernatant (SS fraction) was decanted off and the pellet resuspended in tris Mg^{++} (10^{-3} M) buffer (SP fraction). Each fraction was then examined in the analytical ultracentrifuge (Fig. 4). The SS fraction showed only one peak of soluble components while the SP fraction showed two peaks of CM particles (24 *S* and 31 *S*) and was almost free from other components. The P fraction showed an almost pure 50 *S* peak. The S2 fraction consisted of a mixture of the above 3 fractions.

These fractions were then analysed for protein and RNA. In Table 1 are tabulated

TABLE 1

Chemical analysis of fractions of normal and CM-inhibited cells

Extract	Fraction	Components observed	RNA (mg)	Protein (mg)	RNA / protein	% distribution RNA	% distribution Protein
Control extract	P	50 *S* + 30 *S*	2·80	1·60	1·75	55	27
	S2	Mixture of the other 3 fractions	1·61	1·50	1·07	31	26
	SP	30 *S*	0·36	0·34	1·06	7	6
	SS	5 *S*	0·34	2·38	0·14	7	41
	Total		5·11	5·82	0·88	100	100
CM extract	P	50 *S*	0·79	0·49	1·61	19	21
	S2	Mixture of the other 3 fractions	1·04	0·59	1·77	25	25
	SP	CM particles (24 *S* + 31 *S*)	1·73	0·575	3·00	41	25
	SS	5 *S*	0·63	0·68	0·93	15	29
	Total		4·19	2·34	1·79	100	100

Figures are expressed on the basis of 1 ml. extract (corresponding to 0·17 g wet weight of cells). During the CM treatment (200 μg/ml., 1 hr) the wet weight of cells increased by 30%. We consistently observe that the RNA content of CM extracts is less than expected from the net increase of RNA within CM-inhibited cells. This may be due to the fragile nature of CM cells which results in noticeable lysis during their washing.

the results together with those from a similarly treated control extract. Confirming previous results (Tissières & Watson, 1958) we see that the 30 *S* and 50 *S* particles contain about 60% RNA and 40% protein. The RNA composition of the (24 *S* and 31 *S*) fraction is much higher, 75%. A significant protein component (25%) is observed, suggesting that the (24 *S* and 31 *S*) particles are ribonucleoprotein particles rather than free RNA. To check this point, the following electrophoretic experiments were carried out.

Cell free extracts of both normal and CM treated cells prepared with 10^{-2} M-Mg^{++} were dialysed against 2×10^{-2} M-tris buffer (pH 7·4) containing 10^{-3} M-Mg^{++} and subjected to electrophoresis in the Spinco Model H electrophoresis-diffusion apparatus. The results are shown in Fig. 5. The ultracentrifugal patterns of these extracts

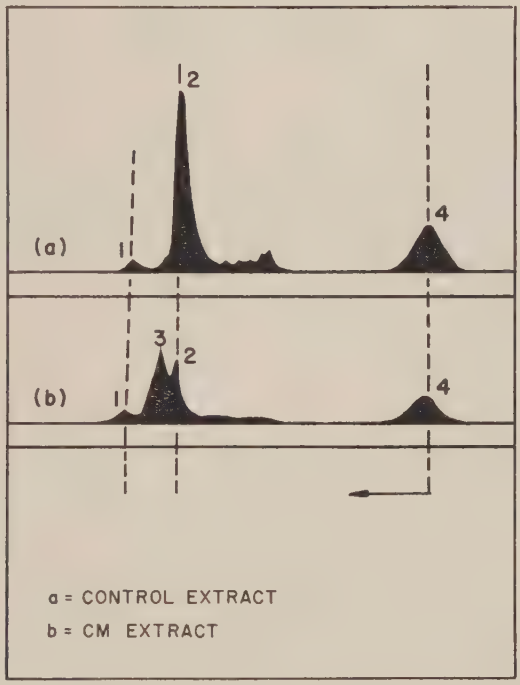

FIG. 5. Electrophoretic patterns of extracts of *E. coli*, (a) control cells, (b) cells exposed to CM. Ascending diagrams obtained after 75 min. Currents are 5 mA. Buffer used is tris buffer (0·02 M, pH 7·4) containing 10^{-3} M-Mg^{++}. 1, Soluble RNA; 2, normal particles; 3, " CM particles"; 4, δ boundary.

simultaneously examined are shown in Fig. 6. The fastest negatively charged component in both extracts is free RNA. This was shown by mixing purified high molecular weight rat liver RNA (supplied by Dr. Benjamin Hall) with the crude extract and observing that this added RNA moved together with the fast component as a single peak. The control extract contains a very large peak which moves toward the anode next to the free RNA. This peak contains the normal (30 *S* and 50 *S*) ribonucleoprotein particles. This was shown by fractionating the extract into particle and supernatant fractions and observing that only the particle fraction exhibited the large peak (Fig. 7). During the usual time (75 min) of our electrophoretic experiments, the particle component moves as a single peak. It showed, however, a tendency to separate into two peaks when the electrophoretic run was continued for 105 min.

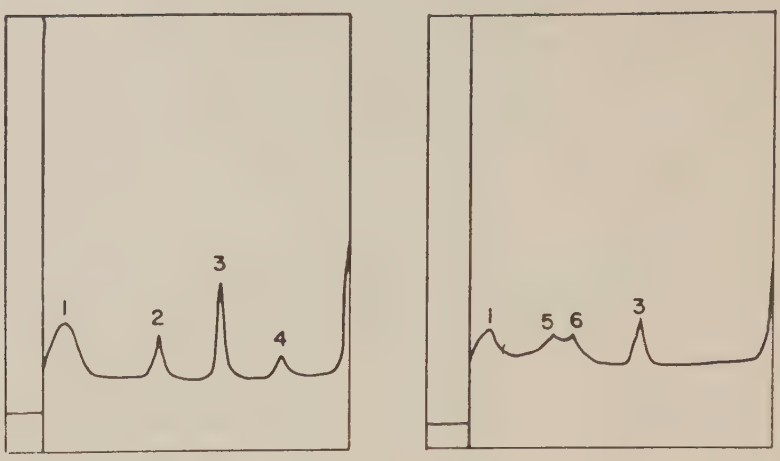

FIG. 6. Ultracentrifuge patterns of samples used for the electrophoretic analysis. (a) Control cells, (b) cells exposed to CM. Extracts were prepared using buffer containing 10^{-2} M-Mg^{++}. They were then dialyzed against 100 volumes of tris buffer (0·02 M, pH 7·4) containing 10^{-3} M-Mg^{++}, and subjected to both electrophoretic analysis (Fig. 5) and ultracentrifuge analysis. Pictures are taken at 10 min after reaching 50,740 rev/min. 1, Soluble component (5 *S*); 2, 30 *S*; 3, 50 *S*; 4, 70 *S*; 5 and 6, CM particles (24 *S* + 31 *S*).

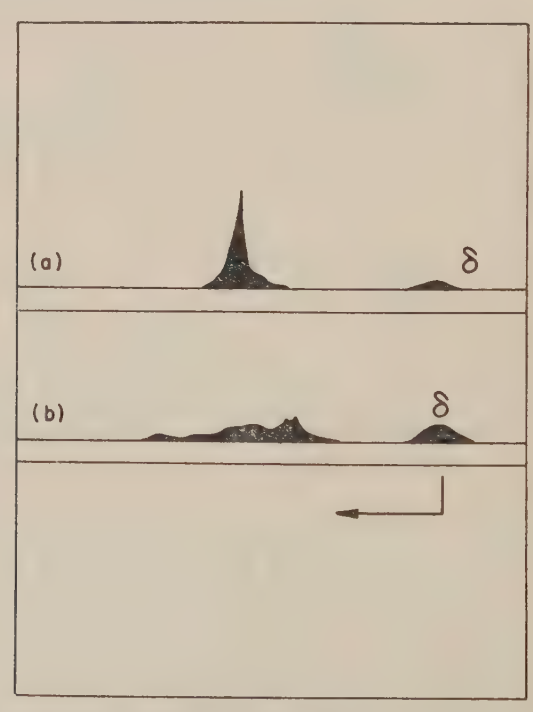

FIG. 7. Electrophoretic patterns of particle fraction (a) and soluble fraction (b) of the normal extract. The extract was prepared using buffer containing 10^{-3} M-Mg^{++}, and then divided into two fractions by centrifugation at 100,000 *g* for 120 min. Each fraction was dialyzed against tris buffer (0·02 M, pH 7·4) containing 10^{-3} M-Mg^{++}. Ultracentrifuge analysis showed the 30 *S* and 50 *S* peaks in particle fraction (a) and the 5 *S* peak in soluble fraction (b). A current of 5 mA was employed and the photographs are ascending diagrams taken after 75 min.

In the CM extract, the particle peak was small as expected from the ultracentrifugal analysis and a large new component appeared between the normal particles and free RNA. Fractionation of the extract reveals (Fig. 8) this to be the (24 *S* and 31 *S*)

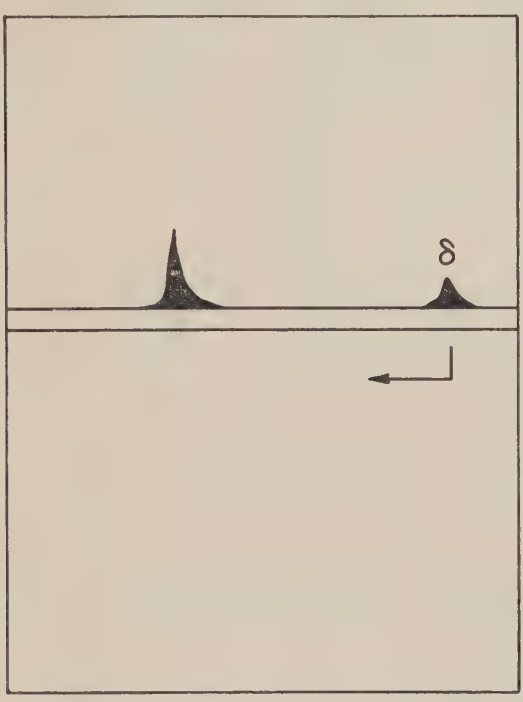

FIG. 8. Electrophoretic pattern of "CM particle" preparation. The "CM particles" were first resuspended in 10^{-3} M-Mg^{++} and then dialyzed against tris buffer (0·02 M) containing 5×10^{-3} M-Mg^{++}. The current is 5 mA and the photograph is an ascending diagram after 75 min. The trailing shoulder is probably due to a small amount of contaminating 50 *S* particles.

particles. The ratio of the area of the CM particle peak to that of the 50 *S* particle peak observed in the electrophoretic pattern (Fig. 5) is similar to that shown in the ultracentrifuge schlieren diagrams (Fig. 6).

The possibility, however, remained that the 15 *S* fraction, in contrast to the (24 *S* and 31 *S*) CM particles, was pure RNA and did not contain protein. To check this point, the 15 *S* component was directly isolated by several cycles of centrifugation. A cell-free CM extract was prepared in tris buffer containing 10^{-3} M-Mg^{++}. It was then centrifuged at 100,000 *g* for 2 hr to pellet the 50 *S* particles. The top 9 ml. from each of two tubes (10·5 ml. volume) was carefully withdrawn and recentrifuged at 100,000 *g* for 7 hr. The pellet enriched in the 15 *S* component was resuspended in 10^{-4} M-Mg^{++} and centrifuged at 100,000 *g* for 2 hr to sediment remaining traces of 50 *S* particles. The supernatant was again centrifuged for 7 hr, after which the supernatant was carefully withdrawn. The pellet was resuspended in tris buffer containing 10^{-4} M-Mg^{++} and then examined in the ultracentrifuge. The ultracentrifuge diagram (Fig. 9) showed a predominant 15 *S* peak with only the slightest traces of soluble protein (5 *S* and 50 *S*) particles.

The purified 15 *S* fraction was then examined for protein and RNA. Table 2 contains the results of this experiment. Again there is a significant protein content,

23% in this experiment and 24% in a second similar centrifugal fractionation. The RNA-protein ratio is thus the same in the 15 *S* and (24 *S* and 31 *S*) CM particles.

Addition of 4×10^{-3} M-Mg^{++} to the purified 15 *S* component converts it to the (24 *S* and 31 *S*) form. This transition is thus not dependent on any factor present in

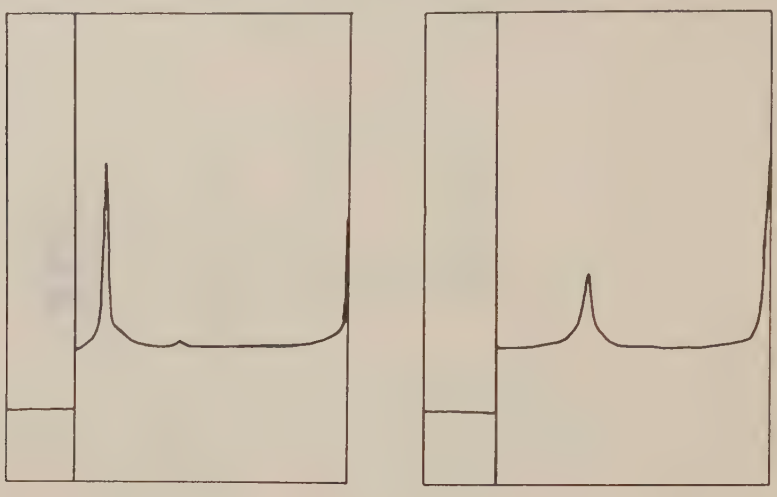

(a) (b)

FIG. 9. Ultracentrifuge patterns of a (15 *S*) preparation suspended in tris buffer (10^{-2} M, pH 7·2) containing 10^{-4} M-Mg^{++}. The photographs shown were taken at (a) 10 min and (b) 34 min after reaching 50,740 rev/min.

the soluble protein and RNA fraction. This observation together with the similarity in protein-RNA content suggests that the (24 *S* and 31 *S*) particles represent either configurational changes or aggregation products of the 15 *S* component.

TABLE 2

Chemical analysis of the 15 *S component*

Sample	RNA (orcinol method)	Protein (biuret)	% Protein
1	1·73 mg/ml.	0·56 mg/ml.	24 %
2	6·00 mg/ml.	1·80 mg/ml.	23 %

(c) *The origin of CM particles*

The fact that CM particles are not found in normal growing bacteria might suggest that they are derived entirely from RNA synthesized after CM addition. Likewise we might predict that all the normal 50 *S* particles seen after CM addition were formed prior to CM inhibition of protein synthesis. Isotopic experiments, however, reveal both these guesses incorrect.

Two types of experiments were performed. In the first, uniformly ^{32}P-labelled bacteria were suspended in isotope-free P medium containing CM. This experiment

measures the fate of phosphorus assimilated prior to CM inhibition. The second type of experiment was complementary in that both CM and ^{32}P were simultaneously added to non-labelled bacteria. Here the location of RNA synthesized after CM inhibition is revealed. Some details of these experiments were as follows.

An overnight bacterial culture (2×10^9 cells/ml.) was diluted 40-fold with fresh P medium and divided into two parts. One (culture B) received $^{32}PO_4^{\equiv}$ while the other (culture A) did not. Both cultures were then grown to a cell concentration of 3×10^8 cells/ml. The cells in culture B were centrifuged, washed once with 0·02 M-phosphate buffer (pH 7·2) and resuspended in isotope-free P medium containing CM (200 μg/ml.). At the same time CM (200 μg/ml.) and $^{32}PO_4^{\equiv}$ were added to culture A. Both cultures were then aerated at 37°C for 2 hr. During this interval the RNA and DNA contents of both cultures increased by 80%. As expected, in neither culture did the protein content change. Cell free extracts were prepared in 10^{-2} M-tris buffer containing 10^{-3} M-Mg^{++} and a fractionation was carried out similar to that described above for the preparation of (24 *S* and 31 *S*) CM particles.

Both the crude extracts and the various fractions were examined in the analytical ultracentrifuge. No differences were observed between the two cultures. In contrast to the extracts of cells grown in L broth some 70 *S* particles together with a small amount of 30 *S* particles were seen. In addition the 15 *S* component was partially converted to the (24 *S* and 31 *S*) form. The isolation method for the (24 *S* and 31 *S*) was therefore slightly modified to give a larger S2 fraction (the bottom part of the supernatant after the first centrifugation), consisting mainly of CM particles with small amounts of 30 *S* and 50 *S* particles.

The results of the chemical and isotopic analyses are summarized in Table 3a. The specific activity of RNA in each fraction was calculated and the value of each fraction in culture A was added to the corresponding value in culture B. These values should be the same, since they represent the specific activity of RNA in the fully labelled culture. The rather close agreement between these numbers show that the two fractionations (A and B) were very similar and that the chemical and isotopic analyses were reasonably accurate. Therefore the origin of the phosphorus of RNA in each fraction can be calculated with confidence (Table 3b).

We first see that 76% of the RNA in the SP fraction (CM particles) is derived from phosphorus assimilated after CM addition. A sizable proportion, 24%, however, is derived from phosphorus compounds assimilated before CM inhibition. Since the SP fraction contains some normal 30 *S* particles, it is conceivable that some of the pre-assimilated ^{32}P belonged to these normal constituents. This possibility was checked by exposing the SP fraction to pancreatic ribonuclease. Previous experiments (Tissières & Watson, 1958) indicated that normal ribonucleoprotein particles (30 *S*, 50 *S*, 70 *S* and 100 *S*) are relatively insensitive to ribonuclease and are thus easily differentiated from the ribonuclease-sensitive CM particles. The exact amount of these particles was therefore determined from the 30 *S* peak size remaining after ribonuclease digestion (1 μg/ml. acting for 30 min at room temperature) of the (24 *S* and 31 *S*) CM particles. Only a very small 30 *S* peak was seen which cannot account for the ^{32}P content of the SP fraction in extract B. The CM particles thus derive a significant fraction of their RNA ^{32}P from normal bacterial constituents.

18 % of the 50 *S* particle RNA contains phosphorus that entered the bacteria after the introduction of CM. This may mean that normal cells contain an excess of RNA-free particle protein and this combines with CM RNA to form normal ribonucleoprotein particles. Alternatively the source of this protein may be the

normal particles some of which we have already seen to break down during CM inhibition. In either case, however, some CM RNA serves as a precursor for particle RNA.

TABLE 3

Isotopic analysis of the origin of RNA in fractions of CM-inhibited cells

(a) Chemical and isotopic data

Culture	Fraction	Chemical amount of RNA mg/ml.	% distribution	^{32}P in RNA (total counts/min) counts/min/ml.	% distribution	Specific activity, counts/min/μg RNA	Sum of specific activity of A and B
A (^{32}P after CM addition)	P	2·94	44	51,800	20	17·6	
	S2	1·75	26	97,400	37	55·7	
	SP	1·02	15	62,600	24	61·3	
	SS	0·93	14	51,100	19	55·0	
	Total	6·64	100	263,000	100		
B (^{32}P before CM addition)	P	2·92	43	228,000	70	78·1	95·7
	S2	1·15	17	33,100	10	28·8	84·5
	SP	1·42	21	27,400	9	19·3	80·6
	SS	1·26	19	37,000	11	29·5	84·5
	Total	6·75	100	326,000			

(b) Calculated value of per cent of origin of RNA of each fraction

Fraction	Phosphorus assimilated before CM addition	Phosphorus assimilated after CM addition	Components observed in ultracentrifuge pattern
	%	%	
P	82	18	Mainly 70 *S* + 50 *S*. Small amount of 30 *S*
S2	34	66	Mainly CM particles. Small amounts of 30 *S* and 50 *S*
SP	24	76	CM particles with trace of 30 *S*
SS	35	65	5 *S*

Table 3b also reveals that a large amount of soluble RNA is synthesized after CM addition. This agrees with the chemical analyses (Table 1) indicating that the amount of soluble RNA increases more than twofold.

3. Discussion and Conclusions

1. Within CM-inhibited cells there appears a new macromolecular component (15 *S*) containing RNA. Large amounts of this material accumulate and it may account for 70% of the total RNA. Since CM blocks protein synthesis we might expect that this 15 *S* fraction is free RNA. We find, however, that 25% of this component

is protein. Further experiments must be done to clarify the nature of this protein and its relationship to the protein of normal ribonucleoprotein particles. It may be relevant that the majority of normal ribonucleoprotein particles break down following CM addition. This could provide a sizable reservoir of protein able to combine specifically with RNA.

2. The precise macromolecular form of the 15 *S* material is unclear. Experiments must be carried out to determine whether it contains one or several RNA chains. Its molecular weight should be determined and the nature of the Mg^{++}-induced transition, 15 *S* → (24 *S* and 31 *S*), needs investigation.

3. The relationship of the 15 *S* component to normal RNA metabolism is unclear. It is possible that it may be similar to a short-lived intermediate in the synthesis of normal ribonucleoprotein particles. The fact that some CM RNA is built into the 50 *S* particle in the presence of CM suggests, without proving, this possibility. A more satisfactory understanding of this problem demands more experiments on the form of RNA within the normal ribonucleoprotein particles.

The analytical ultracentrifuge and electrophoresis experiments were done in the laboratory of Dr. J. T. Edsall. We are also grateful to Miss B. Hollingworth for help with the electrophoresis measurements. This work was supported by grants from The National Science Foundation and an Institutional grant from the American Cancer Society.

REFERENCES

Berg, P. & Ofengand, E. J. (1958). *Proc. Nat. Acad. Sci., Wash.* **44**, 78.
Bolton, E. T., Hoyer, B. H. & Ritter, D. B. (1958). *Microsomal Particles and Protein Synthesis*, p. 18. New York: Pergamon Press.
Burton, K. (1956). *Biochem. J.* **62**, 315.
Elson, D. (1958). *Biochem. biophys. Acta*, **27**, 216.
Gale, E. F. & Folkes, J. P. (1953). *Biochem. J.* **53**, 493.
Hershey, A. D. (1953). *J. Gen. Physiol.* **37**, 1.
Hoagland, M. B., Zamecnik, P. C. & Stephenson, M. L. (1957). *Biochem. biophys. Acta*, **24**, 215.
Neidhardt, F. C. & Gros, F. (1957). *Biochem. biophys. Acta*, **25**, 513.
Pardee, A. B., Paigen, K. and Prestidge, L. S. (1957). *Biochem. biophys. Acta*, **23**, 162.
Pardee, A. B. & Prestidge, L. S. (1956). *J. Bact.* **71**, 677.
Schneider, W. C. (1945). *J. Biol. Chem.* **161**, 293.
Tissières, A. & Watson, J. D. (1958). *Nature*, **182**, 778.
Tomizawa, J. (1958). *Virology*, **6**, 55.
Wisseman, C. L., Smadel, J. E., Hahn, F. E. & Hopps, H. E. (1954). *J. Bact.* **67**, 662.
Zamenhof, S. (1957). *Methods in Enzymology*, Vol. III, p. 702. New York: Academic Press.

J. Mol, Biol. (1959) **1**, 218-220

Is The Nucleic Acid Message in a Two-Symbol Code?

Robert L. Sinsheimer

Division of Biology, California Institute of Technology, Pasadena, California, U.S.A.

(*Received 27 April 1959*)

In order to account for the diversity of adenine : guanine ratios in the deoxyribonucleic acids (DNA) of various microorganisms, it is proposed that the code in DNA is a two-symbol code. Specifically, it is proposed that the code is a sequence of 6-amino or 6-keto groups and thus adenine is equivalent to cytosine and guanine to thymine (or, in RNA, to uracil). This hypothesis also provides a convenient explanation of the near-equivalence of 6-amino and 6-keto nucleotides in the total RNA of various organisms.

1. Introduction

Considerable evidence has accumulated that the genetic information is transmitted from generation to generation in the form of DNA molecules (Sinsheimer, 1957; Crick, 1957). These molecules presumably carry in coded form the information necessary to specify the many features of the particular organism concerned, including notably the various protein components of the organism. It is widely believed that the message coded in DNA is translated into protein through the medium of RNA (Caspersson, 1950; Brachet, 1957; Zamecnik, Stephenson & Hecht, 1958; Crick, 1957).

Various theoretical inquiries have been made into the way in which a DNA molecule could serve to specify an RNA or protein molecule (Gamow, Rich & Ycas, 1956; Crick, Griffith & Orgel, 1957; Golomb, Welch & Delbrück, 1958). All these inquiries have proceded from the assumption that since DNA and RNA molecules are very largely composed of four types of nucleotides, the message in DNA is expressed in four symbols.

However, it has been observed (Belozersky, 1957; Lee, Wahl & Barbu, 1956) that the DNA complements of microorganisms vary widely in composition, ranging in guanine (G)/adenine (A) (and hence cytosine (C)/thymine (T)) ratio from 0·45 to 2·7. There is no evidence that the proteins of these organisms vary widely in composition, and direct measurements of the compositions of the ribonucleic acids of these organisms show much less variation in composition (the range of A + U/G + C is 1·03 to 1·45).

Two hypotheses may be advanced to reconcile these observations with the postulated roles of DNA and RNA. There may be "adaptors" which translate from the DNA code to RNA (analogous to the "soluble RNA fraction" + "pH 5 enzyme" which appear to translate from the RNA code to amino acids) and these "adaptors" may be different in different cells, i.e. there is no universal code relating DNA to RNA or to protein.

Or, alternatively, the code of DNA may not be, as it superficially appeared to be, a four-symbol code. We wish to propose that the code of DNA and RNA may be only a two-letter code—specifically, that the only structural features of importance for coding are the existence on each nucleotide of either a 6-amino group (symbol N) or a 6-keto group (symbol K).

On this hypothesis, in RNA, adenine is equivalent to cytosine and guanine is equivalent to uracil. In DNA, the base pairs adenine-thymine and cytosine-guanine are equivalent as are the base pairs guanine-cytosine and thymine-adenine.

RNA	DNA
$A \approx C = (N)$	A—T ⫽ C—G (N) $\not\approx$ T—A ⫽ G—C (K)
$G \approx U = (K)$	

In deriving an RNA molecule from a DNA molecule, then, the specification of *either* N pair (A—T or C—G) in DNA will specify that the RNA should correspondingly consist of *either* N (A or C) or of *either* K (G or T). (We do not know whether an N in DNA specifies an N or a K in RNA.) Thus, the nucleotide composition of an RNA derived from a particular DNA will be indeterminate as to the A/C and G/U ratios, depending perhaps upon the available supply of nucleotide precursors. However, the sequence of N and K groups will be the same in all RNA molecules derived from the same DNA; this NK sequence will be the code for the protein.

This hypothesis, by permitting free substitution of C—G pairs for A—T pairs in DNA without change of message, permits wide variation of the A/G ratio in DNA without change of message. The mutagenesis of 5-bromouracil is still explicable on an assumption of tautomeric shifts (Watson & Crick, 1953; Benzer & Freese, 1958) as this results in the replacement of an A—T pair by a G—C pair (an N → K transition). The mutagenesis of nitrous acid (Mundry & Gierer, 1958) is to be expected as an N—K conversion.

The replication of DNA, however, is presumed to be precise, involving the detailed complementarity of the Watson-Crick structure.

This hypothesis also provides a convenient explanation for the observations by Elson & Chargaff (1955) that when the composition of the entire RNA of a cell or organ is measured, the sum of the 6-amino groups (N) closely equals the sum of the 6-keto groups (K) although this rule does not appear to be valid for individual species of RNA molecules, such as those of the plant viruses (Magasanik, 1955). There is an elementary theorem in information theory (Shannon & Weaver, 1949) that if a message is to be written in a code of T symbols, the message can be written most efficiently (i.e., make use of the least quantity of symbols) if each symbol is used to an equal extent. In our case the message would be the protein content of a cell; this is to be expressed in a two-symbol (N, K) RNA code. This can be done most efficiently if two symbols are used equally—if the content of N equals the content of K, as Elson & Chargaff found. Of course, this equality cannot apply to each short message, such as each species of RNA molecule.

If the code is in N, K symbols then we may expect to find RNA molecules of considerably variable nucleotide composition, which express the same message.

Brawerman & Chargaff (1959) have recently demonstrated that the RNA composition of etiolated *Chlorella* cells differs slightly but significantly from that of green *Chlorella* cells, although the amounts of RNA per cell do not differ. In both instances N = K, but the ratios A/C and G/U are different. The authors interpreted this observation to be indicative of the formation of a distinct class of RNA molecules associated, indirectly, with photosynthetic processes. We might interpret this result, alternatively, as a consequence of a change in the pattern of supply of nucleotide molecules for RNA synthesis consequent to the change of metabolism with photosynthesis.

Similarly, the parallel between the nucleotide compositions of the RNA fractions synthesised after bacterial infection with phages T2 and T7, and the compositions of the DNA of the respective viruses, may be a reflection of the availability of nucleotide precursors rather than a specific structural relationship (Volkin & Astrachan, 1956; Volkin, Astrachan & Countryman, 1958).

We might note that the models for RNA synthesis proposed by Zubay (1958) could provide a structural basis for precisely the type of indeterminance of RNA structure that we are proposing from coding considerations.

REFERENCES

Belozersky, A. N. (1957). *International Symposium on The Origin of Life on Earth*, p. 194. The Publishing House of the Academy of Sciences of the USSR.

Benzer, S. & Freese, E. (1958). *Proc. Nat. Acad. Sci., Wash.* **44**, 112.

Brachet, J. (1957). *Biochemical Cytology*. New York : Academic Press.

Brawerman, G. & Chargaff, E. (1959). *Biochim. biophys. Acta*, **31**, 164, 172.

Caspersson, T. O. (1950). *Cell Growth and Cell Function*. New York : W. W. Norton and Co., Inc.

Crick, F. H. C. (1957). *Symp. Soc. Exp. Biol.* **12**, 138.

Crick, F. H. C., Griffith, J. S. & Orgel, L. E. (1957). *Proc. Nat. Acad. Sci., Wash.* **43**, 416.

Elson, D. & Chargaff, E. (1955). *Biochem. biophys. Acta*, **17**, 367.

Gamow, G., Rich, A. & Yeas, M. (1956). *Advanc. Biol. Med. Phys.* **IV**, 23.

Golomb, S. W., Welch, L. R. & Delbrück, M. (1958). *Biol. Medd. Kbh.* **23**, no. 9.

Lee, K. Y., Wahl, R. & Barbu, E. (1956). *Ann. Inst. Pasteur*, **91**, 212.

Magasanik, B. (1955). *The Nucleic Acids*, Vol. I, ed. by E. Chargaff & J. N. Davidson, ch. 11. New York: Academic Press.

Mundry, K. W. & Gierer, A. (1958). *Z. indukt. Abstamm-u. Vererbungslehre*, **89**, 614.

Shannon, C. E. & Weaver, W. (1949). *The Mathematical Theory of Communications*. Urbana: Univ. of Illinois Press.

Sinsheimer, R. L. (1957). *Science*, **125**, 1123.

Volkin, E. & Astrachan, L. (1956). *Virology*, **2**, 149.

Volkin, E., Astrachan, L. & Countryman, J. L. (1958). *Virology*, **6**, 545.

Watson, J. D. & Crick, F. H. C. (1953). *Cold Spr. Harb. Symp. Quant. Biol.* **18**, 123.

Zamecnik, P. C., Stephenson, M. L. & Hecht, L. I. (1958). *Proc. Nat. Acad. Sci., Wash.* **44**, 73.

Zubay, G. (1958). *Nature*, **182**, 1290.

J. Mol. Biol. (1959) **1**, 221-233.

Ribonucleoprotein Particles from *Escherichia coli*

A. Tissières, J. D. Watson, D. Schlessinger and B. R. Hollingworth

Biological Laboratories, Harvard University, Cambridge, Mass., U.S.A.

(*Received 14 May 1959*)

In exponential cultures, 25% of the dry weight of *E. coli* is accounted for by RNA. Of this about 80 to 90% is present in ribonucleoprotein particles and 10 to 20% in the "soluble" or "non-sedimentable" fraction. Magnesium stabilizes the particles, and on varying its concentration, four kinds of components are observed, with sedimentation constants of 30, 50, 70 and 100 *S*. 70 *S* is formed of one 30 *S* and one 50 *S*; 100 *S*, of two 70 *S*. Each type of particle has been isolated. They all contain about 63% RNA and 37% protein, and have the same density. The molecular weights of the 30 *S*, 50 *S* and 70 *S* particles are about $0{\cdot}7 \times 10^6$, $1{\cdot}8 \times 10^6$, and $2{\cdot}6 \times 10^6$ respectively.

1. Introduction

Bacteria release on lysis a large number of small particles of uniform size which in electron micrographs seem to constitute the bulk of the bacterial cytoplasm (Luria, Delbrück & Anderson, 1943). These particles contain most of the ribonucleic acid (RNA) of the cells; they form sharp boundaries in the analytical centrifuge, have a molecular weight of the order of 10^6, and are found in all the bacterial species examined (Schachman, Pardee & Stanier, 1952). They resemble in chemical composition and size the ribonucleoprotein particles which have been studied extensively in animal tissues (Petermann & Hamilton, 1952, 1957; Palade, 1955; Palade & Siekewitz, 1956*a* and *b*), in plants (Tso, Bonner & Vinograd, 1956, 1958), and in yeast (Chao & Schachman, 1956; Chao, 1957), and which are believed to be an important site of protein synthesis (Littlefield, Keller, Gross & Zamecnik, 1955; Littlefield & Keller, 1956, 1957; Schweet, Lamfrom & Allen, 1958).

Bacteria in the exponential phase of growth are one of the richest sources of ribonucleoprotein particles. In *Escherichia coli* dividing every 30 min, about 30% of the dry weight of the organism is accounted for by these particles (see below). While they are often firmly attached to the reticulum in animal tissues (Palade, 1955), they are free in bacterial extracts. *E. coli* is therefore convenient for the preparation of ribonucleoprotein particles in amounts sufficient for physical and chemical studies.

Magnesium stabilizes ribonucleoprotein particles from *E. coli* (Bolton, Hoyer & Ritter, 1958) from yeast (Chao, 1957) and from plants (Tso *et al.*, 1956, 1958). In the experiments reported here, in suitable concentrations of magnesium, four kinds of ribonucleoprotein particles were observed, with sedimentation coefficients of 30 *S*, 50 *S*, 70 *S* and 100 *S*. The isolation and some properties of each component will be described, and their molecular weights, based on sedimentation, diffusion, viscosity, and partial specific volume measurements, will be presented and discussed. A preliminary account of some of this work has appeared elsewhere (Tissières & Watson, 1958).

2. Methods

E. coli strain B was grown in enriched broth at 37°C under forced aeration. The broth had the following composition: 1% bactotryptone (Difco), 1% NaCl, 0·5% yeast extract

(Difco), 0·1% glucose, in distilled water. 1 ml. 1 N-NaOH was added to 1 l. of medium to adjust the pH to about 7·0. The cells were harvested in the exponential phase of growth and washed twice in the refrigerated centrifuge with the buffer used to make the extract. They could be kept frozen. Unless otherwise mentioned, the cell-free extract was made by grinding the well packed cells by hand in a cold mortar for 2 to 3 min with 3 parts (wt/wt) of alumina powder (Norton levigated alumina from Norton Abrasives, Worcester 6, Mass.) according to McIlwain (1948), and extracting with 3 vol of buffer. All manipulations were carried out at 0° to 4°C. Deoxyribonuclease (1 μg/ml.) obtained from Worthington Biochemical Corp., Freehold, New Jersey, was added to depolymerize the viscous bacterial deoxyribonucleic acid. The mixture of alumina, broken cells and buffer was centrifuged at 6000 ***g*** for 15 min, giving a sediment composed of two layers: a lower layer of alumina and some unbroken cells and a brown upper layer of large *cell debris*. The supernatant after this centrifugation, which is referred to as *crude extract*, contained the bulk of the ribonucleic acid of the cells, mostly in the form of ribonucleoprotein particles. The crude extract was usually centrifuged once more at 6000 ***g*** for 15 min to sediment any remaining alumina and cell debris. From this the ribonucleoprotein particles were then isolated by high speed centrifugation as described below.

A Model L Spinco ultracentrifuge was used for the preparation of the various particle fractions. The centrifugal forces given here represent ***g*** average, as calculated for the middle of the centrifuge tube. Analytical ultracentrifugation was done with a model E Spinco centrifuge, with either schlieren or ultra-violet optics. The films taken with the latter were analyzed for their optical density with a Spinco Analytrol densitometer. The centrifuge cell had a light path of 12 mm. The sedimentation constants were corrected to 20°C, water and zero concentration. They are expressed in Svedberg units,

$$S\ (= S^{\circ}_{20w} \times 10^{-13}\ \text{cm/sec}).$$

Electrophoresis and diffusion measurements were performed with a Spinco model H apparatus, in an 11 ml. Tiselius cell at 1°C.

Viscosity was measured with Ostwald-Fenske type viscosimeters, solvent running time 350 to 370 sec, at 24·97 $\pm$ 0·02°C.

RNA was estimated by the orcinol method as described by Dische (1953), with correction, when necessary, for deoxyribonucleic acid (Schneider, 1945) by the diphenylamine reaction (Dische, 1955).

Protein was estimated by the biuret test (Gornall, Bardawill & David, 1949).

Dry weight measurements were done on aliquots dried at 110°C to constant weight. The dry weight of the buffer, in which the ribonucleoprotein particles were suspended, was measured in the same way and subtracted from the weight of the particle preparations.

Partial specific volumes were measured in a 25 ml. pycnometer.

The relative amount of each ribonucleoprotein component present in a solution was measured on plates from ultracentrifuge runs by determining (a) the area covered by each peak on the schlieren diagrams and (b) the optical density given by each component on pictures taken with the ultra-violet optics.

Crystalline pancreatic ribonuclease was obtained from Worthington Biochemical Corp.

0·01 M-phosphate buffer pH 7·0 was prepared by mixing 1 vol of 0·01 M-KH_2PO_4 with 3 vol of 0·01 M-Na_2HPO_4. The pH was then adjusted to 7·0 by addition of 0·01 M-KH_2PO_4 or Na_2HPO_4.

Tris(hydroxymethyl)aminomethane was Sigma 7–9 biochemical buffer from Sigma Chemical Company. The pH of tris solutions was adjusted by addition of 0·1 N-HCl. Unless otherwise mentioned, 0·01 M-tris, pH 7·4, was used.

The magnesium salt, added to stabilize the particles, was magnesium acetate.

3. Experimental

(a) *Amount of RNA in E. coli and in fractions from cell free extracts*

RNA and protein were estimated on *E. coli* cells and on the following three fractions: (a) *cell debris*, consisting of pieces of cell walls and cell membranes which sedimented as a brown layer on top of the alumina during the first centrifugation at 6000 ***g*** for 15 min. To obtain this fraction free of crude extract and of intact cells,

which might well modify considerably the RNA content, it was washed five times in the centrifuge with the buffer used to make the extract. Each time the upper layer of the sediment was resuspended in buffer in order to eliminate the intact cells, unbroken during the grinding with alumina, which would, in view of their mass, centrifuge first to the bottom of the tube. This fraction was examined under the microscope and was found free of intact cells; (b) *crude extract*, or supernatant after centrifugation at 6000 *g* for 15 min; (c) *supernatant* obtained by carefully removing 2 ml. on top of the 11 ml. centrifuge tube, after centrifuging the crude extract at 100,000 *g* for 120 min.

TABLE 1

Amounts of RNA and protein in intact cells and fractions from cell free extract. The cells were ground with 3 *parts of alumina and extracted with* 0·001 M-*tris pH* 7·4 *and* 0·01 M-*magnesium acetate.*

(Similar results are obtained when the cells are extracted with 0·01 M-phosphate buffer pH 7·0 and 0·001 M-magnesium acetate. The *cell debris* is formed mostly of pieces from cell walls and cell membranes (see text). The *crude extract* is the fraction obtained after removing the alumina, the intact cells and the large cell debris by 15 min centrifugation at 6000 *g*. The crude extract, centrifuged for 120 min at 100,000 *g*, yields the *supernatant* and a small pellet formed essentially of ribonucleoprotein particles.)

		Protein	RNA	RNA/Protein
Intact cells (% of dry weight)		62·5	24·1	0·386
% of amount in intact cells	cell debris	15·0	0·9	0·06
	crude extract	85·0	97·0	1·17
% of amount in crude extract	supernatant	45·0	17·0	0·378
mg/ml.	crude extract	5·2	3·44	0·66
	supernatant	2·34	0·585	0·25
Difference (mg sedimented in 120 min centrifugation at 100,000 *g* from 1 ml. crude extract)		2·86	2·855	0·99

The results given in Table 1 show that: (a) 24% of the dry weight of the cell is accounted for by RNA; (b) the bulk of the RNA of the cell is present in the crude extract; (c) the debris of cell wall and cell membrane, after washing with buffer, contain less than 1% of the amount of RNA present in the cells; (d) 17% of the RNA in the crude extract is in the form of " non-sedimentable RNA", and is found in the supernatant after centrifugation at 100,000 *g* for 120 min (this value ranged in various experiments from 15 to about 25%); (e) about equal amounts of RNA

and protein are found in the unwashed fraction sedimented from the crude extract in a field of 100,000 *g*. All the RNA and most of the protein in this fraction belong to ribonucleoprotein particles, which are formed, as shown below, of about 63% of RNA and 37% of protein. A few per cent of the protein particles sedimenting with this fraction probably consist of fragments derived from the cell membrane.

(b) *Sedimentation diagrams of crude extracts*

The schlieren diagram of a crude extract made in 0·01 M-Mg^{++} and 0·01 M-tris buffer pH 7·4 showed two ribonucleoprotein peaks with sedimentation constants of 70 *S* and 100 *S*. The latter was predominant. With 0·001 M-Mg^{++}, the 70 *S* peak was the major one and in addition there were small amounts of 100 *S*, 50 *S* and 30 *S* peaks. With still lower magnesium concentrations (0·0001 to 0·0002 M), the ribonucleoprotein particles were present as 30 *S* and 50 *S* peaks. In the crude extracts the bulk of the soluble proteins of the cells appeared as a peak with a coefficient of about 5 *S*.

When the crude extract was made with 0·001 M-Mg^{++} and 0·01 M-phosphate buffer pH 7·0, the ribonucleoprotein particles were present as 30 *S* and 50 *S* components. This can be partly explained by the fact that some of the magnesium is bound to phosphate.

Thus four kinds of ribonucleoprotein particles could be observed in bacterial extracts, with sedimentation coefficients of 30 *S*, 50 *S*, 70 *S* and 100 *S*. The largest particles were predominant in presence of the highest concentration of magnesium. In low magnesium, only the 30 *S* and 50 *S* peaks were visible; these two components always appeared together and in the same ratio.

Schachman *et al.* (1952) found that extracts made by breaking the cells in different ways showed essentially similar sedimentation patterns. This was confirmed here: extracts made by sonic vibration or by lysing the protoplasts formed following the addition of penicillin to the culture medium according to Lederberg (1956) gave identical schlieren diagrams.

(c) *Isolation of the 70 S component*

The crude extract was made with 0·01 M-Mg^{++} and tris buffer pH 7·4. Under these conditions, the schlieren diagram showed a main 100 *S* component and a small amount of a 70 *S* peak. The 30 *S* and 50 *S* peaks were not visible. This extract was centrifuged at 78,000 *g* for 180 min. The supernatant was poured off and the yellow brown gelatinous pellet was resuspended in 0·005 M-Mg^{++} and 0·01 M-tris buffer by means of a teflon homogenizer used directly in the nitrocellulose centrifuge tube. The suspension was first centrifuged at 8000 *g* for 15 min in order to sediment and discard some aggregated material; then it was centrifuged at 78,000 *g* for 180 min. Washing the particles by resuspending them in buffer, followed by low and high speed centrifugation, as described above, was repeated twice. Finally the pellet was resuspended in tris buffer containing 0·001 M-Mg^{++} and the suspension was centrifuged at 8000 *g* for 15 min. The sediment was discarded. In the supernatant there was a major 70 *S* component, with in addition 10 to 15% of a 100 *S* peak and smaller amounts of 30 *S* and 50 *S* peaks. In one preparation 1 g (dry weight) of particles was obtained from 70 g (wet weight) of bacteria. The yield varied somewhat from preparation to preparation.

The 100 *S* particle is obtained by increasing the magnesium concentration of a 70 *S* preparation to 0·005–0·01 M. Sedimentation and viscosity measurements suggest

that it is formed of two 70 *S* particles. This view is supported by electron micrographs of 100 *S* (Dr. C. Hall, personal communication) showing large numbers of two particle aggregates.

All the 70 *S* and 100 *S* pellets were yellow-brown, although the intensity of this color was reduced by repeated centrifugation. When a 70 *S* pellet was examined as such in a 3 mm thick cell, with the Cary spectrophotometer, in the presence and in the absence of a reducing agent, the typical absorption spectrum of all the cytochrome pigments found in *E. coli* (Keilin & Harpley, 1941) was observed. It is likely that the ribonucleoprotein particles are contaminated at this stage by nonparticle protein, to the extent of about 5%. This view is consistent with the percentages of RNA and protein reported in Table 2.

(d) *Conversion of* 70 *S particles into* 30 *S and* 50 *S components*

The observations with the crude extracts described above suggested that the 70 *S* and 100 *S* particles were formed by the aggregation of 30 *S* and 50 *S* particles. Experiments with isolated 70 *S* particles proved this conjecture and showed that as the magnesium concentration is decreased 70 *S* breaks down to 30 *S* and 50 *S*. Two procedures were used to effect this transition.

(i) A 70 *S* preparation was centrifuged at 78,000 *g* for 180 min and the sedimented particles were resuspended in sufficient 0·00025 M-Mg^{++} and tris buffer to give a concentration of ribonucleoprotein of about 5 mg/ml. This was then dialyzed overnight in the cold with stirring against 0·00025 M-Mg^{++} and tris buffer. In some cases this treatment led to a complete conversion of 70 *S* particles into 30 *S* and 50 *S* components. However, in many instances a small amount of the 70 *S* peak was still visible on the schlieren diagram. The amount of this remaining 70 *S* component can be further reduced by lowering the magnesium concentration or by exposure to 45°C for several hours.

(ii) The pellet of particles after high speed centrifugation was resuspended in 0·001 M-Mg^{++} and 0·01 M-phosphate buffer pH 7·0. This procedure gave a 100% conversion of 70 *S* into the two smaller units, and was therefore adopted in most cases for the preparation of 30 *S* and 50 *S*. The conversion could also be obtained by dialysis against the phosphate-magnesium mixture.

(e) *Relative amounts of* 30 *S and* 50 *S arising from* 70 *S*

70 *S* was split to 30 *S* and 50 *S* and the resulting solutions were examined in the analytical ultra-centrifuge. For two different preparations, the areas of the 30 *S* and 50 *S* peaks on the schlieren plates were in the ratio of about 1 : 2. Applying the Johnston & Ogston (1946) correction would somewhat lower this ratio. Since, as shown below, the RNA and protein composition of 30 *S* and 50 *S* is the same, the optical density for each component on films taken with the ultra-violet optics is also a measure of their relative proportions. In four such experiments the ratio of 30 *S* to 50 *S* varies from 1 : 2 to 1 : 2·5. The errors in these measurements were possibly as great as 20%.

The molecular weights of the 30 *S* and 50 *S*, calculated from sedimentation and diffusion rates (see Table 3), are in the ratio of 1 to 2·5. Furthermore the molecular weight of the 70 *S* is approximately the sum of those of the 30 *S* and 50 *S*. These data show clearly that the 70 *S* particle is formed of one 30 *S* and one 50 *S*.

(f) *Isolation of the* 30 *S component*

The mixture of 30 *S* and 50 *S*, in concentrations of 5 to 10 mg/ml., was centrifuged at 100,000 ***g*** for 360 min. 7/10ths of the supernatant fluid was carefully removed without stirring and discarded while the remaining fluid was shaken gently by hand for about 5 sec in order to resuspend the upper layer of the pellet. This fluid was poured off and saved. It consisted of 30 *S* particles with 10 to 30 % of 50 *S*. With one or two more cycles of centrifugation at 100,000 ***g*** for 360 min and gentle resuspension of the upper layer of the pellet, the ratio of 30 *S* to 50 *S* could be brought to about 20 to 1, as judged by the area covered by each peak under the schlieren curve. The 30 *S* preparation could be sedimented by centrifugation at 100,000 ***g*** for 360 min. The pellet thus obtained was colorless. The buffer was either tris with 0·00025 M-Mg^{++} or phosphate with 0·001 M-Mg^{++} depending on whether procedure (a) or (b) was used to make 30 *S* and 50 *S*.

(g) *Isolation of the* 50 *S component*

The pellet after the first centrifugation at 100,000 ***g*** for 360 min was resuspended in buffer and magnesium mixture (either 0·01 M-tris pH 7·4 and 0·00025 M-Mg^{++}, or 0·01 M-phosphate pH 7·0 and 0·001 M-Mg^{++}). It was then centrifuged at 15,000 ***g*** for 15 min, the sediment was discarded and the supernatant was centrifuged at 100,000 ***g*** for 90 min. This last step was repeated twice. Further purification could be achieved by lowering the pH of the preparation to 5·0 with 0·1 N-CH_3.COOH, centrifuging at 8000 ***g*** for 15 min and finally bringing the pH of the supernatant to 7·0 with 0·1 N-NH_4OH. This treatment removed some cell debris derived probably from the membrane and the cell wall (see below) and also small amounts of 30 *S* which may still be present at this stage. After this last step the preparation showed only one peak on the sedimentation diagram and upon high speed centrifugation formed a colorless pellet. In addition it moved as a single symmetrical peak on electrophoresis at pH 7·6 or 4·7.

(h) *Formation of* 70 *S particles from purified* 30 *S and* 50 *S*

30 *S* and 50 *S* particles (in tris buffer and 0·00025 M-Mg^{++}) were mixed together in equal number amounts and magnesium added to a final concentration of 0·001 M. No aggregation occurred. On raising magnesium to 0·005 M, 70 *S* particles appeared and at 0·01 M the majority of particles were in the 70 *S* form. Subsequent lowering of the magnesium level to 0·001 M reveals a majority of 70 *S* particles. Thus a higher magnesium concentration is required to form 70 *S* particles than to effectively stabilize them. Our data are summarized by the equation

$$\text{increasing } Mg^{++} \longrightarrow$$
$$2\,(30\,S) + 2(50\,S) \rightleftarrows 2(70\,S) \rightleftarrows (100\,S) \qquad (1)$$

When a mixture of peaks is observed, they are usually very sharp. This would not be true if the various particle types were in rapid equilibrium, as the peaks would blend into each other. This implies that the transitions need not occur immediately, but that an activation energy is required when 70 *S* splits into 30 *S* and 50 *S*. This is supported by the observation that incubation of 70 *S* particles in low magnesium (0·00025 M) does not lead to immediate breakdown and that the transition is hastened by incubation at 45°C. The same reason may explain why the 70 *S* particle is not formed at 0·001 M-Mg^{++} even though once formed it initially seems stable and can be isolated at this magnesium level. In fact, prolonged incubation (several days to a

week) of 70 *S* particles at 45°C leads to their breakdown to 30 *S* and 50 *S* particles. It is thus probable that the 70 *S* particles are completely stable only at magnesium concentrations greater than 0·005 M where in fact they begin to further aggregate to 100 *S* particles.

(i) *Chemical composition*

The results of RNA and protein estimations, together with dry weights and extinctions at 260 mμ on a dry weight basis, are given in Table 2. The dry weights corresponded, within the limits of error, to the sum of the weights of RNA and protein found by chemical estimation. The errors in these estimations were probably 3 to 4%. Thus it appears that the particles are formed mostly, if not exclusively, of RNA and protein. It is likely that the ratio of RNA to protein is the same in the three kinds of particles, 30 *S*, 50 *S* and 70 *S*, and that the small variations shown in Table 2 are due to varying amounts of impurities. This view is supported by the finding (see below) that the densities of the three kinds of particles are very similar. The values for the extinction at 260 mμ suggest that the purest preparations are those of 30 *S* and of 50 *S*, the latter after treatment at pH 5·0.

TABLE 2

Dry weight, chemical composition and specific extinction coefficients at 260 mμ *of* 30 *S*, 50 *S and* 70 *S ribonucleoprotein particle preparations.*

Particle fraction	Dry weight mg/ml.	RNA mg/ml.	Protein mg/ml.	RNA + Protein mg/ml.	% RNA	% Protein	Specific extinction coefficient at 260 mμ = $E^{1\%}_{1\,cm}$
30 *S*	3·72	2·38	1·50	3·88	62·0	38·0	167·0
30 *S*	1·58	0·95	0·60	1·55	61·3	38·7	162·0
50 *S*	2·26	1·39	0·83	2·22	62·5	37·5	—
50 *S*	1·06	0·63	0·37	1·00	63·4	36·6	182·0
50 *S*	2·82	1·80	1·00	2·80	64·0	36·0	—
50 *S*†	6·96	3·94	2·85	6·79	58·0	42·0	149·0
70 *S*	39·00	23·50	17·60	41·10	57·3	42·7	147·0
70 *S*	—	—	—	—	—	—	145·0
70 *S*	13·60	8·80	5·70	14·50	60·7	39·3	157·0

† 50 *S*: this preparation had not been treated at pH 5·0.

(j) *Absorption spectrum*

The absorption curves of the 30 *S*, 50 *S* and 70 *S* in the ultra-violet region were nearly identical. They all showed an absorption peak with a maximum at 259 mμ. The RNA in 30 *S*, 50 *S* and 70 *S* was found to react with formaldehyde, as described by Fraenkel-Conrat (1954) for several plant viruses: the absorption in the 260 mμ region increased by about 20% and the maximum was shifted about 3 mμ towards the longer wavelengths. The spectrum of a 50 *S* preparation and the effect of formaldehyde are shown in Fig. 1.

(k) *Relative densities*

A particle preparation containing 30 *S* and 50 *S* components was added to salt solutions to give an optical density of 1·0 at 260 mμ. The resulting samples contained

0·01 M-phosphate pH 7·0 and 0·001 M-Mg^{++} in 0·0, 0·5, 1·5, 3·5, and 5·0 molal CsCl. The sedimentation rates observed with ultra-violet optics are shown in Fig. 2. Corrected for the viscosity and density of the medium, they correspond to 30 *S* and 50 *S*. In all cases, the relative sedimentation constants of the two components were the same, indicating that they had similar if not identical partial specific volumes. Further experiments were performed in varying concentrations of sucrose and NaCl with identical results. In one experiment involving 70 *S* particles in NaCl solution, the sedimentation run was done before complete 70 *S* breakdown (see below) and the sedimentation rate of 70 *S* was reduced at the same rate as those of 30 *S* and 50 *S*.

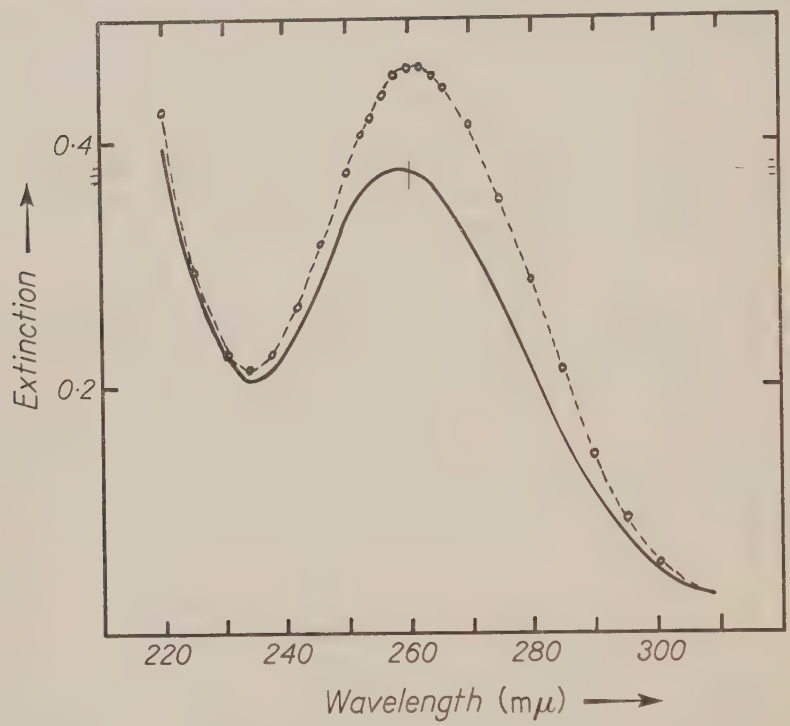

FIG. 1. Absorption spectra of 50 *S* particles. The solid line represents the spectrum of 50 *S* (20·6 μg/ml.) in 0·01 M-phosphate and 0·001 M-Mg^{++}, before and after 70 hr at 45°C. The dashed line shows the spectrum after similar incubation in 2% HCHO.

(l) *Stability*

(i) *Effect of magnesium*. The four kinds of particles were usually stable in the presence of magnesium for over a month in the cold in 10 μg/ml. streptomycin, although occasionally after a few weeks the particles were found to break down. Buffer was not necessary; preparations remained intact for several days in distilled water and magnesium.

Magnesium is required not only for the existence of the 70 *S* and 100 *S*, but also for the integrity of the 30 *S* and 50 *S* subunits. If 30 *S* or 50 *S* is dialyzed against buffer containing no magnesium, or against distilled water, or if 0·01 M-ethylene-diamine tetra-acetate (versene) is added, breakdown of the particles occurs.

It has been mentioned that 0·003 to 0·01 M-Mg^{++} causes aggregations to the 100 *S* component. The particles are stable up to 0·02 M-Mg^{++}, above which breakdown was observed.

(ii) *Effect of freezing.* The particles could be kept frozen for several months without any noticeable change of their properties.

(iii) *Effect of pH.* The 50 *S* was stable for 24 hr at pH 4·7 and 9·5. The 30 *S*, 70 *S* and 100 *S* broke down under these conditions.

If the pH of a suspension of 30 *S*, 50 *S* and 70 *S* (1·5 mg/ml.) was lowered to 4·4 with 0·01 M-ammonium acetate or 0·1 N-CH_3.COOH, and the resulting mixture dialyzed for 15 hr against 100 vol of 0·001 M-Mg^{++} and 0·01 M-ammonium acetate pH 4·4, a completely diffuse peak, suggesting random aggregation, was seen in the

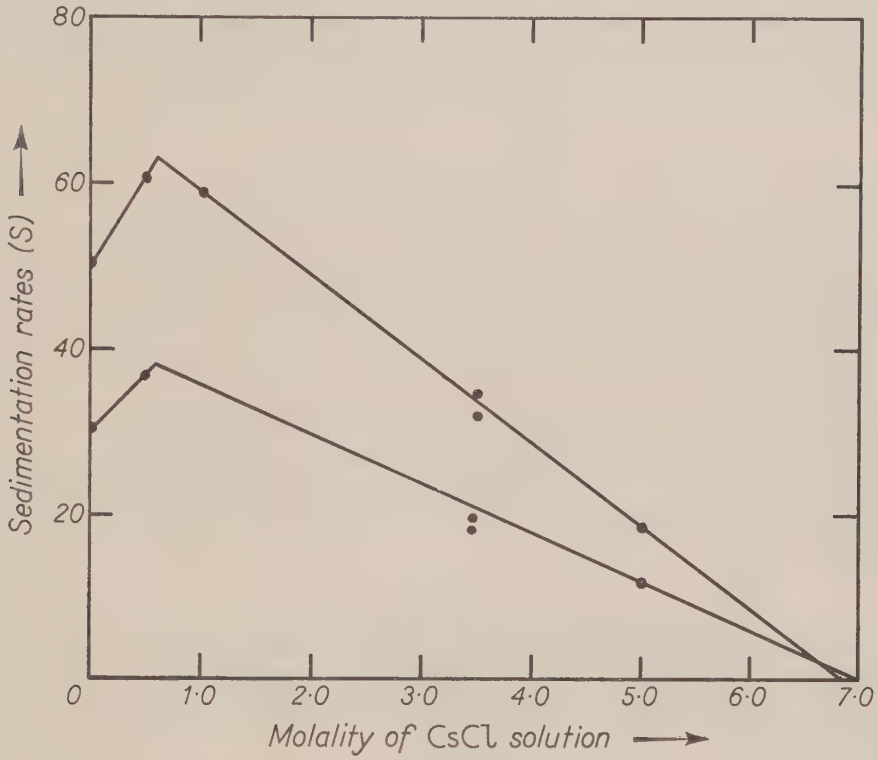

FIG. 2. Sedimentation rates in CsCl. Mixtures of 30 *S* and 50 *S* were examined in the analytical ultracentrifuge with ultra-violet optics, immediately after dilution in different concentrations of CsCl. The ratio of sedimentation rates was always 50 : 30. The graphs extrapolate to a particle density in CsCl of 1·73 ± 2% for both components. The initial rise in sedimentation rate is probably attributable to initial replacement of Na^+ in the particles by Cs^+.

analytical ultracentrifuge. If the same sample was then dialyzed for 15 hr against 0·01 M-tris, pH 7·4, a 50 *S* peak was again visible, with traces of 30 *S* and 70 *S*. If the pH was lowered further to 4·2, a white precipitate was observed. The precipitate did not revert to ribonucleoprotein components on raising the pH.

(iv) *Effect of ribonuclease.* 1 to 5 μg/ml. of pancreatic ribonuclease, at pH 7·6, had no effect on most particle preparations, even after 4 to 6 hr at room temperature, as judged by the appearance of the peak in the analytical ultracentrifuge. In some cases, however, the peak heights were reduced. The reason for these discrepancies is not clear.

(v) *Effect of NaCl and CsCl.* 30 *S*, 50 *S*, or 70 *S*, or mixtures of them, in 0·001 M-Mg^{++} solutions, were allowed to stand at 4°C in different NaCl or CsCl concentrations. After

15 hr, samples were examined in the analytical centrifuge with the ultra-violet optics. 30 *S* and 50 *S* were stable below about 0·15 and above 2·0 molal NaCl and CsCl. They broke down in the intermediate range and consequently no sedimentation rate greater than 5 *S* was observed. 70 *S* was stable in low salt concentrations up to about 0·15 molal. In higher concentrations it split to 30 *S* and 50 *S*.

Elson (1958) has shown that a latent ribonuclease is present in ribonucleoprotein particle preparations from *E. coli*. The unusual stability of the particles in salt reported here may be partly explained by the presence of this enzyme, assuming that above 0·15 molal NaCl or CsCl the particle structure is altered in such a way that the endogenous ribonuclease can degrade the particulate RNA. The stability of the particles above 2·0 molal NaCl or CsCl might be due to inhibition of ribonuclease by high salt concentrations, or else simply to salt effect on the particles.

(m) *Molecular weights*

Values shown in Table 3 are based on the following data:

(i) *Sedimentation constants.* The coefficients for 30 *S*, 50 *S* and 70 *S* were measured both with the ultra-violet optics at concentrations of about 60 μg/ml., and with the schlieren optics at concentrations of 0·5 to 5·0 mg/ml., in 0·01 M-tris and the suitable magnesium concentrations. The results are shown in Fig. 3. The salt concentration had no appreciable effect between 0·01 and 0·05 M-phosphate and 0·001 and 0·05 M-tris.

(ii) *Diffusion coefficients.* Free diffusion was allowed to proceed for 2 to 3 days. Measurements were made on two different preparations of 30 *S* (both at 0·11%, in 0·01 M-tris), three of 50 *S* (at 0·06%, in 0·01 M-phosphate; 0·07%, in 0·05 M-phosphate; and 0·20%, in 0·01 M-phosphate), and one of 70 *S* (at 0·10% and 0·20%, in 0·01 M-tris).

TABLE 3

Physical constants and molecular weights. Percentages of error are given as the average deviation from the mean. The molecular weights are consistent with equation (1).

Components	Precise S ($S^0_{20,w} \times 10^{13}$ cm/sec)	D ($D^0_{20,w} \times 10^7$ cm²/sec)	$\bar{V}$	$\eta_{int.}$ cm/dl.	Molecular weights from S & D (Svedberg & Pedersen, 1940)	Molecular weights from S & η (Scheraga & Mandelkern, 1953)
30 *S*	30·6 ± 1	2·95 ± 4 %	0·64	0·080 ± 8 %	0·7 × 10⁶ ± 8 %	1·0 × 10⁶ ± 16 %
50 *S*	50·0 ± 1	1·91 ± 1 %	0·64	0·054 ± 8 %	1·8 × 10⁶ ± 4 %	1·8 × 10⁶ ± 16 %
70 *S*	69·1 ± 1	1·83 ± 2 %	0·64	0·061 ± 10 %	2·6 × 10⁶ ± 6 %	3·1 × 10⁶ ± 18 %
100 *S*	100·0 ± 2		0·64	0·071 ± 12 %		5·9 × 10⁶ ± 20 %

Because of the impossibility of forming infinitely sharp initial boundaries with proteins, the calculated values of D decreased with time. Plots of D against $1/t$, which were linear, when extrapolated to infinite time, gave corrected values of D. Zero-time corrections were of the order of 20 to 50 min. The values of D were then corrected to 20°C in water. For 30 *S*, they were 2·81 and 3·10 × 10^{-7} cm²/sec; for 50 *S*, 1·88, 1·90, and 1·95 × 10^{-7}; and for 70 *S*, 1·82 and 1·84 × 10^{-7}. Averaged values are shown in Table 3.

(iii) *Partial specific volume.* The values obtained were 0·64 and 0·66 for two 50 *S* preparations, and 0·63 for one 70 *S*, at concentrations varying from 0·5 to 4%. Since the density and chemical composition of the three kinds of particles is probably the same (see above), an average value of 0·64 was used in all calculations.

(iv) *Viscosity.* The preparations used contained at least 85% of one ribonucleoprotein component, as measured on plates taken with the schlieren optics. For various 30 *S*, 50 *S* and 70 *S* preparations, and for one of 100 *S*, series of viscosity measurements were extrapolated to an average intrinsic viscosity (Table 3). Concentrations were calculated assuming that 67 μg/ml. corresponded to an optical density of 1·0 for 50 *S*, 70 *S* and 100 *S*, and 61 μg/ml. for 30 *S*. These values were deduced from the specific extinction coefficients at 260 mμ given in Table 2.

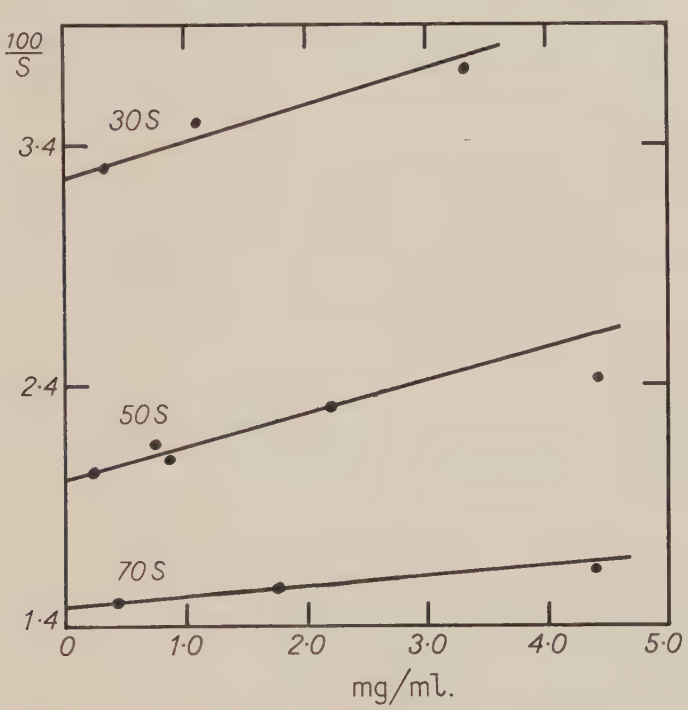

FIG. 3. Concentration dependence of sedimentation constants.

The molecular weight of the 50 *S* particles calculated from sedimentation, diffusion and partial specific volume data agrees well with that derived from sedimentation, viscosity and partial specific volume. As the value involving the diffusion coefficient is independent of the shape of the particle, while that using intrinsic viscosity assumes a spherical shape, this result, in agreement with the electron micrographs (Hall & Slayter, 1959), suggests a spherical shape for the 50 *S* particle.

In contrast the molecular weight of the 30 *S* particles obtained by using intrinsic viscosity seems high when compared to that based on diffusion values, and may reflect the less symmetrical form shown in electron micrographs.

4. Discussion

The construction of ribonucleoprotein particles from two unequal units which join in presence of a suitable magnesium concentration seems to be a general phenomenon.

With both pea seedlings (Tso *et al.*, 1956) and yeast (Chao, 1957) 80 *S* particles break down reversibly to 60 *S* and 40 *S*, and we have seen that in *E. coli* the 70 *S* component is made of one 30 *S* and one 50 *S*, the molecular weights of which are in the ratio of about 1 : 2·5. Viscosity measurements suggest greater asymmetry of 30 *S* than of 50 *S* and 70 *S*, and the electron micrographs (Hall & Slayter, 1959) show that 30 *S* is definitely asymmetric, while 50 *S* and 70 *S* appear nearly spherical. A simple model for the structure of 70 *S* would thus be a capped sphere or acorn shape.

The particles from *E. coli* seem to differ from those of other sources in at least three ways: (a) the molecular weight is lower ($2{\cdot}8 \times 10^6$ for 70 *S*, while values varying between 4 and $4{\cdot}5 \times 10^6$ have been reported for animal (Dintzis, Borsook & Vinograd, 1958), plant (Tso *et al.*, 1956), and yeast particles (Chao & Schachman, 1956)); (b) the percentage of RNA (60 to 65%) is higher than that reported for particles from other sources (Tso *et al.*, 1956; Chao & Schachman, 1956; Petermann & Hamilton, 1957; Dintzis *et al.*, 1958) with the exception of particles from rabbit appendix (Takata & Osawa, 1957); (c) the magnesium requirement for the integrity of the *E. coli* particles appears to be greater.

If we take the weight of one *E. coli* cell to be 10^{-12} gm, with 25% RNA in exponential cultures, there is $2{\cdot}5 \times 10^{-13}$ gm of RNA per cell. One 70 *S* particle contains $2{\cdot}74 \times 10^{-18}$ gm RNA. Thus there are about 90,000 particles in one bacterium. In the stationary phase, or upon incubation in phosphate buffer, this number decreases by a factor of 4 to 5 (Mendelsohn & Tissières, 1959), or to about 20,000 particles per cell.

We wish to thank Dr. J. T. Edsall for his interest and encouragement of this work, and Dr. D. M. Skinner and Miss C. Laumont for their assistance in some of these experiments. This work has been supported by grants from the U.S. National Science Foundation and an institutional grant from the American Cancer Society.

REFERENCES

Bolton, E. T., Hoyer, B. H. & Ritter, D. B. (1958). *Microsomal Particles and Protein Synthesis*, p. 18. New York: Pergamon Press.
Chao, F. C. (1957). *Arch. Biochem. Biophys.* **70**, 426.
Chao, F. C. & Schachman, H. K. (1956). *Arch. Biochem. Biophys.* **61**, 220.
Dintzis, H. M., Borsook, H. & Vinograd, T. (1958). *Microsomal Particles and Protein Synthesis*, p. 95. New York: Pergamon Press.
Dische, Z. (1953). *J. Biol. Chem.* **204**, 983.
Dische, Z. (1955). *The Nucleic Acids*, Vol. I, p. 287. New York: Academic Press.
Elson, D. (1958). *Biochem. biophys. Acta*, **27**, 216.
Fraenkel-Conrat, H. (1954). *Biochem. biophys. Acta*, **15**, 307.
Gornall, A. G., Bardawill, C. T. & David, M. M. (1949). *J. Biol. Chem.* **177**, 751.
Hall, C. E. & Slayter, H. S. (1959). *J. Mol. Biol.* **1**, in press.
Johnston, J. P. & Ogston, A. G. (1946). *Trans. Faraday Soc.* **42**, 789.
Keilin, D. & Harpley, C. H. (1941). *Biochem. J.* **35**, 688.
Lederberg, J. (1956). *Proc. Nat. Acad. Sci., Wash.* **42**, 574.
Littlefield, J. W. & Keller, E. B. (1956). *Fed. Proc.* **15**, 302.
Littlefield, J. W. & Keller, E. B. (1957). *J. Biol. Chem.* **224**, 13.
Littlefield, J. W., Keller, E. B., Gross, J. & Zamecnik, P. C. (1955). *J. Biol. Chem.* **217**, 111.
Luria, S. E., Delbruck, M. & Anderson, T. F. (1943). *J. Bact.* **46**, 57.
McIlwain, H. (1948). *J. Gen. Microbiol.* **2**, 288.
Mendelsohn, J. & Tissières, A. (1959). *Biochem. biophys. Acta*, in press.
Palade, G. (1955). *J. Biophys. Biochem. Cytol.* **1**, 59.
Palade, G. & Siekewitz, P. (1956*a*). *J. Biophys. Biochem. Cytol.* **2**, 171.
Palade, G. & Siekewitz, P. (1956*b*). *J. Biophys. Biochem. Cytol.* **2**, 671.

Petermann, M. L. & Hamilton, M. G. (1952). *Cancer Research*, **12**, 373.
Petermann, M. L. & Hamilton, M. G. (1957). *J. Biol. Chem.* **224**, 723.
Schachman, H. K., Pardee, A. B. & Stanier, R. Y. (1952). *Arch. Biochem. Biophys.* **38**, 245.
Scheraga, H. A. & Mandelkern, L. (1953). *J. Amer. Chem. Soc.* **75**, 179.
Schneider, W. C. (1945). *J. Biol. Chem.* **161**, 293.
Svedberg & Pedersen, K. O. (1940). *The Ultracentrifuge*, p. 5. Oxford: Clarendon Press.
Schweet, R., Lamfrom, H. & Allen, E. (1958). *Proc. Nat. Acad. Sci., Wash.* **44**, 1029.
Takata, K. & Osawa, S. (1957). *Biochem. biophys. Acta*, **24**, 207.
Tissières, A. & Watson, J. D. (1958). *Nature*, **182**, 778.
Tso, P. O. P., Bonner, J. & Vinograd, J. (1956). *J. Biophys. Biochem. Cytol.* **2**, 451.
Tso, P. O. P., Bonner, J. & Vinograd, J. (1958). *Biochem. biophys. Acta*, **30**, 570.

J. Mol. Biol. (1959) **1**, 234-236

High Resolution Electron Microscopy of Beet Yellows Virus Filaments

R. W. Horne

Electron Microscopy Group, Cavendish Laboratory, Cambridge, England

G. E. Russell and A. R. Trim

Plant Breeding Institute, Maris Lane, Trumpington, Cambridge, England

(*Received 2 June 1959*)

In preparations of sap removed from sugar beet infected with beet yellows virus, filaments have been concentrated in sufficient numbers to be studied in the electron microscope. Using the negative staining technique, the virus appears as a filamentous structure 10 mμ in diameter and one to several microns long. The filaments have a regular periodicity and a central hollow core. Small hollow particles 10 mμ in diameter, observed in infected sap, may be short pieces of filament.

The methods of preparation are discussed and dimensions compared with tobacco mosaic virus.

1. Introduction

Leyon (1951) reported the presence of long filamentous particles approximately 10 mμ in diameter in leaf sap from sugar beet infected with beet yellows virus (Beta Virus 4, Smith) and in serological precipitates from the reaction of specific antiserum to beet yellows virus with sap from infected beet. These reports have since been confirmed by several workers. Some have indicated that the filaments may not be the only specific antigenic particles associated with beet yellows virus infection (Nixon & Watson, 1951).

Nixon & Watson thought that the serological behaviour of sap from infected plants suggested the presence of an additional specific antigenic component which was present in a higher concentration than the filaments. The character of the serological precipitates suggested that this component was spherical and might resemble the spherical particles which are present in large numbers in healthy sugar beet sap. These workers thought that the filaments and antigenic spherical particles might be different forms of the virus. However, at that time there was no easy means of transmitting the virus mechanically and, therefore, no method of testing the infectivity of either component.

Brandes and Zimmer (1955) found that filaments from sugar beet (*Beta vulgaris*), *Tetragonia expansa*, *Tetragonia echinata*, *Chenopodium album* and *Mesembryanthemum crystallinum*, infected with sugar beet yellows virus, had a mean length of 1250 mμ, and Mundry (1958) separated filaments of different lengths from the sap of infected plants by centrifuging in a sucrose gradient. Testing infectivity by mechanical inoculation to several different hosts he found that the filaments of "normal" length (1250 mμ) were the infective component, and that the shorter filaments were not infective. There was no evidence that spherical particles were necessary for infection. On the basis of these results it can be assumed, as a working hypothesis, that the filaments are an infective form of the virus.

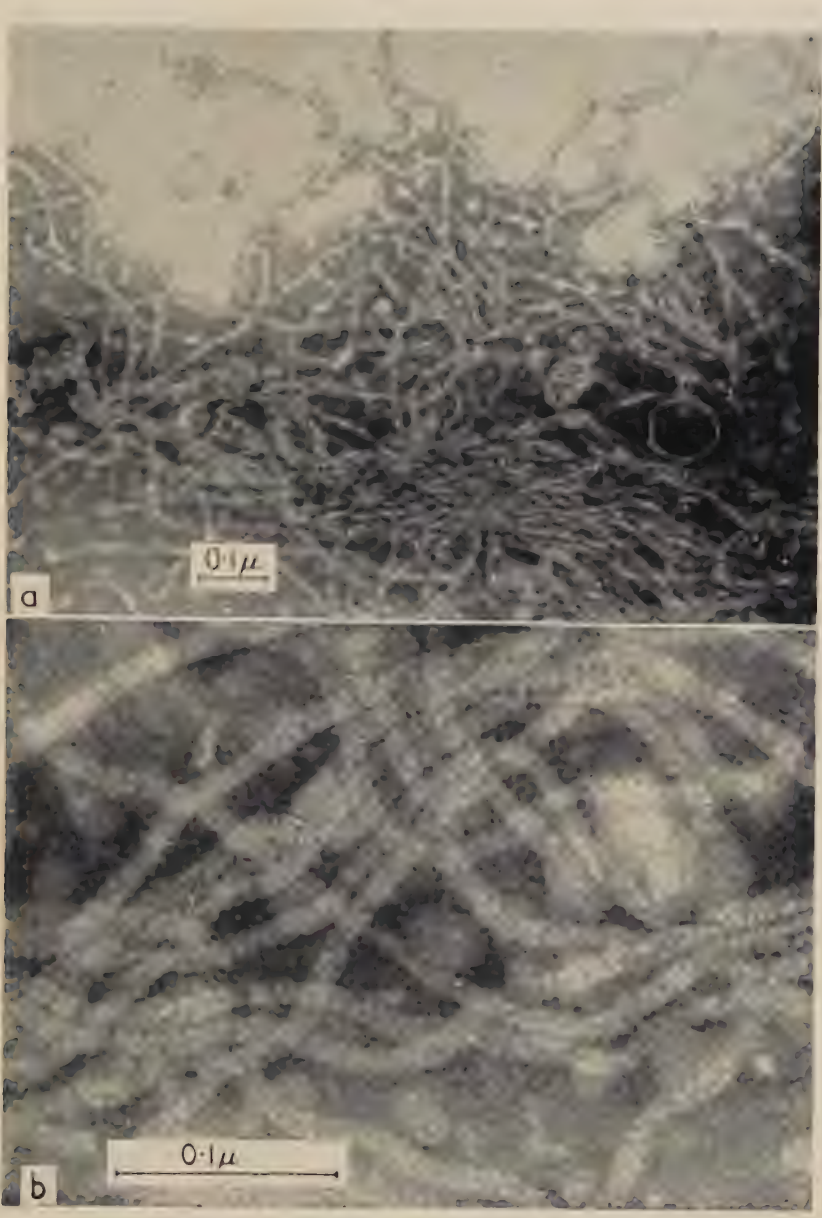

PLATE I. Beet yellows virus (phosphotungstate (PTA) preparations):

(a) Low magnification of droplet pattern showing filaments "embedded" in PTA. No staining of filaments is apparent.

(b) High magnification of similar area to (a) showing regular periodicity along the axis of the filaments.

[*To face page* 234.

PLATE II. Beet yellows virus (PTA preparations):

(a and b) Filaments showing periodic structure of 26 to 30 Å.

(c) Trypsin-treated preparation showing penetration of PTA along the central region of the filament revealing hollow centre 30 to 40 Å in diameter. Flexibility of the structure is shown by the loop.

PLATE III.

(a) Part of through-focal series of a mixed preparation of sugar beet yellows virus and tobacco mosiac virus.

(b) Area at the edge of droplet pattern showing periodic structure confined to filament.

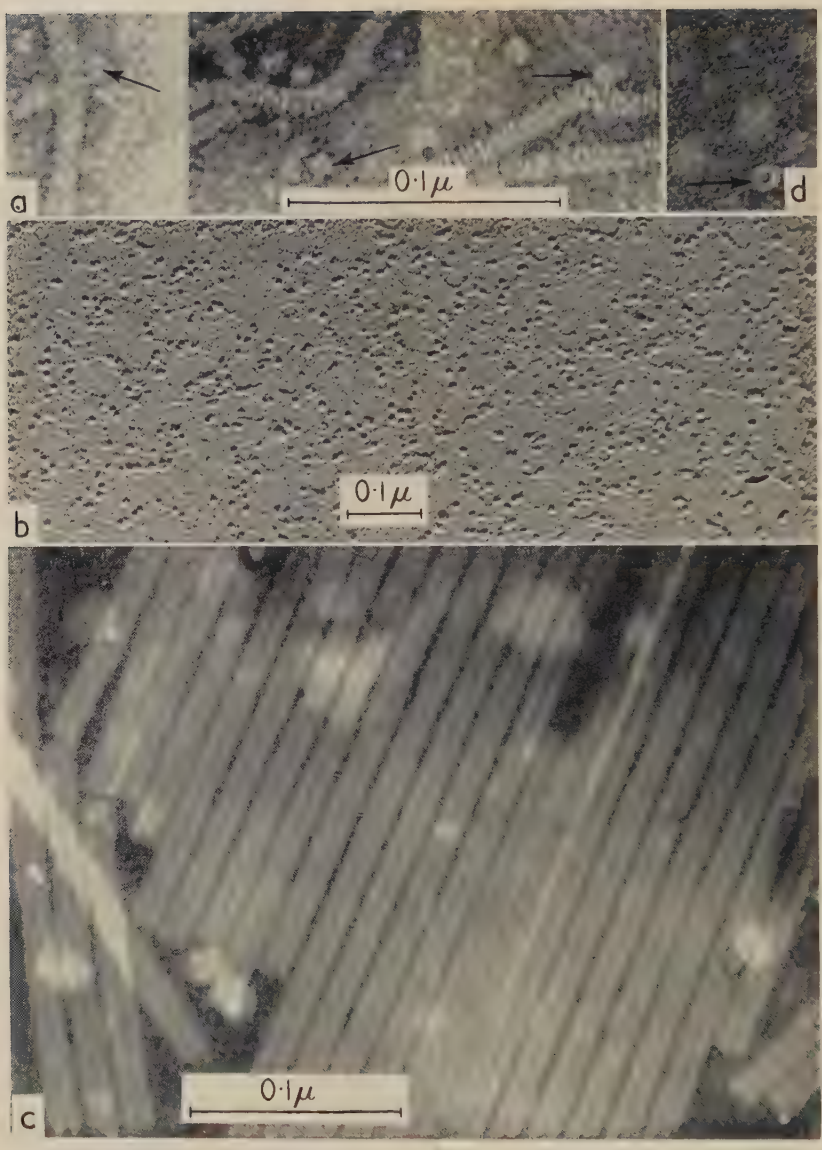

PLATE IV

(a) Beet yellows virus: PTA preparations showing "spheres" or " discs " with central hole and external diameter 10 mμ as in filaments.

(b) Shadowed preparation (from sugar beet infected with beet yellows virus) from supernatant liquid of sap centrifuged at 40,000 ***g*** showing "spherical" particles as seen in both healthy and infected plants.

(c) Tobacco mosiac virus "embedded" in PTA showing preservation of rods and hollow central region of 35 to 40 Å diameter.

(d) As (b) but using PTA method showing hollow structure of small "spherical" particle.

In this paper preliminary results of work on the preparation and structure of the filaments from plants infected with beet yellows virus will be reported and discussed. Comparisons will be made with the particles of tobacco mosaic virus.

2. Materials and Methods

Healthy sugar beet seedlings (variety Sharpes Kleinwanzleben, E), raised in an insect-proofed glasshouse, were inoculated with a strain of beet yellows virus which produces severe etch symptoms in sugar beet seedlings. Infection was carried out by placing five viruliferous *Myzus persicae* (Schulz) on each plant immediately after they had fed for 24 hr on leaves of sugar beet plants infected with sugar beet yellows virus. After a further feeding period of 24 hr on the test seedlings they were killed by fumigation and the plants were grown on in the greenhouse for a period of 4 to 5 weeks, during which time they developed vein-etch and yellowing symptoms. Leaves showing severe symptoms were minced, the sap squeezed out through muslin and clarified by centrifuging at 0°C for 10 min at 10,000 ***g*** and then for 10 min at 20,000 ***g***. The pellets were discarded and the final supernatant liquid was centrifuged at 0°C for 1 hr at 40,000 ***g*** in a Spinco Model L centrifuge. The pellet was re-suspended in 2 to 3 ml. of distilled water for examination in the electron microscope. Using the negative staining method of Brenner & Horne (1959) a freshly prepared 2% solution of phosphotungstic acid (PTA) was adjusted to pH 7·0 with N-KOH and 0·5 ml. added to 0·5 ml. of the pellet suspension in a Vaponefrin atomiser. The mixture was sprayed onto electron microscope supports covered with a carbon substrate. Specimens were examined in the Siemens Elmiskop electron microscope at instrumental magnifications of × 8,000 and × 40,000 using an illuminating beam diameter of 20 microns.

3. Results

Droplet patterns from sprayed PTA preparations of sugar beet yellows virus showed areas containing large numbers of filaments with a mean diameter of 10 mμ, and lengths ranging from one micron to several microns (Plate I(a)). Isolated filaments and highly concentrated aggregates were observed in the same droplet areas (Plate I(b)).

At very high magnifications individual filaments were observed to have a regular periodic structure along the axis (Plates II(a) and (b)). The mean distance measured between the small regular structures was about 26 to 30 Å and the width of the individual units approximately 20 Å (Plate III(a) and (b)). They appear to have a well defined, central, hollow core with a diameter of 30 to 40 Å. This is best shown in preparations treated with trypsin (0·01% aqueous solution of crystalline trypsin) for 5 min at room temperature and pH 7 before mixing with phosphotungstic acid (Plate II(c)).

In addition to long filaments, the preparation from infected plants contained small particles with a mean diameter of 10 mμ which corresponded in size to the "spherical" particles which are present in both healthy and infected sap (Plate IV(b)). Some of these were hollow (Plate IV(a)).

Plate IV(c) shows tobacco mosaic virus (*Nicotiana* virus 1, Smith) rods embedded in phosphotungstic acid with a well defined central hole 35 to 40 Å in diameter, as described by earlier workers (Franklin & Holmes, 1958; Huxley, 1956).

Examination of the supernatant liquids from saps obtained from both healthy and infected beet leaves after centrifuging at 40,000 ***g*** and using the shadow casting technique showed the presence of many "spherical" particles. Preparations using the negative staining technique suggested that a small proportion of these particles from plants infected with beet yellows virus were hollow (Plate IV(d)), with hole diameters and external diameters corresponding to the longer filamentous particles. A detailed study of the small particles of healthy and infected plants is in progress.

4. Discussion

It is important to compare the observed structure of beet yellows virus filaments with viruses of better known structure. The prediction from X-ray diffraction measurements that tobacco mosaic virus rods contain a hollow core 40 Å in diameter (Franklin & Holmes, 1958) has been confirmed by Huxley (1956) and later by Brenner & Horne (1959), using the negative staining method. The preservation of structure and infectivity during this procedure has been studied in detail using other viruses and it has been concluded that structures and dimensions of less than 20 Å can be clearly resolved, apparently without distortion, moreover the three-dimensional preservation of adenovirus (Horne, Brenner, Wildy & Waterson, 1959) and bacteriophage (Brenner & Horne, 1958) at the molecular level has been clearly demonstrated. The detailed dimensions of the beet yellows virus filaments are within these limits.

The beet virus resembles tobacco mosaic virus in having a central hole 30 to 40 Å in diameter. The postulated helical structure of tobacco mosaic virus cannot be seen in the electron micrographs. In view of these observations, evidence of periodic structures in air dried, shadowed or replicated specimens must be interpreted with caution (Matthews, Horne & Green, 1956). However, with beet yellows virus the structures observed in the electron microscope correspond best to a loose, hollow helix. It is less likely that the filaments consist of chains of disc-like structures. Plate III(a) shows part of a through-focal series where the helix is well defined. It is of interest that X-ray diffraction studies on potato X virus have suggested a periodic structure of 22 Å.

The small particles present in the supernatant liquids from the sap of sugar beet infected with beet yellows virus after centrifuging at 40,000 *g*, having a diameter of 10 mμ and a central hole, may be short pieces of the virus filaments and may account for the results of Nixon & Watson (1951).

This work has been done in connection with the programme of breeding for resistance to beet yellows virus in sugar beet at the Plant Breeding Institute, Cambridge, England. We are indebted to the Director, Dr. G. D. H. Bell, and Mr. G. K. G. Campbell for their help and encouragement.

We wish to thank Dr. S. Brenner and Dr. R. Markham for valuable discussion. Acknowledgement is also due to Mr. Boon of the Department of Biochemistry, Cambridge University, for technical assistance. The Siemens Elmiskop electron microscope was purchased with a generous grant from the Nuffield Foundation. One of us (R.W.H.) wishes to thank the Agricultural Research Council for financial aid.

REFERENCES

Brandes, J. & Zimmer, K. (1955). *Phytopath. Z.* **24**, 221.

Brenner, S. & Horne, R. W. (1958). *4th International Conference on Electron Microscopy.* Berlin, in press.

Brenner, S. & Horne, R. W. (1959). *Biochim. biophys. Acta*, **34**, 103.

Franklin, R. & Holmes, K. C. (1958). *Acta Cryst.* **11**, 213.

Horne, R. W., Brenner, S., Wildy, P. & Waterson, A. (1959). *J. Mol. Biol.* **1**, 84.

Huxley, H. E. (1956). *First Regional Conference on Electron Microscopy, Stockholm*, p. 266.

Leyon, H. (1951). *Ark. Kemi Min. Geol.* **3**, 105.

Matthews, R. E. F., Horne, R. W. & Green, E. M. (1956). *Nature*, **178**, 635.

Mundry, K. W. (1958). *Z. Naturf.* **136**, 19.

Nixon, H. L. & Watson, M. A. (1951). *Nature*, **168**, 523.

J. Mol. Biol. (1959) **1**, 237-239.

Nucleotide Composition of Ribonucleoprotein Particles from *Escherichia coli*

P. F. Spahr and A. Tissières

Biological Laboratories, Harvard University, Cambridge, Massachusetts, U.S.A.

(*Received 12 June 1959*)

The nucleotide composition of the four principal nucleotides is the same in the three different kinds of ribonucleoprotein particles from *E. Coli*, with sedimentation constants of 30 *S*, 50 *S* and 70 *S*.

1. Introduction

The ribonucleoprotein particles from *Escherichia coli* are formed of two subunits with sedimentation constants of 30 *S* and 50 *S* and molecular weights of $0{\cdot}7 \times 10^6$ and $1{\cdot}8 \times 10^6$. These two subunits join together in the presence of sufficient magnesium ions to yield a particle with a sedimentation coefficient of 70 *S* and a molecular weight of $2{\cdot}5 \times 10^6$. The three kinds of particles contain about 63% of RNA and 37% of protein (Tissières, Watson, Schlessinger & Hollingworth, 1959).

In this communication the nucleotide compositions of the ribonucleic acid (RNA) of the 30 *S*, 50 *S* and 70 *S* ribonucleoprotein particles are reported. This study has been limited to the determination of the ratios of the four principal nucleotides. The results show that, within the limits of error, the nucleotide composition of the three kinds of particles is approximately the same.

2. Material and Methods

The cultivation of *E. coli*, strain B, preparation of the cell free extracts, and the isolation of the 30 *S*, 50 *S* and 70 *S* ribonucleoprotein particles were carried out as previously described (Tissières *et al.*, 1959). RNA was prepared for hydrolysis by hot NaCl extraction followed by alcohol precipitation, according to Davidson & Smellie (1952). Ribonucleoprotein particles were also hydrolyzed to ascertain that the total nucleotide mixture obtained in this way had the same composition as that of RNA extracted with hot salt.

Samples of RNA (10 mg in 2 ml.) or particles (20 mg in 2 ml.) were hydrolyzed in 0·3 N-KOH at 37° C for 18 hr and treated with perchloric acid as described by Smith (1955). A small precipitate formed after hydrolysis of intact particles. It was removed by centrifugation, washed with 0·3 N-KOH, and the washings added to the supernatant. This precipitate did not give any reaction with orcinol (Dische, 1953) but reacted with the Folin phenol reagent (Lowry, Rosebrough, Farr & Randall, 1951), indicating that it was of protein nature.

Samples of hydrolysates containing 4 to 5 mg of nucleotide mixture were brought to pH 8·0 with 2 N-NaOH, diluted five times with water, and adsorbed on a column of Dowex CG-1 × 8, minus 400 mesh (California Corporation for Biochemical Research, 3625 Medford Street, Los Angeles, Calif.) according to Cohn (1950). The column was 1 cm in diameter and 18·5 cm in length. The nucleotides were eluted with formic acid, 10 ml. fractions collected, and their optical density (OD) determined at 260 mμ. The amount of nucleotide in each chromatographic peak was determined by integrating the values of the optical densities of the individual fractions, using the molar extinction coefficients given by Beaver, Holiday & Johnson (1955). The ratio OD_{280}/OD_{260} was calculated for each fraction of the nucleotide peaks.

3. Results

The nucleotide composition of RNA from the three kinds of particles, 30 *S*, 50 *S* and 70 *S*, is shown in Table 1. The values reprseent the mean of chromatographic analysis on four different preparations for each kind of particles. Of these, two were performed on hydrolysates from NaCl-extracted RNA, and two on particles hydrolyzed as such. The errors are expressed as average deviation from the mean. The recoveries from the columns, estimated by optical density measurements, were 100 ± 2%. Of this, in all cases 96% was accounted for by the four main nucleotides and the remaining 4% was distributed in three small chromatographic peaks which were not further characterized. In the fourth column of Table 1, the nucleotide composition is given for 70 *S* particles as calculated from the values for 30 *S* and 50 *S* particles (columns 1 and 2, Table 1). In this calculation the weight ratio of RNA in 30 *S* and 50 *S* particles was taken as 1 : 2·5 (Tissières *et al.*, 1959).

Table 1

Nucleotide composition of 30 *S*, 50 *S and* 70 *S ribonucleoprotein particles*

The values represent the mean of four chromatographic analyses. They are given as moles per 100 moles of the four principal nucleotides, thus not including the unidentified chromatographic peaks (4% of the total optical density).

The errors are expressed as average deviation from the mean.

	30 *S*	50 *S*	70 *S*	70 *S* values calculated from those of 30 *S* and 50 *S* (see text)
Adenylic acid	24·6 ± 0·6	25·6 ± 0·6	25·0 ± 0·5	25·2 ± 0·5
Guanylic acid	31·6 ± 0·7	31·4 ± 0·7	31·5 ± 0·6	31·5 ± 0·7
Cytidylic acid	22·8 ± 0·7	20·9 ± 0·5	22·1 ± 0·2	21·6 ± 0·6
Uridylic acid	21·0 ± 0·6	22·1 ± 0·6	21·4 ± 0·6	21·7 ± 0·6
Purines/pyrimidines	1·28	1·32	1·30	1·30
†6-Am/6-K	0·90	0·87	0·89	0·88
‡(A + U/G + C)	0·84	0·91	0'86	0·88

†6-Am = 6-amino nucleotides (adenylic and cytidylic acids).
6-K = 6-keto nucleotides (guanylic and uridylic acids).
‡A, G, C, U stand for adenylic, guanylic, cytidylic and uridylic acids respectively.

4. Discussion and Conclusion

The composition of the ribonucleic acid appears to be the same in the three different particles, with the possible exception of the cytidylic acid, which seems slightly lower in the 50 *S* than in the 30 *S* particles. This difference, which was found in all preparations, might be significant. Our values differ in some respects from those given by Pardee & Prestidge (1956) and Lombard & Chargaff (1957) for total *E. coli* RNA. The presence of soluble RNA in the preparations from whole cells may account for some of these differences.

We wish to thank Dr. J. T. Edsall for his interest and encouragement. This work has been supported by grants from the National Science Foundation (G-3230) and the United States Public Health Service (H-3169).

REFERENCES

Beaven, G. H., Holiday, E. R. & Johnson, E. A. (1955). *The Nucleic Acids*, Vol. I, ed. by E. Chargaff & J. N. Davidson, p. 493. New York: Academic Press.
Cohn, W. E. (1950). *J. Amer. Chem. Soc.* **72**, 1471.
Davidson, J. N. & Smellie, R. M. S. (1952). *Biochem. J.* **52**, 594.
Dische, Z. (1953). *J. Biol. Chem.* **204**, 983.
Lombard, A. & Chargaff, E. (1957). *Biochim. biophys. Acta*, **25**, 549.
Lowry, O. H., Rosebrough, N. J., Farr, A. L. & Randall, R. J. (1951). *J. Biol. Chem.* **193**, 265.
Pardee, A. B. & Prestidge, L. S. (1956). *J. Bact.* **71**, 677.
Smith, J. D. (1955). *The Nucleic Acids*, Vol. I, ed. by E. Chargaff & J. N. Davidson, p. 267. New York: Academic Press.
Tissières, A., Watson, J. D., Schlessinger, D. & Hollingworth, B. R. (1959). *J. Mol. Biol.* **1**, 221.

J. Mol. Biol. (1959) **1**, 240-259

Phosphorolyse et Configuration Macromoléculaire des Polyribonucléotides Biosynthétiques et des Acides Ribonucléiques

Marianne Grunberg-Manago †

Institut de Biologie Physico-Chimique, Service de Biochimie, 13 rue Pierre Curie, Paris 5e, France

(*Received 16 February 1959*, and in revised form *29 June 1959*)

Investigation of the phosphorolysis of polyribonucleotides by polynucleotide phosphorylase was undertaken in order to clarify the role *in vivo* of this enzyme which might catalyze the two following reactions:

(1) The synthesis of ribonucleic acid.

(2) The formation of nucleotides from cellular RNA.

Biosynthetic polynucleotides containing only one base unit are phosphorolyzed very readily in the presence of Mg and inorganic phosphate, as might be predicted from the apparent equilibrium of the reaction catalyzed by polynucleotide phosphorylase. The rates of phosphorolysis of poly A, U and C are about the same. A preparation of poly G was phosphorolyzed at about one quarter of the rate of the other polymers.

Polynucleotides containing four different bases, poly AGUC, are phosphorolyzed at about one third of the rate of the polymers containing one base unit such as poly A, poly U, or poly C. The rate is the same for the two AGUC polymers studied, one containing about three times more guanine than the other.

Several poly AU samples, containing different ratios of the two bases, were synthesized by polynucleotide phosphorylase, starting from different mixtures of ADP and UDP, and their phosphorolysis was studied. They are all phosphorolyzed more slowly than the homopolymers containing only adenine or uracil. The one containing the largest percentage of adenine was phosphorolyzed the most rapidly.

The rate of phosphorolysis of most of the RNA preparations is very slow. TYM RNA, highly polymerized yeast RNA, microsomal particle RNA, S-RNA and commercial yeast RNA are phosphorolyzed six to ten times more slowly than poly A. However, although the RNA preparations are phosphorolyzed slowly, most are completely degraded in the presence of an excess of enzyme. There are two exceptions: TMV RNA which is phosphorolyzed as rapidly as poly A at 37 to 40°C and S-RNA which is only degraded to 40% of completion. The behaviour of the soluble RNA is peculiar to several S-RNA preparations.

The fact that commercial RNA preparations containing a large percentage of chains ending in 3′-PO_4 are phosphorolyzed to completion, indicates that these chains can be degraded by polynucleotide phosphorylase. Therefore, the results found with small oligonucleotides, which indicated that these compounds are not phosphorolyzed if they are terminated by a phosphate in the 3′ position, do not appear to be applicable to the larger polynucleotide chain. The slow rate of phosphorolysis of most of the RNA preparations cannot be explained by the presence of a terminal phosphate in the 3′ position.

† Une partie de ce travail a été effectuée dans les laboratoires du Dr. P. Doty, Department of Chemistry, Harvard University, Cambridge (Mass.), grâce à une subvention U.S. Public Health, Service C 2170, et du Dr. L. A. Heppel, National Institute of Arthritis and Metabolic Diseases, Bethesda (Md) où l'auteur a travaillé en tant que " Visiting Scientist."

The length of the polymer chain does not explain the phosphorolysis rate either, since small oligonucleotides are phosphorolyzed as rapidly as the polymers.

The fact that poly A and poly U can interact in aqueous solution to form two different stable helical complexes, depending on the relative concentration of the two polyacids, makes it possible to further evaluate the effect of the structure of the polynucleotides on their rate of degradation. It has indeed been found that the rate of phosphorolysis of the mixture of poly A and poly U depends markedly on the proportions of these two polyacids. When poly A and poly U are in equimolecular amount forming a two-stranded helix structure, their rate of phosphorolysis is about one third of that of poly A or poly U and decreases rapidly. The mixture of poly A and poly U in proportion 3 : 1 (2/3 of the poly A is not in a complex under these conditions) is phosphorolyzed at about the same rate as poly A, and mostly ADP is liberated. This suggests that only the fraction of poly A not involved in the complex is degraded. The mixture containing an excess of poly U (a triple-stranded helix is formed between the two polyacids under these conditions) is degraded very slowly, and only UDP is liberated, probably from the poly U not involved in the complex.

It appears therefore, that polynucleotide phosphorylase rapidly attacks polymers having a single chain structure, but reacts at a slow rate with polymers which have a multistranded configuration. This is confirmed by the effect of salt on the rate of phosphorolysis of poly I. This polymer exists as a single chain in dilute salt, and is then phosphorolyzed as well as poly A. But it forms a triple-stranded helix in the presence of high salt, and is then phosphorolyzed very poorly, while the rate of phosphorolysis of poly A or poly U is not decreased by salt, their molecular structure not being affected to a very great extent.

The slow rate of phosphorolysis of some biosynthetic polynucleotides and of most of the RNA preparations can therefore be explained, at least in part, by their molecular configuration (assuming that they exist as complexes or contain helical regions resulting from the formation of internal molecular hydrogen bonds). The direct evidence that this is really the case was found by the studies of the effect of the temperature on the rate of phosphorolysis of several RNA and poly AGUC samples. An increase in the temperature produces optical density changes of the RNA preparations, which can be attributed to the cleavage of the internal hydrogen bond. From the optical density changes it was suggested that, at any given temperature, different RNA samples exhibit different degrees of hydrogen bonding. Since the latter would interfere with their rate of phosphorolysis, the rates were measured at 40°C and 25°C for a number of different samples. The increase in optical density at the two temperatures was also measured, and the results indicate that the relative increase in the rate of phosphorolysis of polynucleotides is linearly related to the increase in optical density. On raising the temperature from 25°C to 40°C the rate of phosphorolysis of poly U, which does not have any internal hydrogen bonding, is only doubled; on the other hand, the phosphorolysis of TMV RNA is stimulated tenfold and 59% of its hydrogen bonds are split. The microsomal particle RNA and poly AGUC, which have only 17% and 23% respectively of the hydrogen bonds cleaved at 40°C, have their rate of phosphorolysis stimulated 4·5 and 5 fold.

These results explain why at 40°C the TMV RNA is phosphorolyzed as well as poly A or poly U: most of its internal hydrogen bonds are cleaved, in contrast to the other RNA preparations tested. Under the conditions where the hydrogen bonds of the TMV RNA are preserved (25°C or 40°C in presence of high salt concentration), the TMV RNA is phosphorolyzed at a rate comparable to the other RNA, and more slowly than poly A or poly U.

These results show clearly that the phosphorolysis of polyribonucleotides and RNA does not depend only on the relative concentrations of the substrate determining the equilibrium of the reaction, but also on their molecular configuration, and particularly on the degree of hydrogen bonding between different nucleotides. It is then conceivable that RNA in the living cell could escape from being phosphorolyzed even in the presence of a high amount of orthophosphate.

1. Introduction

Le rôle physiologique de la polynucléotide phosphorylase n'est pas encore éclairci. Cet enzyme qui est très actif et largement répandu chez les bactéries (Brummond, Staehelin & Ochoa, 1957) peut catalyser *in vitro* (Grunberg-Manago, Ortiz & Ochoa, 1956):

(1) la synthèse des polyribonucléotides ;

(2) la formation de nucléotides par phosphorolyse des polyribonucléotides.

On est ainsi amené à concevoir que la polynucléotide phosphorylase pourrait catalyser *in vivo* deux réactions différentes, toutes deux importantes du point de vue biologique:

(1) la synthèse des acides ribonucléiques ;

(2) la formation à partir des acides ribonucléiques cellulaires de nucléotides pouvant servir de co-facteurs dans les réactions essentielles du métabolisme.

Il a été montré (Singer, Hilmoe & Grunberg-Manago, résultats non publiés) que la phosphorolyse procède par étapes successives, en détachant du polyribonucléotide un nucléotide après l'autre et fournissant ainsi des nucléosides diphosphates. La phosphorolyse est donc au sens strict l'inverse de la polymérisation (Singer, Heppel & Hilmoe, 1956).

Nous n'avons pas encore de données précises sur la constante d'équilibre de la réaction. Comme pour la polysaccharide phosphorylase, la concentration du polymère ne semble pas influer sur cet équilibre. Dans nos conditions expérimentales, quel que soit le polymère synthétisé, la réaction catalysée par la polynucléotide phosphorylase se stabilise lorsque le rapport de concentration: mononucléotide restant/Pm† est d'environ 0·6 (Grunberg-Manago *et al.*, 1956). Ceci suggère que l'acide ribonucléique pourrait être facilement phosphorolysé en présence d'un excès de phosphate minéral, conditions probablement réalisées *in vivo* dans la cellule, à cette réserve près que ces conditions peuvent être différentes au lieu de synthèse.

Il a déjà été montré que la phosphorolyse n'est pas spécifique (Grunberg-Manago, Ortiz & Ochoa, 1955): tous les polynucléotides biosynthétiques, de même que les acides ribonucléiques, sont phosphorolysés en libérant les diphosphates. Cependant les vitesses de phosphorolyse sont très différentes et les expériences rapportées dans le présent mémoire montreront qu'en fait la plupart des préparations d'acide ribonucléique sont phosphorolysées très lentement, ce qui indique que d'autres facteurs

† *Abréviations:* adénine, uracile, cytosine, guanine, hypoxanthine: A, U, C, G, I.
5′-diphosphates (pyrophosphates d'adénosine, inosine, guanosine, uridine et cytidine): ADP, IDP, GDP, UDP, CDP
5′-monophosphates des mêmes nucleosides: AMP, IMP, GMP, UMP, CMP
3′-monophosphates correspondants: 3′AMP, etc . . .
5′-triphosphates des mêmes nucléosides: ATP, ITP, GTP, UTP, CTP
TRIS: tri(hydroxymethyl)aminométhane
EDTA: acide éthylènediamine tétraacétique
Pm: orthophosphate
coups/min: coups par minute
ApApApUp: tétranucléotide contenant 3 adénines, 1 uracile, et terminé par un P estérifié au carbone 3′
ApApAp: triadénylate terminé par un PO_4 estérifié au carbone 3′ du ribose
pApApA: triadénylate terminé par un PO_4 estérifié au carbone 5′ du ribose
ARN: acide ribonucléique
TMV: virus de la mosaïque du tabac
TYM: virus de la mosaïque jaune du navet
S-ARN: ARN soluble (non lié aux particules)
Poly: est utilisé pour indiquer un homo- ou un copolymère de(s) nucléotide(s) de la (ou les) base(s) indiquée(s)
PM: poids moléculaire.
S: ct de sédimentation.

que l'équilibre de la réaction peuvent intervenir pour empêcher la phosphorolyse. Nous serons amenés ainsi à envisager l'importance de la configuration macromoléculaire des polyribonucléotides pour leur résistance à la dégradation enzymatique. Ainsi, certaines configurations des polyribonucléotides leur permettent de résister à la phosphorolyse, même en présence d'un excès de phosphore minéral. D'autre part, on verra que l'étude de la vitesse de phosphorolyse des acides ribonucléiques peut nous apporter des indications quant à leur structure macromoléculaire, structure sur laquelle nous ne possédons jusqu'ici que peu de renseignements.

2. Partie Experimentale

(a) *Phosphorolyse des homopolymères*

Les polymères biosynthétiques formés seulement d'une seule base sont phosphorolysés très rapidement en présence de Mg^{++} et d'un excès de phosphate minéral ainsi que le laissait prévoir la stoechiométrie de la réaction (Grunberg-Manago *et al.*, 1956).

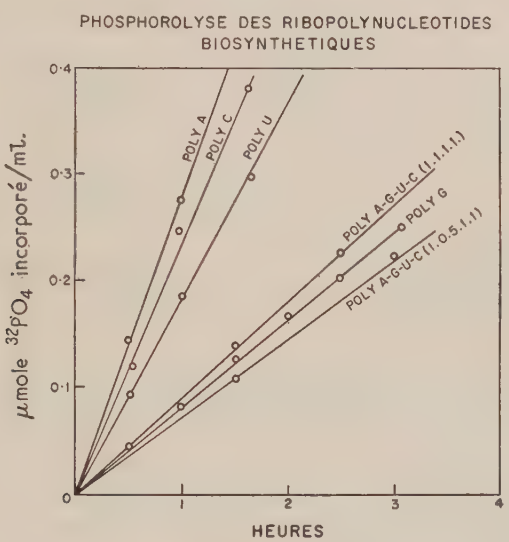

FIG. 1. Le mélange d'incubation contient: 0·3 µmoles $MgCl_2$, 0·89 µmoles tampon $^{32}PO_4$ pH 7·4 (activité spécifique = 330 000 coups/min par µmoles), 0·1 mg de polymère et 3·9 µg de polynucléotide phosphorylase de *E. coli* d'activité spécifique $\simeq$ 20–22 dans un volume total de 0·1 ml. Incubation à 40°C. Les polymères utilisés étaient les suivants: poly A_1, poly U_3, poly C, poly $AGUC_1$ et $AGUC_3$. Les détails sur les polymères et le test sont décrits dans la section Méthodes.

La vitesse de phosphorolyse dépend de la concentration des polymères, mais dans toutes les expériences rapportées dans ce mémoire les polynucléotides sont ajoutés en quantité saturante. Leur concentration est de 2×10^{-3} M.

Les courbes de la Fig. 1 montrent que la vitesse de phosphorolyse des poly A, U et C est environ la même. Elle varie d'ailleurs d'un échantillon à l'autre de ces polynucléotides, mais reste en général grande†. La vitesse de phosphorolyse d'une

† Il faut noter cependant que certains échantillons de poly A préparés à l'aide d'enzymes de faible activité spécifique contaminés peut-être par des nucléases, ou qui ont pu être partiellement dégradés en cours de manipulation comme le poly A_6, montrent une vitesse de phosphorolyse faible. Il est possible que les échantillons dégradés soient terminés par un PO_4 estérifié au carbone 3′ du ribose, ce qui, comme nous le verrons par la suite, peut influer sur la vitesse de phosphorolyse. D'autre part, nous avons observé que 2 échantillons de poly A_7 lyophylisés dans l'eau distillée, puis mis en suspension dans le tampon citrate salin, avaient une vitesse de phosphorolyse moitié de celle de l'échantillon non lyophylisé. L'effet de la lyophylisation sur le poly A n'est pas claire.

préparation d'acide polyguanylique obtenue en ajoutant biosynthétiquement des unités d'acide guanylique sur un triadénylate servant d'amorceur (Singer, 1957; Singer, Heppel, Hilmoe, Ochoa & Mii, sous presse), est environ 4 fois plus faible que celle des trois autres polymères. Cependant cette vitesse reste relativement grande et il faut noter qu'on n'observe aucune phase de latence. La phosphorolyse du poly G n'exige donc aucun amorceur au contraire de sa formation qui requiert la présence d'un oligonucléotide. Ceci est en accord avec ce que l'on sait du mécanisme d'action de la polynucléotide phosphorylase. La phosphorolyse observée est bien celle de

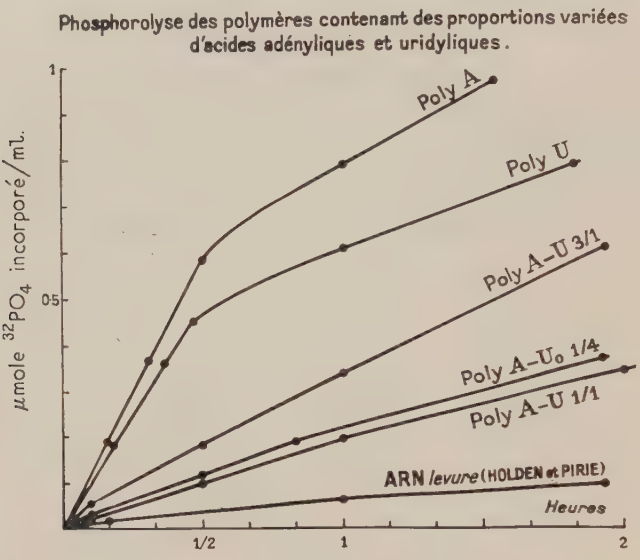

FIG. 2. Le mélange d'incubation contient: 7 µmoles $MgCl_2$, 50 µmoles tampon Tris pH 7·45, 8 µmoles tampon $^{32}PO_4$ pH 7·4 (activité spécifique = 68 000), ≃ 1·2 µmoles de polymère, 69 µg de polynucléotide phosphorylase *d'Azotobacter vinelandii* d'activité spécifique = 14·8 dans un volume final de 1 ml.

Incubation à 30°C. Des prises de 0·1 ml. sont effectuées à des intervalles de temps déterminés pour le test d'incorporation de $^{32}PO_4$ et pour l'élution des nucléotides.

Les polymères utilisés étaient les suivants: poly A_2, poly U_2. Les détails sur les polymères et le test sont décrits dans la section Méthodes.

l'acide polyguanylique et non du triadénylate contenu dans la molécule: la phosphorolyse procède par étapes (Singer, Hilmoe & Grunberg-Manago, résultats non publiés) et commence par le bout de la chaine contenant le poly G; ainsi en présence d'une quantité minimum d'enzyme, seul le diphosphate de guanosine est libéré.

Les expériences qui viennent d'être décrites ont été faites en milieu salin minimum, en présence de 3×10^{-3} M-$MgCl_2$, alors que la quantité optimum de $MgCl_2$ pour la phosphorolyse des poly U et poly A est de 10^{-2} M (la vitesse de phosphorolyse de chacun de ces polymères est alors doublée). Le milieu salin minimum a été choisi pour éviter l'aggrégation de certains polyribonucléotides (poly I, ARN de TMV), ce qui a une répercussion sur leur vitesse de phosphorolyse comme on le verra par la suite.

Il est possible qu'il soit en rapport avec la faculté qu'a le poly A de former dans l'eau distillée un complexe qui serait stabilisé par la lyophylisation. Même remis à pH neutre, il subsisterait des aggrégats qui, comme nous le verrons par la suite, sont phosphorolysés moins rapidement. Ceci est appuyé par le fait qu'un tel effet de la lyophylisation n'a pas été observé sur le poly U qui ne forme pas de complexe de ce genre. Cependant, le chauffage à 80°C pendant 1 heure des échantillons de poly A_7 lyophylisés ne ramène pas les vitesses de phosphorolyse à leurs valeurs avant la lyophylisation.

(b) *Phosphorolyse des copolymères*

Il avait déjà été noté (Grunberg-Manago *et al.*, 1955) que les copolymères qui contiennent diverses bases dans une même chaine sont phosphorolysés à des vitesses plus faibles que les polymères à une unité de base. Nous avons entrepris ici une étude plus détaillée des vitesses de phosphorolyse des différents polymères.

Les polynucléotides contenant les 4 bases, adénine, guanine, uracile et cytosine (poly AGUC), sont phosphorolysés à une vitesse d'environ 1/3 de celle des poly A, U ou C et à une vitesse comparable à celle de l'échantillon de poly G (Fig. 1). Les deux polymères AGUC 1 et 3, l'un 3 fois plus riche en guanine que l'autre (voir Méthodes), sont phosphorolysés à la même vitesse. La Fig. 2 montre que le polymère contenant seulement les 2 bases, adénine et uracile, en proportion équimoléculaire (poly AU 1/1) est phosphorolysé plus lentement que les poly A ou poly U et à la même vitesse que les polymères AGUC.

Tableau 1

Influence de la concentration des nucléosides diphosphates sur la composition des polynucléotides

Le mélange d'incubation contient: 100 μmoles de tampon Tris pH 8·1, 10 μmoles $MgCl_2$, 124 μg de polynucléotide phosphorylase *d'Azotobacter vinelandii* d'activité spécifique = 14·8, dans un volume final de 1 ml.

Incubation de 23 à 36 heures à 30°C. Les détails sur l'hydrolyse des polymères et le dosage des nucléotides sont donnés dans la section Méthodes.

	μmoles de nucléotides par ml. dans le mélange d'incubation			μmoles de nucléotides élués après hydrolyse alcaline de A-U			
Exp.	ArPP	UrPP	$\frac{\text{ArPP}}{\text{UrPP}}$	μmoles de poly AU hydrolysé	ArP	UrP	$\frac{\text{ArP}}{\text{UrP}}$
1	21·2	64	$\frac{1}{3}$	2 2	0·334 0·32	1·55 1·54	$\frac{1}{4·7}$
2	21	65	$\frac{1}{3·1}$	2·2 1·3	0·315 0·225	1·36 0·96	$\frac{1}{4·3}$
3	41	43	$\frac{1}{1·05}$	0·98 0·98	0·37 0·35	0·38 0·33	$\frac{1}{1}$
4	61	22	$\frac{2·8}{1}$	1·75 1·75	1 0·89	0·32 0·27	$\frac{3·2}{1}$

La correction a été faite pour les impuretés présentes dans les échantillons de nucléosides diphosphates utilisés. L'ADP contenait 2 % d'ATP et d'AMP, l'UDP contenait 5 % d'UMP.

$\Sigma 260$ pour l'AMP_3 = 13·9 à pH acide

$\Sigma 262$ „ UMP_3 = 9·9 „

La question se pose de savoir pourquoi la vitesse de phosphorolyse d'un polymère contenant les 2 bases, adénine et uracile, est bien inférieure à celle de chacun des polymères A et U pris séparément. Pour avoir une idée plus nette de ce phénomène, nous avons synthétisé des polymères contenant les 2 bases en différentes proportions et étudié leur vitesse de phosphorolyse. La synthèse des divers polymères AU a été

faite à partir de mélanges d'adénosine et d'uridine diphosphates en proportions variées. Chaque nucléotide est employé en quantité inférieure à celle qui est nécessaire pour saturer l'enzyme.

Le tableau 1 montre que la composition en nucléotides des polymères † dépend étroitement des concentrations relatives initiales des nucléosides diphosphates à partir desquels ils sont synthétisés. La proportion de l'acide adénylique par rapport à l'acide uridylique est pratiquement la même que celle des nucléosides diphosphates de départ dans le cas des polymères AU synthétisés à partir des mélanges d'ADP et d'UDP en proportion 1/1 ou 3/1. Il faut remarquer qu'elle s'en écarte légèrement lorsque le mélange contient 3 fois plus d'uridine que d'adénosine diphosphate: le polymère AU obtenu contient alors 4 et non pas 3 fois plus d'acide uridylique. Cependant, même dans ce cas, la proportion des acides uridylique et adénylique dans le polynucléotide est voisine des concentrations relatives des nucléosides diphosphates utilisés pour leur synthèse.

Nous avons ainsi à notre disposition un moyen de synthétiser des polynucléotides AU de composition voulue. Il faut remarquer que dans le cas de la synthèse des polymères AGUC, la proportion des bases du polymère dépend également de celle des diphosphates, mais s'écarte de leur concentration initiale relative (voir Méthodes, composition des poly AGUC 1 et 3 synthétisés à partir de deux mélanges différents de nucléosides diphosphates).

La Fig. 2 montre les vitesses de phosphorolyse de différents polymères AU comparées à celles des poly A, U et d'un ARN. On voit que les 3 polymères AU sont phosphorolysés plus lentement que les poly A ou U, le polymère contenant un excès d'acide adénylique étant phosphorolysé le plus rapidement des trois. La proportion des nucléotides libérés au bout d'une heure s'écarte peu de celle des nucléotides du polymère (Tabl. 2).

TABLEAU 2

Le mélange d'incubation contient: 7 μmoles $MgCl_2$, 50 μmoles tampon Tris pH 7·45, 8 μmoles tampon $^{32}PO_4$ pH 7·4 (activité spécifique = 68 000), $\approx$ 1·2 μmoles de polymère, ou lorsqu'on ajoute 2 polymères différents 0·6 μmoles de chaque, 69 μg de polynucléotide phosphorylase *d'Azotobacter vinelandii* SA = 14·8 dans un volume final de 1 ml.

Incubation à 30°C. Des prises de 0·1 ml. sont effectuées à des intervalles de temps déterminés pour le test d'incorporation de $^{32}PO_4$ et pour l'élution des nucléotides. Les polymères utilisés étaient les suivants: poly A_2, poly U_2. Les détails sur les polymères et le test sont décrits dans la section Méthodes. Les résultats sont exprimés en μmoles.

	Polynucléotides ajoutés	PO_4 incorporé	ADP élué	UDP élué	$\frac{ADP}{UDP}$
Exp. 1	A (1·22)	0·76	0·76	—	—
	U (0·8)	0·53	—	0·44	—
	AU 1:1 (1·23)	0·145	0·06	0·09	1:1·5
	AU 3:1 (1·25)	0·34	0·27	0·07	4:1
	AU 1:4 (1·2)	0·26	0·05	0·23	1:4
Exp. 2	A (1·22)	0·8	0·76	—	—
	U (0·8)	0·65	—	0·54	—
	A + U (0·61 + 0·58)	0·33	0·27	0·06	4·5:1
	A + U (0·9 + 0·29)	0·75	0·74	0·03	25:1
	A + U (0·3 + 0·98)	0·08	0	0·06	—

† Tous ces polymères ont été synthétisés avec la même fraction de polynucléotide phosphorylase.

(c) *Phosphorolyse des préparations d'acides ribonucléiques*

La vitesse de phosphorolyse de la plupart des préparations d'acide ribonucléique naturel est faible, exception faite, comme il a déjà été montré par Ochoa (1957), de l'ARN du virus de la mosaïque du tabac qui dans nos conditions expérimentales est phosphorolysé aussi rapidement que le poly A (Fig. 3). L'ARN du virus de la mosaïque

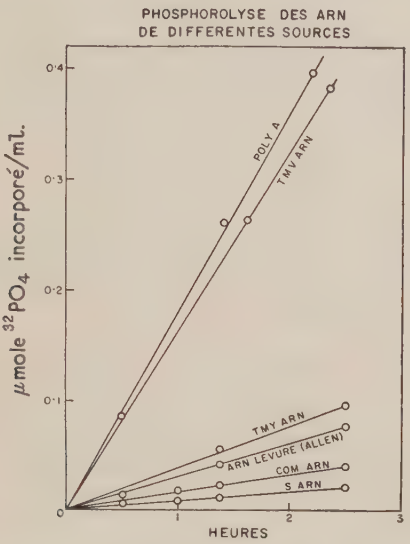

FIG. 3. Le mélange d'incubation contient: 0·3 μmoles $MgCl_2$, 0·78 μmoles tampon $^{32}PO_4$ pH 7·4 (activité spécifique = 320 000 coups/min par μmole), 0·1 mg de ribonucléotides ou 0·2 μmoles S-ARN, 3·9 μg de polynucléotide phosphorylase de *E. Coli* d'activité spécifique ≈ 20 à 22 dans un volume total de 0·1 ml.

Incubation à 37°C. Les polymères utilisés étaient les suivants: poly A_1, TMV ARN_1, S-ARN_1. Les détails sur lespolymères et le test sont décrits dans la section Méthodes.

jaune du navet et l'ARN hautement polymérisé préparé à partir de la levure selon la methode de Crestfield, Smith & Allen (1955), sont phosphorolysés 5 à 6 fois plus lentement que le poly A. Les autres échantillons d'ARN testés sont phosphorolysés à la même vitesse que l'ARN commercial de levure, 10 fois plus lentement environ que le poly A (ARN des particules de microsomes PM 1 000 000, ARN de levure préparé selon la méthode de Holden & Pirie (1955)). Il avait déjà été noté que d'autres préparations d'acide ribonucléique étaient phosphorolysés également très lentement (Grunberg-Manago *et al.*, 1955).

Enfin, deux échantillons d'acide ribonucléique soluble, S-ARN (Hoagland, Zamecnik & Stephenson, 1957) 1 et 2 sont phosphorolysés également très lentement, 1/10ème à 1/20ème de la vitesse du poly A.

3. Facteurs Responsables de la Vitesse de Phosphorolyse des Différents Polyribonucléotides

Comment expliquer la vitesse faible de phosphorolyse des copolymères et de la plupart des préparations d'acide ribonucléique? Plusieurs facteurs peuvent *a priori* déterminer la vitesse de phosphorolyse des polynucléotides.

(a) *Influence de la nature de la base sur la vitesse maximum de la réaction (Vm)*

A concentration saturante, la nature de la base, exception faite du poly G, n'influe pas d'une manière appréciable sur la vitesse de phosphorolyse des homopolymères, de même qu'elle n'influe pas sur la vitesse de polymérisation (Grunberg-Manago *et al.*, 1956). La vitesse de formation du poly G est beaucoup plus faible, mais le mécanisme de polymérisation du poly G n'est pas encore éclairci et il est probable que cette faible vitesse n'est pas simplement la conséquence de la diminution de la vitesse maximum de la réaction, cette vitesse dans la réaction d'échange orthophosphate P minéral avec le nucléoside diphosphate étant sensiblement la même avec le GDP qu'avec les autres diphosphates (Singer, Hilmoe & Grunberg-Manago, résultats non publiés). Il en est probablement de même dans le cas du polymère AGUC dont la vitesse de formation dépend de son contenu en guanine.

La vitesse de formation du copolymère AU 1/1 n'est que légèrement plus faible que celle des poly A et U (d'environ 25%) et il est peu probable que la valeur de la vitesse maximum de la réaction enzymatique suffise à elle seule à expliquer la faible vitesse de phosphorolyse des différents polymères AU.

(b) *Longueur de la chaine*

Il semble improbable que ce soit la longueur de la chaine de la préparation qui intervienne. Singer (1958) a déjà noté que les vitesses de phosphorolyse des oligonucléotides et des polynucléotides sont comparables. Effectivement, les hauts polymères de poly A de poids moléculaire aux environs de 800 000 et les oligonucléotides composés de 3 ou 4 unités d'acide adénylique sont phosphorolysés à une vitesse comparable s'ils sont en quantité suffisante pour saturer l'enzyme (Tabl. 3). D'autre part, l'ARN

Tableau 3

Phosphorolyse du poly A et des oligonucléotides

Le mélange d'incubation contient: 4 μmoles Tris pH 8·1, 0·4 μmoles $MgCl_2$, 2·4 μmoles $NaK^{32}PO_4$pH 7·2 (activité spécifique = 236 000 coups/min par μmole), le substrat comme indiqué dans le tableau et 2·4 μg de polynucléotide phosphorylase de *E. Coli* d'activité spécifique 20 à 22 dans un volume total de 0·1 ml.

Incubation 1 heure à 37°C.

Substances ajoutées μmoles adénine/ml.		$^{32}PO_4$ incorporé μmoles/ml.
poly A_1	(1·8)	0·58
poly A_7 lyophylisé	(1·9)	1·04
pApApA	(2·84)	0·5
pApApApA	(3·3)	1·4

des particules de microsomes et le poly A_7, dont les poids moléculaires sont comparables (aux alentours de 1 000 000) ont une vitesse de phosphorolyse très différente. Enfin, l'ARN des particules de microsomes chauffé 10 min à 85°C de PM = 100 000 est phosphorolysé à la même vitesse que l'ARN non chauffé à poids moléculaire aux environs de 1 000 000.

(c) *Position du radical PO_4 en fin de chaine*

Les polynucléotides biosynthétiques sont tous terminés par un radical PO_4 en 5′, mais il n'en est pas de même pour les préparations d'ARN, aussi l'un des facteurs qui

peuvent intervenir dans la vitesse de phosphorolyse des ARN peut-il être la position du radical PO_4 en fin de chaine. Singer (1958) a trouvé que les oligonucléotides terminés par un PO_4 estérifié au carbone 3′ du ribose ne sont pas phosphorolysés contrairement aux oligonucléotides terminés par un PO_4 en 5′ ou ne possédant aucun PO_4 en bout de chaine. Singer et coll. (résultats non publiés) ont montré que, de plus, les oligonucléotides terminés par un PO_4 en 3′ inhibent la phosphorolyse des chaines plus courtes terminées par un PO_4 en 5′. C'est ainsi que les tétranucléotides $3'PO_4$ inhibent de 70% la phosphorolyse des trinucléotides $5'PO_4$ mais seulement de 8% celle des tétranucléotides 5′. Le " core " qui est terminé par un PO_4 en 3′ n'est pas phosphorolysé et inhibe également de 70% la phosphorolyse des trinucléotides $5'PO_4$. Son pouvoir inhibiteur est moindre sur les tétranucléotides. Le pouvoir inhibiteur des chaines $3'PO_4$ n'est donc pas très grand. On pouvait néanmoins supposer que si la préparation d'acide ribonucléique contient de nombreuses chaines en $3'PO_4$ et quelques chaines plus courtes en 5′, seules ces dernières seraient phosphorolysées et avec une vitesse plus faible puisque des chaines en 3′ sont présentes, et la phosphorolyse ne serait pas complète.

Nos connaissances sur la question des groupements terminaux des acides ribonucléiques sont encore très sommaires: Fraenkel-Conrat (Communication au Colloque sur la spécificité dans la biogénèse des protéines, Louvain, 1959) a montré que l'ARN du TMV est terminé par un radical PO_4 en 3′. Markham & Smith (1952) ont trouvé que les ARN du commerce sont composés pour une grande part de chaines relativement courtes (15 à 20 nucléotides) terminés par un PO_4 en 3′, ce qui est en accord avec le fait que durant la préparation commerciale il peut y avoir hydrolyse chimique partielle avec libération de groupes $3'PO_4$.

Tableau 4

Le mélange d'incubation contient: 0·3 μmoles $MgCl_2$, 0·78 μmoles tampon $^{32}PO_4$ pH 7·4 (activité spécifique = 162 000 coups/min par μmole), le polymère ou l'ARN (exprimé en μmoles de P organique) et 39 μg de polynucléotide phosphorylase de *E. coli* d'activité spécifique = 20 à 22 dans un volume total de 0·1 ml.

Incubation à 37°C. Des prises de 0·04 ml. sont effectuées à des intervalles de temps déterminés. Les polymères utilisés étient les suivants: poly A_1, S-ARN, poly $AGUC_2$. Les détails sur les polymères et le test sont décrits dans la section Méthodes.

Degré de phosphorolyse des acides ribonucléiques de différentes sources

Substances ajoutées (μmoles P organique/ml.)		Phosphorolyse % 19 heures	27 heures
Poly A	(1)	100	100
Poly AGUC	(183)	89	—
ARN levure (Allen)	(2·52)	88	96
ARN TYM	(139)	86	100
ARN commercial	(2·25)	67	100
ARN soluble	(0·59)	35	50
	(1·48)	35	43
ApApApUp	(4·2)	5	5

Or les résultats du tableau 4 montrent que les ARN (à l'exception du S-ARN) s'ils sont phosphorolysés lentement, le sont complètement en présence d'un excès d'enzyme. Contrairement aux oligonucléotides en $3'PO_4$, comme le tétranucléotide à

3 adénines et une uridine ApApApUp qui n'est dégradé que de 5% dans nos conditions expérimentales†, l'ARN du commerce malgré la forte proportion probable de chaines en 3′ est dégradé totalement. Ainsi, les résultats trouvés sur les oligonucléotides ne peuvent pas s'appliquer directement aux chaines plus longues. Il est possible que dans ce dernier cas, et comme cela se produit avec la phosphodiestérase du venin de serpent (Razzel & Khorana, 1958), l'attaque se produise à quelque distance de la fin de la chaine et non à son extrémité. Il apparait donc que toutes les chaines d'ARN sont phosphorolysées quel que soit leur groupe terminal. Il est cependant possible que la vitesse de phosphorolyse des chaines terminées par un PO_4 en 3′ soit plus faible que celles dont le PO_4 est en position 5′, et que cela puisse expliquer, au moins en partie, la vitesse lente de phosphorolyse des préparations d'ARN commercial contenant de nombreuses chaines en 3′.

Par contre, cette explication n'est pas satisfaisante dans le cas des préparations d'ARN très polymérisé, comme celles des particules de microsomes ou de la levure (Crestfield *et al*, 1955 ; Holden & Pirie, 1955) qui ne doivent contenir que peu de radicaux terminaux. En effet, ceux-ci sont éliminés au cours de la phosphorolyse: si la lenteur de la phosphorolyse était due à la présence des radicaux, on devrait observer une courbe de phosphorolyse autocatalytique, ce qui n'est pas le cas. De plus cette explication ne parait pas valable non plus dans le cas des préparations du S-ARN. En effet, d'après les études de Canellakis (1957), Edmonds & Abrams (1957), Zamecnik, Stephenson, Scott & Hoagland (1957), Chung & Malher (1958) et d'autres auteurs sur l'incorporation des nucléotides 5′PP dans l'ARN soluble, cet ARN soluble serait terminé par un nucléoside à groupement oxhydrile libre en 3′. Ceci implique que le radical phosphate libre du nucléotide terminal à l'autre extrémité de la chaine est en 5′; or cet ARN est phosphorolysé à une vitesse très lente. Il est vrai que parmi les ARN les préparations du S-ARN occupent une place très particulière car elles ne sont phosphorolysées qu'à 35 à 50%, même en présence d'un excès d'enzyme. Le fait de traiter le S-ARN par l'alcali dilué pour enlever les amino-acides éventuels ($S\text{-}ARN_3$) ne modifie ni la vitesse, ni le pourcentage de la phosphorolyse. La phosphorolyse partielle de ce S-ARN pourrait être due en particulier à ce que le résidu non attaquable serait composé de bases ou de sucres inhabituels (Littlefield & Dunn, 1958 ; Cohn, 1958, 1959; Yu & Allen, 1959).

(d) *Structure macromoléculaire des polyribonucléotides*

Si la vitesse de phosphorolyse des polynucléotides est déterminée en partie par leur structure macromoléculaire, on doit s'attendre à trouver de grandes différences dans les vitesses de phosphorolyse des mélanges en proportion variée de poly A et poly U.

En effet, nous savons d'après les travaux de Warner (1957*a*, *b*), Rich (1957), Felsenfeld, Davies & Rich (1957), Fresco & Doty (1957) et Fresco & Klemperer (1959) que les poly A et poly U en solution aqueuse réagissent, en absence de tout système enzymatique, pour former des complexes stables présentant différentes configurations moléculaires suivant les conditions expérimentales et les proportions des deux polyacides.

La Fig. 4 montre que, bien que la vitesse initiale de phosphorolyse de ces deux échantillons de polymères A et U soit sensiblement la même, celle des mélanges de ces deux polymères dépend de leur proportion relative.

† La faible phosphorolyse est probablement due à une impureté contaminant le tétranucléotide ApApApUp en accord avec les résultats de Singer (1958).

Le mélange des polymères A et U en proportion 3/1 est phosphorolysé presque aussi rapidement que le polymère A seul. Or dans ces conditions, il y a peu de complexe formé et on constate que la phosphorolyse † libère un très gros excès d'ADP par rapport à l'UDP: ceci suggère que ce sont les chaines de poly A, qui ne prennent pas part au complexe, qui sont attaquées.

Le mélange des poly A et U en proportion 1/1 (complexe à double hélice maintenue par des liaisons hydrogène) est attaqué avec une vitesse environ trois fois plus faible que celle des deux polyacides testés séparément, ainsi qu'il avait déjà été noté par Ochoa (1957), et la vitesse va diminuant alors que la plus grande partie des polymères n'est

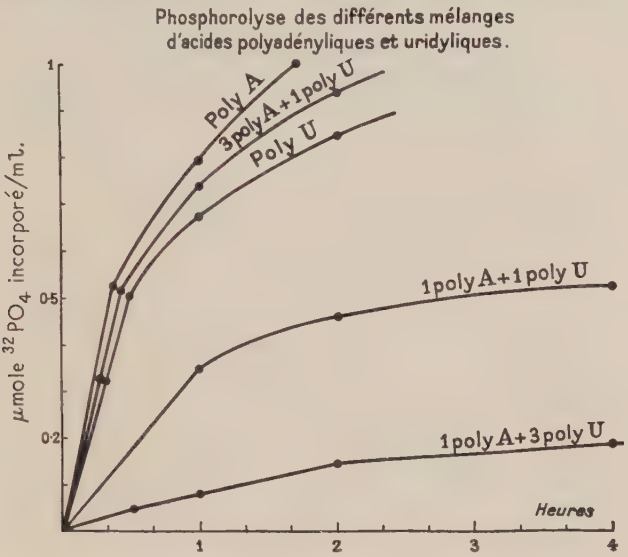

FIG. 4. Le mélange d'incubation contient: 7 µmoles $MgCl_2$, 50 µmoles tampon Tris pH 7·45, 8 µmoles tampon $^{32}PO_4$ pH 7·4 (activité spécifique = 68 000), $\simeq$ 1·2 µmoles de polymère, ou lorsqu'on ajoute 2 polymères différents 0·6 µmoles de chaque, 69 µg de polynucléotide phosphorylase d'*Azotobacter vinelandii* d'activité spécifique = 14·8 dans un volume final de 1 ml.

Incubation à 30°C. Des prises de 0·1 ml. sont effectuées à des intervalles de temps déterminés pour le test d'incorporation de $^{32}PO_4$ et pour l'élution des nucléotides. Les polymères utilisés étaient les suivants: poly A_2, poly U_2. Les détails sur les polymères et le test sont décrits dans la section Méthodes.

pas encore degradée. On peut supposer que la première partie de la courbe correspond à l'attaque des chainons libres provenant d'une discontinuité de l'hélice. La diminution considérable de vitesse observée ensuite correspondrait à l'attaque du complexe. L'ADP étant libéré en excès par rapport à l'UDP (Tabl. 2), il est possible que les chainons libres soient composés en majeure partie de poly A.

Lorsqu'il y a un excès de poly U par rapport au poly A, la vitesse de phosphorolyse est très faible. Or dans ce cas, d'après Rich, un complexe à triple hélice est formé. Seul l'UDP est libéré ; la polynucléotide phosphorylase attaque donc probablement l'excès de poly U qui ne fait pas partie du complexe.

Ces résultats montrent que les polyribonucléotides ayant une structure à plusieurs brins maintenus par des liaisons hydrogène résistent à la phosphorolyse, le complexe à trois brins n'étant pratiquement pas attaqué.

† Les expériences de phosphorolyse des poly AU et des mélanges de polymères A et U ont été réalisées en présence des concentrations optima de $MgCl_2$ (10×10^{-3} M) qui favorisent la formation des complexes.

Cette interprétation est confirmé par l'étude de la phosphorolyse du Poly I. Il a été montré par Rich (1958), Haselkorn, Fresco et Doty (communication personnelle) que ce polymère possède deux configurations macromoléculaires suivant la concentration en sel du milieu: en milieu salin dilué il n'a pas de structure ordonnée, en milieu riche en sel il se présente sous forme d'hélice à trois brins. La Fig. 5 montre qu'en milieu salin dilué les vitesses de phosphorolyse des poly A et poly I sont comparables (légèrement plus grande pour l'échantillon de poly I utilisé). Au contraire, en milieu salin concentré (0·6 M) le poly I n'est attaqué que très lentement, et certains échantillons comme le poly I_7 conservés en milieu KCl 1 M et congelés en présence de cette forte concentration en sel, ne sont pas du tout attaqués. La forte concentration en sel

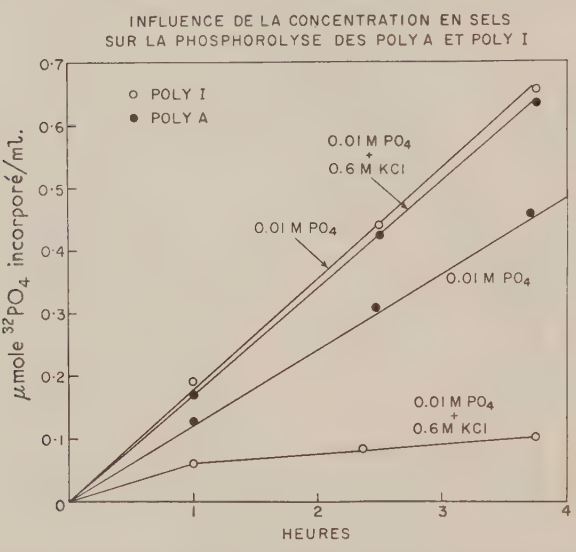

Fig. 5. Le mélange d'incubation contient: 0·3 µmoles $MgCl_2$, 0·78 µmoles tampon $^{32}PO_4$ pH 7·4 (activité spécifique = 244 000 coups/min par µmole), 0·1 mg de poly A_1 ou de poly I, 3·9 µg de polynucléotide phosphorylase de *E. Coli* d'activité spécifique ≈ 20 à 22 dans un volume total de 0·1 ml.

Incubation à 37°C. Dans les expériences réalisées en présence de KCl, les polymères A et I ont été préalablement incubés 30 min à 20°C en présence de KCl 0·6 M. Les détails sur les polymères et le test sont décrits dans la section Méthodes.

n'inhibe pas la polynucléotide phosphorylase: au contraire les poly A et poly U sont attaqués avec une vitesse plus grande en présence de 0·6 M-KCl qu'en milieu salin dilué. La vitesse est doublée pour le poly U et est stimulée de 30 à 50% pour le poly A. Comme le poly U ne possède pas de liaisons hydrogène (Fresco & Alberts, résultats non publiés) cette activation est probablement due à l'action des sels sur la vitesse maximum de la réaction enzymatique, comme cela se produit dans certains cas pour la polynucléotide phosphorylase de *M. lysodeikticus* (Beers, 1958). Dans le cas du poly A deux effets se superposent probablement: d'une part, l'action des sels qui augmente la vitesse, et d'autre part, l'augmentation du nombre des liaisons hydrogène intramoléculaires (Fresco & Klemperer, 1959), qui tend à la diminuer.

Il ressort de ces expériences que la polynucléotide phosphorylase n'attaque que très lentement ou pas du tout les polymères quand ils sont sous forme de complexes à plusieurs brins. Il est possible qu'il en soit de même pour certaines formations dans

lesquelles l'existence de liaisons hydrogène entre les bases donne naissance à des complexes quelconques. On expliquerait ainsi la faible vitesse de phosphorolyse des polymères à deux ou à quatre bases et celle de beaucoup de préparations d'ARN.

Des données plus directes en faveur de cette interprétation ont été obtenues en étudiant l'effet de la température sur la vitesse de phosphorolyse des ARN du TMV et des particules de microsomes de foie ainsi que sur le polymère AGUC.

4. Effet de la Temperature sur la Phosphorolyse des Polyribonucléotides Biosynthétiques et des Acides Ribonucléiques

Il a été montré que les liaisons hydrogène des structures des polymères biosynthétiques et de l'acide désoxyribonucléique sont détruites par la chaleur et que le passage de la forme ordonnée à la forme non ordonnée a lieu à des températures définies et

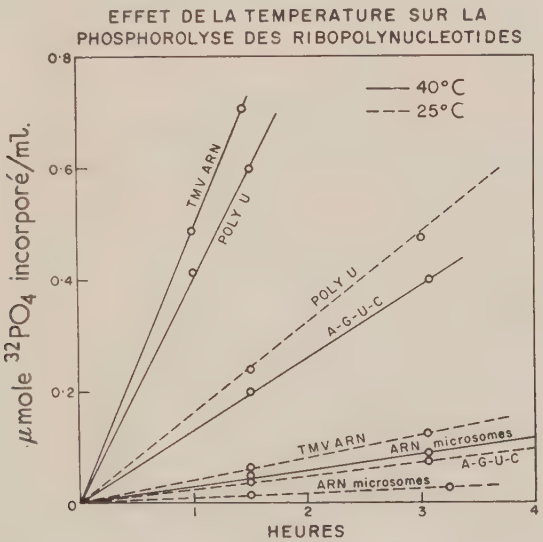

Fig. 6. Le mélange d'incubation contient: 0·3 μmoles $MgCl_2$, 0·89 μmoles tampon $^{32}PO_4$ pH 7·4 (activité spécifique = 278 000 coups/min par μmole), 0·1 mg de ribopolynucléotides et 15 μg de polynucléotide phosphorylase d'*Azotobacter vinelandii* d'activité spécifique ≈ 10 dans un volume total de 0·1 ml.

Incubation à 40° ou 25°C. Les polymères utilisés étaient les suivants: poly U_3, $AGUC_3$, TMV ARN_2. Les détails sur les polymères et le test sont décrits dans la section Méthodes.

se manifeste par un accroissement marqué de la densité optique (Warner, 1957 *a* & *b* ; Fresco & Doty, 1957; Fresco & Klemperer, 1959; Doty, Boedtker, Fresco, Haselkorn & Litt, 1959; Doty, Boedtker, Fresco, Haselkorn & Hall, 1959). Les ARN du TMV et des particules de microsomes présentent des changements similaires de leur densité optique. Par analogie avec les résultats trouvés sur les polymères et l'acide désoxyribonucléique, cette augmentation de densité optique est attribuée à la dissociation des bases par rupture thermique des liaisons hydrogène qui les réunissent (Doty *et al.*, 1959). Dans les ARN les diverses bases ont de nombreuses possibilités de s'apparier entre elles par formation de liaisons hydrogène, et suivant les bases couplées il en résulterait des structures à stabilités différentes plus ou moins sensibles à la température. Quand la température passe de 25 à 40°C, le changement de densité optique de l'ARN du TMV

correspond à 59% du changement total de densité optique (OD) qui peut se produire par chauffage (Boedtker, 1959). Les valeurs correspondantes pour l'ARN des particules de microsomes (Hall & Doty, 1959) et le polymère AGUC (Doty *et al.*, 1959) sont seulement de 17% et de 23%. Le calcul est fait en se basant sur le rapport

$$\frac{OD_{40°C} - OD_{25°C}}{OD_{90°C} - OD_{25°C}}$$

A une température donnée les différents ribopolynucléotides posséderaient ainsi différents degrés de liaison hydrogène. Si la vitesse de phosphorolyse des ARN est déterminée par leur structure macromoléculaire, on doit s'attendre à ce que la rupture des liaisons hydrogène intramoléculaires ait une répercussion sur cette vitesse. La vitesse de phosphorolyse de l'ARN du TMV, en accord avec ce que l'on a vu précédemment, doit donc être stimulée très significativement par l'élevation de température qui ne doit donc avoir que peu d'effet sur la phosphorolyse de l'ARN des particules de microsomes.

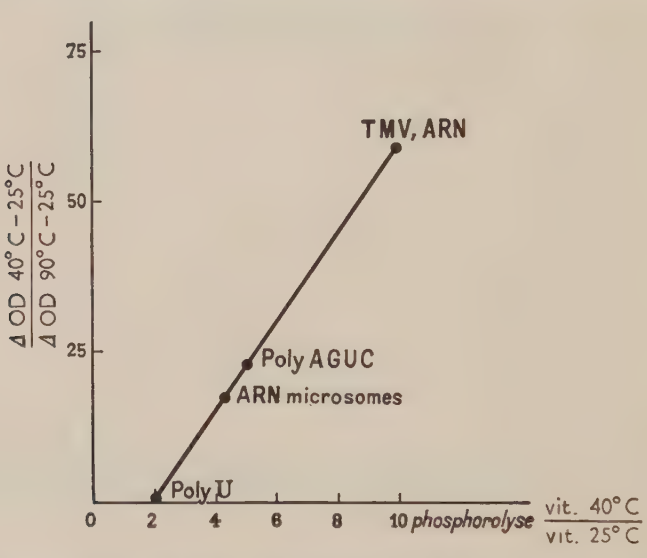

Fig. 7. Vitesse de phosphorolyse des ribopolynucléotides en fonction des changements de leur densité optique. (Les détails sur le test sont donnés dans la Fig. 6.)

La Fig. 6 montre que c'est effectivement ce qui se produit. La vitesse de phosphorolyse de l'ARN du TMV est 10 fois plus grande à 40 qu'à 25°C alors qu'elle n'est que 4·5 fois plus rapide pour l'ARN des particules de microsomes et 5 fois plus rapide pour le polymère AGUC; ceci est vrai pour les 2 échantillons ARN_1 et ARN_2 du TMV. Le polymère U, dont les bases ne peuvent pas s'apparier et dont la densité optique n'est par conséquent pas affectée par la température, n'est phosphorolysé que 2 fois plus rapidement à 40 qu'à 25°C; cet accroissement de vitesse peut être attribué à l'activation de l'enzyme par la température.

Il ressort donc nettement de la Fig. 6 que dans les conditions où les liaisons hydrogène intramoléculaires des ARN sont préservées, leur vitesse de phosphorolyse est faible: à 25°C les ARN du TMV, des microsomes et le poly AGUC, sont phosphorolysés plus lentement que le poly U. Par contre, à 40°C un fort pourcentage des liaisons hydrogène du TMV étant clivées, on constate que sa vitesse de phosphorolyse est du même ordre de grandeur que celle du poly U, tandis qu'elle reste faible pour l'ARN des

particules de microsomes dont les liaisons hydrogène résistent à une telle température. De plus, en présence d'une forte concentration de sels qui stabilisent ses liaisons hydrogène (Boedtker, 1959), la vitesse de phosphorolyse de l'ARN du TMV est seulement doublée (comme celle du poly U) au lieu d'être décuplée quand la température passe de 25 à 40°C.

La Fig. 7 montre en outre que lorsque l'on passe de 25 à 40°C, la stimulation de la vitesse de phosphorolyse des différents polyribonucléotides (AGUC, ARN du TMV en présence ou en absence de sel, ARN des particules de microsomes) est linéaire par rapport à l'augmentation relative de densité optique.

Il ressort de cette étude que l'on peut étendre aux ARN l'interprétation qui découle des résultats obtenus avec les polymères biosynthétiques: c'est leur structure macromoléculaire qui est responsable, pour une grande partie, de leur vitesse de phosphorolyse. En effet, dans les conditions favorisant le clivage des liaisons hydrogène (température élevée, milieu salin dilué) la phosphorolyse est plus rapide. Elle est ralentie, au contraire, lorsque les liaisons hydrogène sont stabilisées (milieu salin concentré, basse température).

5. Conclusions

Les résultats exposés montrent que la phosphorolyse des polyribonucléotides ne dépend pas seulement des concentrations relatives des substrats en présence qui déterminent l'équilibre de la réaction, mais qu'elle est encore étroitement liée à la structure des polymères et particulièrement à la quantité de complexes formés entre les différents nucléotides au moyen de liaisons hydrogène inter- ou intramoléculaires.

Les polyribonucléotides biosynthétiques, s'ils possèdent une structure ordonnée à plusieurs brins, ne sont pas attaqués par la polynucléotide phosphorylase. Ainsi, peuvent-ils échapper à la dégradation même en présence d'un excès de phosphate minéral, conditions qui au contraire devraient favoriser la phosphorolyse si l'on ne tenait compte que de l'équilibre de la réaction. Il semble que cette interprétation qui découle des résultats obtenus avec les polyribonucléotides biosynthétiques est applicable aux préparations d'acide ribonucléique naturel: une des raisons de la vitesse lente de phosphorolyse des ARN serait due à la formation dans les chaines de complexes maintenus par des liaisons hydrogène intramoléculaires. En effet, si celles-ci sont clivées la vitesse de phosphorolyse est augmentée.

On n'a malheureusement que peu de renseignements sur la configuration macromoléculaire des préparations isolées d'ARN. D'après Doty *et al.* (1959), celle-ci comprendrait des petites régions hélicoïdales. On possède encore moins de renseignements sur la structure de l'acide ribonucléique tel qu'il est *in vivo*, aussi est-il difficile à l'heure actuelle de décider si l'ARN peut ou non être phosphorolysé *in vivo*. De plus, une grande partie de l'ARN se trouve sous forme de nucléoprotéines ou lié à des peptides. Il est possible que sous cette forme il ne puisse être attaqué comme le suggèrent nos essais de phosphorolyse du virus intact et des particules de microsomes. Ceux-ci dans les conditions où les acides nucléiques sont attaqués, ne le sont pas. Les recherches préliminaires de Doty *et al.* (1959), et Hall & Doty (1959), sur la structure des particules de microsomes indiquent qu'une structure secondaire analogue à celle des ARN existerait dans ces particules. On peut ainsi penser que l'ARN des cellules pourrait échapper à la phosphorolyse malgré un excès de phosphate minéral. On peut alors concevoir que dans certaines conditions pouvant affecter sa configuration (variation du milieu cellulaire, température, sels) l'ARN pourrait être dégradé par la polynucléotide phosphorylase et servir de source de diphosphates.

Les vitesses de phosphorolyse des ribopolynucléotides dépendent étroitement de leurs configurations. L'étude de ces vitesses peut alors nous aider à élucider les structures macromoléculaires des acides ribonucléiques. C'est ainsi que l'étude de la vitesse de phosphorolyse de l'ARN du virus de la mosaïque du tabac suggère qu'il possède une configuration avec des liaisons hydrogène intramoléculaires labiles à des températures relativement basses. Cette interprétation est en accord avec les résultats de Boedtker (1959), de Gierer (1957), Staehelin (1958) et Doty *et al.* (1959).

6. Matériels et Méthodes

(a) *Enzymes*

La polynucléotide phosphorylase d'*Azotobacter vinelandii* a été préparée suivant la méthode de Grunberg-Manago *et al.* (1956) et fractionnée jusqu'au stade $SO_4(NH_4)_2$ II inclus. Elle avait une activité spécifique de 14·8 exprimée en unités Grunberg-Manago et coll.

Une autre préparation de polynucléotide phosphorylase d'*Azotobacter vinelandii* a été préparée suivant la méthode de Ochoa & Mii (résultats non publiés) et correspondait à un éluat du gel $(PO_4)_2\ Ca_3$; elle avait une activité spécifique de 10. La polynucléotide phosphorylase de *E. Coli*† a été préparée suivant la méthode de Littauer & Kornberg (1957) et fractionnée jusqu'à la première précipitation alcoolique inclue. La préparation utilisée avait une activité spécifique de 50 exprimée en unités de Littauer et coll., ce qui correspond environ à 20 des unités précédentes.‡

(b) *Polyribonucléotides*

§ Les polymères biosynthétiques ont été synthétisés et isolés suivant les méthodes habituelles (Grunberg-Manago *et al.*, 1956). Ils étaient, sauf indication contraire, dissout à la concentration de 10 mg/ml. dans l'eau distillée neutralisée à pH 7.

Poly A_1, poly C, poly I_1: préparations lyophylisées; poly A_7: PM $\approx$ 800 000 préparé par la polynucléotide phosphorylase d'*Az. vinelandii* SA = 90, dissout dans le citrate salin (0·015 M tampon citrate pH 7·3, 0·15 M-NaCl); poly A_6: PM $\approx$ 50 000 préparé par la polynucléotide phosphorylase d'*Az. vinelandii* SA = 7, utilisé pour des mesures physiques, puis dialysé, lyophylisé et dissout dans le tampon citrate salin; poly U_3 PM $\approx$ 100 000; poly I_2: gardé congelé dans une solution de KCl M; poly A_2, poly U_2, poly AU 1/4, poly AU 3/1, poly AU 1/1: préparés par la polynucléotide phosphorylase d'*Az. vinelandii* SA = 14·8; poly G: préparé suivant la méthode de Singer *et al.* (sous presse) en incubant un triadénylate

† Les polynucléotides phosphorylases de *E. Coli* et d'*Az. vinelandii* d'A.S. 10 ont été préparées par les Dr. M. F. Singer, R. J. Hilmoe et L. A. Heppel, qui les ont gracieusement mises à notre disposition.

‡ Ce sont les unités Grunberg-Manago et coll. qui sont indiquées dans les figures ou tableaux.

§ Le poly A_1 a été préparé par les Dr. M. F. Singer, R. J. Hilmoe, L. A. Heppel.

Les poly A_7, A_6, U_3, I_2 par les Dr. J. R. Fresco et R. Haselkorn.

Les poly C et I_1 par le Dr. A. Rich.

Les poly AGUC nous ont été envoyé par Mrs. P. J. Ortiz et le Dr. S. Ochoa.

L'acide ribonucléique de levure préparé par la méthode de M. Holden et N. W. Pirie nous a été donné par le Dr. W. S. Pierpoint.

L'acide ribonucléique de levure preparè par la methode de Crestfield *et al.* (1955) est une préparation offerte au Dr. L. A. Heppel par le Dr. F. W. Allen.

L'acide ribonucléique du TMV: ARN_1 (TMV) a été préparé par les Dr. M. Staehelin et H. Fraenkel-Conrat.

L'acide ribonucléique du TMV: ARN_2 (TMV) a été préparé par le Dr. H. Boedtker.

L'acide ribonucléique de la mosaïque jaune du navet est une préparation offerte au Dr. L. A. Heppel par le Dr. R. Markham.

L'acide ribonucléique des particules de microsomes a été préparé par le Dr. B. Hall.

L'acide ribonucléique S-ARN_1 nous a été envoyé congelé par le Dr. P. C. Zamecnik et l'acide ribonucléique S-ARN_2 a été préparé par le Dr. J. Cantoni.

Les oligonucléotides ApApAp et pApApApU ont été préparés par les Dr. M. F. Singer, R. J. Hilmoe et L. A. Heppel.

Je suis heureuse de remercier tous ceux qui ont bien voulu me fournir si aimablement et généreusement ces précieux échantillons de ribopolynucléotides.

$5'PO_4$, pApApA comme amorceur avec la guanosine diphosphate et l'enzyme en présence de Mg; le polymère formé à été précipité par l'éthanol et dialysé, il contenait 7 unités d'acide guanylique et 3 unités d'acide adénylique; poly $AGUC_3$: préparé à partir des nucléosides diphosphates d'adénosine, guanosine, uridine, cytosine en proportion 1 : 1 : 1 : 1 (préparation lyophylisée), le contenu en bases de cette préparation est A = 10·0 G = 15·0 U = 8·3 C = 8·8; poly $AGUC_2$: préparé à partir des nucléosides diphosphates d'adénosine, guanosine, uridine, cytosine en proportion 1 : 1 : 1 : 1 (préparation lyophylisée); poly $AGUC_1$: préparé à partir des nucléosides diphosphates d'adénosine, guanosine, uridine, cytosine en proportion 1 : 0·5 : 1 : 1, le contenu en bases déterminé sur une préparation identique (Ochoa & Heppel, 1957) était A = 10·0 G = 5·9 U = 7·1 C = 9·9 (préparation lyophylisée).

Les échantillons d'acides ribonucléiques utilisés en solution à 10 ou 5 mg/ml. dans le tampon Tris pH 7·4 0·18 M, étaient les suivants:
l'acide ribonucléique commercial: préparation de Schwarz S = 2·0 PM moyen $\approx$ 12 000; l'acide ribonucléique de levure: préparé par la méthode de Holden et Pirie (1955); l'acide ribonucléique de levure: préparé par la methode de Crestfield *et al.* (1955); l'ARN_1 du TMV: préparation lyophylisée, préparé par la méthode au dodecyl SO_4 (Fraenkel-Conrat, Singer & Williams, 1957); l'ARN_2 du TMV: préparé par Boedtker (1959), préparation de PM $\approx$ 2 000 000 et biologiquement active, précipité par l'éthanol à froid; l'acide ribonucléique soluble S-ARN_1 et $_2$ fraction pH 5 du foie de veau, préparé par la méthode au phénol; S-ARN_3 provient du S-ARN_1 traité par l'ammoniaque 0·01 N 15 min à 37°C; l'ammoniaque est ensuite éliminée par un courant d'air; l'ARN des particules de microsomes du foie de veau, préparé par la méthode au phénol, S = 81, PM $\approx$ 1 000 000, qui, par chauffage, 10 min à 85°C, se transforme en ARN PM $\approx$ 100 000 (Hall & Doty 1959); l'ARN du virus de la TYM S = 7·1 PM moyen = 125 000; pApApApU: tétranucléotide contenant 4 adénine 1 uridine, a été préparé suivant la méthode de Singer, Hilmoe & Heppel (résultats non publiés).

(c) *Test*

La phosphorolyse est mesurée en incubant le polymère biosynthétique avec l'enzyme en présence d'orthophosphate marqué ^{32}P et en déterminant, à différents intervalles de temps, la quantité d'orthophosphate incorporée dans les nucléotides. Les résultats sont exprimés en μmoles de PO_4 en se basant sur l'activité spécifique du PO_4 minéral incorporé. Les nucléotides radioactifs sont séparés du P minéral par adsorption sur charbon suivant la technique de Littauer & Kornberg (1957) ou par élimination du complexe phosphomolybdique soluble dans l'isobutanol suivant la technique décrite précédemment (Grunberg-Manago *et al.*, 1956).

L'adsorption sur norite a été effectuée de la manière suivante: le mélange expérimental (0·1 ml.) est incubé dans un pot de centrifugeuse d'Internationale de 5 ml.; la réaction est arrêté en ajoutant à ce mélange 1 ml. d'acide perchlorique froid à 2·5%; 0·1 ml. d'une suspension de norite lavée à l'acide à 10g/100 (poids/poids) est ajouté pour adsorber les nucléotides. Après 10 min à 0°C la suspension est centrifugée et le charbon lavé 3 fois avec des portions de 2·5 ml. d'eau distillée froide. Le charbon est ensuite mis en suspension dans 0·8 ml. d'éthanol à 50% contenant 0·3 ml. d'ammoniaque concentré pour 100 ml. Une partie de cette suspension (généralement 0·1 ml.) est placée sur une planchette de cuivre, séchée, et la radioactivité déterminée avec un compteur Flow à fenêtre étroite; on utilise un facteur d'adsorption de 1·15. Un blanc ne contenant pas d'enzyme est effectué et les résultats corrigés pour la faible radioactivité adsorbée sur le charbon de ces échantillons.

L'élimination du P minéral par la technique à l'isobutanol a été décrite† (Grunberg-Manago *et al.*, 1956); on ajoute à 0·1 ml. du mélange expérimental 1 ml. d'acide perchlorique froid à 2·5%. On prélève 0·9 ml. pour l'extraction.

(d) *Dosage des nucléotides*

La décomposition en nucléotides des poly AU a été déterminée après hydrolyse des polymères en milieu alcalin 0·4 N, 40 h à 37°C, et chromatographie sur Whatman No. 1 lavé

† L'acide sulfurique employé est 10 N et non 10 M comme il a été publié par erreur.

suivant la technique de Krebs & Hems (1953). Les nucléotides sont élués en les laissant en contact avec 5 ml. HCl 0·01 N, 48 h à 20°C. Les nucléotides sont dosés sur les éluats par leur coefficient d'adsorption dans l'U.V., les blancs (papier seul) sont défalqués.

Dans les expériences de phosphorolyse les nucléotides diphosphates ^{32}P formés ont été dosés après élution, non seulement en utilisant leur coefficient d'absorption à 260 mμ, mais aussi par leur contenu en P radioactif. Les résultats concordent.

(e) *Effet de la temperature sur la densité optique des ribopolynucléotides*

La densité optique des acides ribonucléiques est déterminée dans les fioles de Beckmann bouchées à l'émeri; la température est maintenue par un thermostat qui la contrôle à ± 0·5°C.

Je tiens à remercier chaleureusement les Dr. P. Doty, Department of Chemistry, Harvard University, Cambridge (Mass.) et L. A. Heppel, Nationale Institute of Arthritis and Metabolic Diseases, Bethesda, Md. pour m'avoir offert l'hospitalité de leurs laboratoires et pour l'intérêt qu'ils ont bien voulu porter à ce travail.

J'ai grand plaisir à remercier le Dr. J. R. Fresco pour le concours qu'il m'a apporté, en particulier pour la détermination des constantes de sédimentation de l'ARN commercial et de celui du TMV et l'établissement des courbes de densité optique du poly AGUC et de l'ARN du TMV en fonction de la temperature.

Je voudrais enfin remercier Mr. Dan Broida de la Maison Sigma, St Louis (Mo) pour m'avoir offert gracieusement une partie des nucléosides diphosphates; sans son concours, ce travail n'aurait pu être mené à bien.

REFERENCES

Beers, R. F., Jr. (1958). *Arch. Biochem. Biophys.* **75**, 497.
Boedtker, H. (1959). *Biochim. biophys. Acta*, **32**, 519.
Brummond, D. O., Staehelin, M. & Ochoa, S. (1957). *J. Biol. Chem.* **225**, 835.
Cannellakis, E. S. (1957). *Biochim. biophys. Acta*, **25**, 217.
Chung, W. & Malher, H. R. (1958). *J. Amer. Chem. Soc.* **80**, 3165.
Cohn, W. E. (1958). *Fed. Proc.* **17**, 203.
Cohn, W. E. (1959). *Biochim. biophys. Acta*, **32**, 569.
Crestfield, A. M., Smith, K. C. & Allen, F. W. (1955). *J. Biol. Chem.* **216**, 185.
Doty, P., Boedtker, H., Fresco, J. R., Haselkorn, R. & Hall B. (1959). *Ann. N.Y. Acad. Sci.* in the press.
Doty, P., Boedtker, H., Fresco, J. R., Haselkorn, R. & Litt, M. (1959). *Proc. Nat. Acad. Sci., Wash.* **45**, 482.
Edmonds, M. & Abrams, R. (1957). *Biochim. biophys. Acta*, **26**, 226.
Felsenfeld, G., Davies, D. R. & Rich, A. (1957). *J. Amer. Chem. Soc.* **79**, 2023.
Fraenkel-Conrat, H., Singer, B. & Williams, R. C. (1957). *Biochim. biophys. Acta*, **25**, 87.
Fresco, J. R. & Doty, P. (1957). *J. Amer. Chem. Soc.* **79**, 3928.
Fresco, J. R. & Klemperer, E. (1959). *Ann. N.Y. Acad. Sci.* in the press.
Gierer, A. (1957). *Nature*, **179**, 1297.
Grunberg-Manago, M., Ortiz, P. J. & Ochoa, S. (1955). *Science*, **122**, 907.
Grunberg-Manago, M., Ortiz, J. P. & Ochoa, S. (1956). *Biochim. biophys. Acta*, **20**, 269.
Hall, B. D. & Doty, P. (1959). *J. Mol. Biol.* **1**, 111.
Hoagland, M. B., Zamecnik, P. C. & Stephenson, M. L. (1957). *Biochim. biophys. Acta*, **24**, 215.
Holden, M. & Pirie, N. W. (1955). *Biochem. J.* **60**, 46.
Krebs, H. A. & Hems, R. (1953). *Biochem. biophys. Acta*, **12**, 172.
Littauer, U. Z. & Kornberg, A. (1957). *J. Biol. Chem.* **226**, 1077.
Littlefield, J. W. & Dunn, D. B. (1958). *Nature*, **181**, 254.
Markham, R. & Smith, J. D. (1952). *Biochem. J.* **52**, 565.
Ochoa, S. (1957). *Arch. Biochem. Biophys.* **69**, 119.
Ochoa, S. & Heppel, L. A. (1957). *The Chemical Basis of Heredity*, p. 626. Baltimore: Johns Hopkins Press.

Razzel, W. E. & Khorana, H. G. (1958). *J. Amer. Chem. Soc.* **80**, 1770.
Rich, A. (1957). *The Chemical Basis of Heredity*, p. 557. Baltimore: Johns Hopkins Press.
Rich, A. (1958). *Biochim. biophys. Acta*, **29**, 502.
Singer, M. F. (1957). *Fed. Proc.* **16**, 250.
Singer, M. F. (1958). *J. Biol. Chem.* **232**, 211.
Singer, M. F., Heppel, L. A. & Hilmoe, R. J. (1956). *Biochim. biophys. Acta*, **26**, 447.
Singer, M. F., Heppel, L. A., Hilmoe, R. J., Ochoa, S. & Mii, S. *Third Canadian Cancer Conference*. New York: Academic Press, in the press.
Staehelin, M. (1958). *Biochem. biophys. Acta*, **29**, 410.
Warner, R. C. (1957*a*). *Ann. N.Y. Acad. Sci.* **69**, 314.
Warner, R. C. (1957*b*). *J. Biol. Chem.* **229**, 711.
Yu, C. T. & Allen, F. W. (1959). *Biochem. biophys. Acta*, **32**, 393.
Zamecnik, P. C., Stephenson, M. L., Scott, J. F. & Hoagland, M. B. (1957). *Fed. Proc.* **16**, 275.

J. Mol. Biol. (1959) **1**, 260-276

Synthesis of Phage-Precursor Protein in Bacteria Infected with T2 †

Gebhard Koch ‡ and A. D. Hershey

Department of Genetics, Carnegie Institution of Washington, Cold Spring Harbor, New York U.S.A.

(*Received 22 June 1959*)

Measurable synthesis of the principal phage-precursor proteins begins about 7 min after infection of bacteria with T2. By the 20th minute, such proteins have accumulated to the extent of about 28 phage-particle equivalents per bacterium. During the steady state of phage growth prevailing after this time, atoms of labeled sulfur or molecules of labeled arginine pass from the culture medium into phage-precursor protein in less than 1 min and then appear in phage particles about 5 min later. The 28 equivalents of precursor protein therefore make up an intrabacterial pool in which the rate of protein synthesis is matched by a similar rate of subsequent incorporation into phage particles.

After artificial lysis of the infected bacteria, the precursor proteins can be separated into three categories: large particles precipitable by antiphage serum (presumably empty phage heads); smaller particles similarly precipitable; and materials that are not precipitable. These three form roughly equal parts in the pool and all must be chiefly precursors of the coats of the finished phages. Surprisingly, a pulse of radioactive isotope passes from the culture medium into phage particles almost simultaneously through all three components of the pool; none of them is mainly a precursor of the others. Thus several classes of protein structures found in lysates are precursors of phage particles or, more likely, are derived by breakdown during extraction of other structures that are precursors. In either case it is clear that the more-or-less finished head portion of a phage particle is formed from phage-precursor nucleic acid and amino acids in a time that is short relative to the time required for the remaining steps in the production of an infective phage particle.

Serologically phage-specific proteins that are not phage precursors are also formed at slow and doubtfully significant rates. Other proteins that are not precursors are formed faster, but these probably are not related to the precursor materials.

1. Introduction

Growth of bacteriophage T2 consists of at least two separable phases: synthesis of deoxyribonucleic acid, probably the chemical equivalent of genetic replication, and protein synthesis, the measurable aspect of particle formation (Hershey & Melechen, 1957; Watanabe, 1957; Tomizawa, 1958). The first of these is understandable in principle (Watson & Crick, 1953) and seems to be yielding to experiment (Meselson & Stahl, 1958; Lehman *et al.*, 1958). The second involves numerous biochemical and morphogenetic problems that are obscure individually and collectively (Kellenberger, 1959). Definition of these problems evidently calls for the characterization of protein precursors of phage particles and ordering them with respect to time of formation.

† Aided by grant C2158 from the National Cancer Institute, National Institutes of Health, United States Public Health Service.

‡ Present address: Laboratorium der Stiftung zur Erforschung der spinalen Kinderlähmung und der multiplen Sklerose, Hamburg-Eppendorf.

Lysates of bacteria infected with phage T2 (or T5) contain, besides phage particles and phage-precursor nucleic acid, several phage-specific structures that have been recognized microscopically (Levinthal & Fisher, 1952; Kellenberger & Séchaud, 1957) or by serological means (DeMars, Luria, Fisher & Levinthal, 1953; Maaløe & Symonds, 1953; Lanni, 1954; DeMars, 1955, Watanabe, 1957). Among these the so called doughnuts, identified as empty phage heads composed of protein and containing little or no nucleic acid, are pertinent in the present context (Anderson, Rappaport & Muscatine, 1953; DeMars *et al.*, 1953; Watanabe, Stent & Schachman, 1954). It seems probable that the empty heads are breakdown products of particles that contained nucleic acid at the time of their formation (Kellenberger, 1959). Such breakdown could occur inside the infected bacterium, during extraction from the bacterium, or both.

Except for some preliminary tracer experiments reported without details (Maaløe & Symonds, 1953; Hershey, 1956), there has been no clear indication that any of the phage-related materials (other than nucleic acid) detected in lysates are phage precursors rather than by-products of phage growth (Lanni, 1954; DeMars, 1955; Kellenberger & Séchaud, 1957). Infected bacteria do contain appreciable amounts of phage-precursor protein, however (Hershey, Garen, Fraser & Hudis, 1954; Hershey & Melechen, 1957). The experiments reported below were designed to analyze the kinetics of synthesis and incorporation into phage particles of such proteins, and to gain information about the sequence of events by which a phage particle is formed.

In the following experiments, the proteins formed in infected bacteria are labeled specifically by feeding radioactive arginine or sulfate. The bacteria are then lysed and the lysates are fractionated, after removal of insoluble bacterial debris, to yield several components in which radioactivity can be separately assayed. The fractionation is achieved by a combination of centrifugal and serological methods. The components recognized in these ways may be characterized as finished phage particles, as large particles lighter than phage particles but precipitable by antiphage serum (presumably empty phage heads), as smaller particles likewise precipitable, and as materials that are not precipitable by antiphage. By analysis of continuously labeled cultures, the amounts of protein in these fractions are measured at different times during phage growth. By similar analysis of cultures to which radioactive substrates are admitted only briefly, it can be shown that the protein in finished phage particles is derived from all three of the other categories of protein mentioned.

Three general conclusions about protein synthesis in bacteria are pertinent to the interpretation of results presented in this paper, and should be made clear at the outset. First, bacteria do not contain appreciable amounts of sulfur, arginine, or lysine that serve as precursors of protein. Second, uninfected bacteria do not contain appreciable amounts of proteins that contribute sulfur, arginine, or lysine to phage particles formed after infection. Third, atoms of sulfur or carbon once incorporated into intrabacterial proteins in general do not subsequently re-enter the protein-precursor pools. These conclusions have been reached by previous investigators (Hershey *et al.*, 1954; Hogness, Cohen & Monod, 1955; Hershey & Melechen, 1957) and are further documented below. Thus if we feed radioactive substrates to bacterial cultures beginning at the time of infection, we label all protein synthesized after infection and all proteins of potential interest as phage precursors. Similarly, if we feed radioactive substrates during a short time period only, we are labeling nearly all the protein synthesized (to an acid-insoluble stage) during that period and very little synthesized afterward.

2. Materials and Methods

Phage T2H and *Escherichia coli* strain H grown in a glucose-ammonium medium are used in the experiments reported in this paper. "Diluting fluid" contains 3·0g NaCl, 1·0 g Bacto peptone, and 0·12 g $MgSO_4$ per liter. The principal experiments are performed as follows (see also Hershey & Melechen, 1957).

Appropriately seeded bacterial cultures are aerated at 36°C for about 2·5 hr until they contain 5×10^8 bacteria per ml. The bacteria are then sedimented and resuspended in fresh culture medium. Aeration is resumed and, at zero time of the experimental schedule, the culture is infected with 5 phage particles per bacterium. Radiosulfate (carrier-free) or uniformly labeled [^{14}C]-L-arginine (not less than 0·1 μmole per ml. of culture) is added at the start of the specified labeling period. To terminate the assimilation of radiosulfur 1 mg per ml. of sulfur in the form of a neutralized solution of ammonium sulfate and 2·5 mg per ml. of DL-methionine are added. To terminate the assimilation of radiocarbon, L-arginine is added in 100-fold excess of the radioactive arginine.

Samples of the culture are lysed at intervals by mixing in a chilled tube 2·5 ml. of culture, $1{\cdot}5 \times 10^{12}$ phage particles irradiated with ultraviolet light to a survival fraction of 10^{-5}, 0·05 ml. of M-KCN (bringing the pH to about 8·0), and 200 μg of egg white lysozyme. After thorough chilling the mixtures are warmed for 30 min at 36°C, refrigerated overnight, and brought to 10 ml. total volume with diluting fluid. By this time the bacteria are satisfactorily lysed, with the possible exception of samples taken during a refractory period beginning about 3 min after infection and ending about 12 min after infection. The added lysozyme aids lysis during this period: otherwise the results of the analysis described below are the same with or without lysozyme. A large excess of the enzyme seems, however, to precipitate some of the labeled proteins, and so must be avoided.

The lysates are spun at 5000 rev/min for 10 min to separate low speed pellets that contain chiefly bacterial debris. The pellets are sampled for phage titrations and washed with trichloroacetic acid preliminary to radio-assay. The low speed supernatant fluids contain most of the phage particles, which are sedimented three times at 15,000 rev/min for 30 min, resuspending the pellets in 10 ml. of diluting fluid the first two times and pooling the three supernatants.

The final 15,000 rev/min pellets are resuspended in diluting fluid, digested with 0·5 mg of commercial pancreatin for 30 min at 36°C, sampled for phage titrations, and precipitated and washed with trichloroacetic acid preliminary to radio-assay. The digestion with pancreatin renders acid-soluble small amounts (3 to 5 phage equivalent units per bacterium in continuously labeled cultures) of radioactivity derived from contaminating bacterial debris.

The pooled 15,000 rev/min supernatants are titrated for phage content, and samples are fractionated by precipitation with antiphage serum as follows. To 3 ml. of the supernatants are added 10^{12} phage particles and 3 drops of high-titer antiphage serum diluted 1 : 5. (This amount of antiserum represents a several-fold excess over the minimum amount needed to cause prompt precipitation. Antisera from three animals, as well as larger amounts of antiserum and various conditions of precipitation, gave identical results in this fractionation.) The mixtures are warmed for 10 min at 36°C, allowed to stand for an additional 20 min at room temperature, diluted to 5 ml. total volume, and centrifuged. Precipitate and supernatant fractions are both assayed for acid-insoluble radioactivity.

Other samples of the pooled 15,000 rev/min supernatant fluids are spun with admixed carrier ghosts (empty phage coats prepared by osmotic shock) for 60 min at 20,000 rev/min, which carries down the remaining phage particles and the added ghosts. The supernatant fluids from this centrifugation (usually discarded) contain low molecular weight proteins, including part of the material precipitable by antiphage. Much of the specifically precipitable protein that fails to sediment at 20,000 rev/min also fails to sediment at 26,000 rev/min. We assume, therefore, that the labeled material other than phage particles in the 20,000 rev/min sediment represents relatively intact head membranes, though probably not all of them, and that the supernatant fraction is more heterogeneous.

The 20,000 rev/min pellet fraction is resuspended in diluting fluid and precipitated with antiphage serum in the presence of whole phage carrier as already described. The precipitate, containing practically all the labeled protein in the fraction, is assayed for acid-insoluble radioactivity.

In addition to the assays mentioned, the phage content of the unfractionated lysates, and the acid-insoluble radioactivity of additional samples of the unlysed culture, are determined, and prove to be in good agreement with the sums of the appropriate assays made after fractionating.

The results of the radio-assays are expressed in phage equivalent units whose numerical value is checked directly within each experiment. In terms of sulfur, the measured unit is $1{\cdot}5 \times 10^{-12}$ μg per phage particle, close to the smallest value previously reported (Hershey, 1957). In continuously labeled cultures, the assays measure the total sulfur content of phage particles and phage precursors, since the unlabeled bacterial constituents make no appreciable contribution. In the pulse labeling experiments to be described, the assays measure only the contribution made by sulfur assimilated during the specified labeling period, usually a small fraction of the total sulfur.

In the experiments employing arginine label, the computations are made in the same way. The measured arginine content per phage is about $1{\cdot}3 \times 10^{-11}$ μg.

Our fractionation procedure does not, of course, yield pure fractions. For example, most of the fractions contain appreciable numbers of phage particles. Since these numbers can be counted with precision, satisfactory corrections can be made, and the data shown in the body of this paper have been adjusted by pooling together all the radioactivity attributable to phage particles. An example of the computation is shown in Table 1, which also summarizes the scheme of fractionation.

Table 1

Sample calculation of results

Fraction	Phage per B	^{35}S per B	^{35}S in phage	^{35}S per B, corrected
1. 5,000 rev/min pellet	**8·1**	**32**	8	24
2. 15,000 rev/min pellet	**53**	**57**	57	78
3. Supernatant	**13**	—	—	—
4. Antiphage precipitate from 3	13	**33**	13	20
5. Remainder from 4	0	**62**	0	62
6. 20,000 rev/min pellet from 3	13	**20**	13	7

Analysis at 44 min of a culture labeled continuously after infection (Fig. 2). Actual measurements are shown in bold face type. The data are expressed as phage particles per bacterium measured by plaque counts, and as phage-equivalent units ($1{\cdot}5 \times 10^{-12}$ μg) of sulfur per bacterium assimilated after infection, computed from the radio-assays and from the measured specific radioactivity of the culture medium. Totals are obtained by summing lines 1, 2, 4, and 5. The correction in the last column consists in moving all sulfur attributable to phage particles into line 2.

In pulse-labeling experiments the radiosulfur per phage measured in line 2 differs systematically for each time of sampling and must be used in place of the standard unit to make the corrections.

3. Results

Our principal results are given by experiments in which we label infected cultures continuously, or during a few minutes only, and measure the radioisotope content of various materials as a function of time. We first present the results of these two types of experiment, and then record some tests that serve principally to evaluate the methods of analysis already described.

(a) *Distribution among the several fractions of protein synthesised after infection*

In the first type of experiment, the radioactive substrate is fed continuously beginning 1 min after infection of the culture. Samples of the culture are then lysed at

intervals, fractionated, and assayed for radioactive protein in the several fractions. Results for labeling with arginine radiocarbon are given in Fig. 1 and for labeling with radiosulfur in Fig. 2. Certain points were checked also by labeling with [^{14}C]-L-lysine. We note that the results are virtually identical and describe chiefly those shown in Fig. 2.

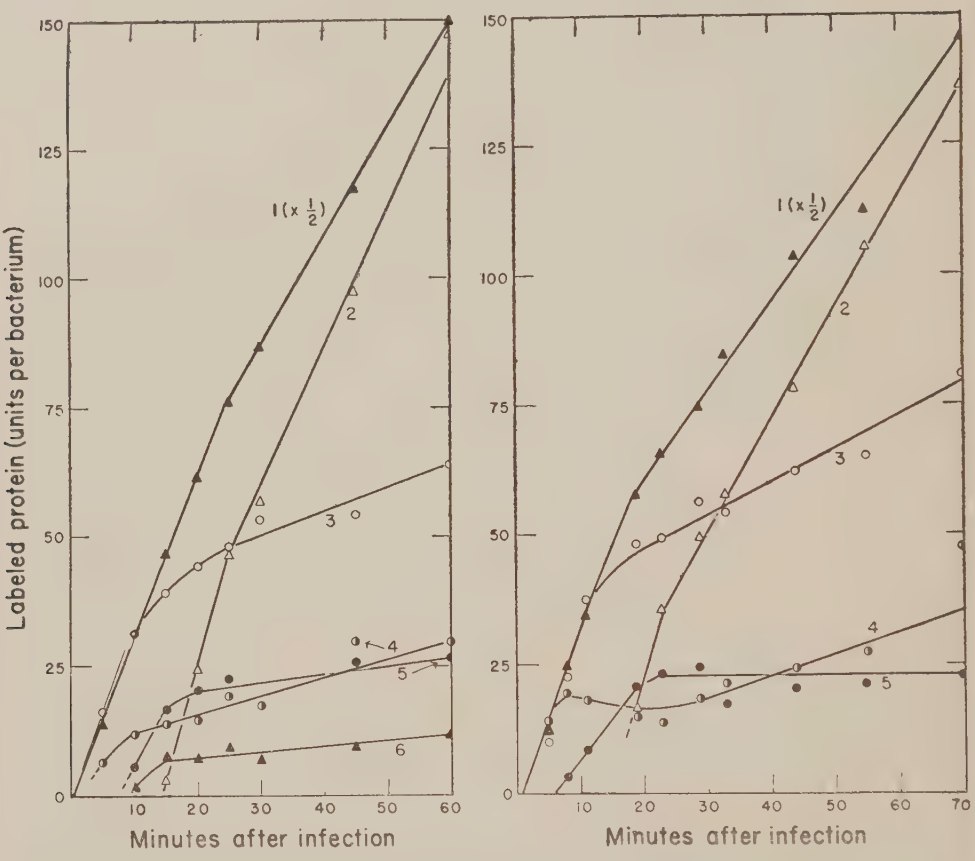

Fig. 1 (left). Incorporation of arginine radiocarbon, fed continuously after infection, into several acid-insoluble fractions of infected bacteria. The phage-equivalent unit is $1{\cdot}3 \times 10^{-11}$ μg of arginine derived from arginine in the culture medium, representing all or most of the arginine incorporated into protein synthesized after infection (Hershey, 1957). Multiply ordinate scale by two to read points on curve 1.

Curve 1, total protein. Curve 2, phage particles. Curve 3, soluble protein not precipitated by antiphage serum. Curve 4, bacterial debris. Curve 5, antiphage precipitate exclusive of phage particles. Curve 6, antigenic particles, exclusive of phage particles, sedimented at 20,000 rev/min and precipitated by antiphage.

Fig. 2 (right). Incorporation of radiosulfur, fed continuously after infection, into several acid-insoluble fractions of infected bacteria. The unit is $1{\cdot}5 \times 10^{-12}$ μg of sulfur assimilated from the labeled medium. Multiply ordinate scale by two to read points on curve 1. Curves numbered as in Fig. 1.

The initial rate of protein synthesis is about 6·2 phage-equivalent units ($1{\cdot}5 \times 10^{-12}$ μg of sulfur each) per bacterium per minute. Since an uninfected bacterium contains about 660 units of protein sulfur, and grows at a rate of 1·15% per min (Hershey & Melechen, 1957), the rate of protein synthesis is about the same before and immediately after infection (Hershey *et al.*, 1954). By the 30th min after infection, the rate has

fallen (rather excessively in Fig. 2) to about 3·3 units per bacterium per minute, but protein synthesis continues at a linear rate thereafter at least until the 90th min. Some cells lyse at about 25 min after infection, but the number is probably too small to account for the decreasing rate of synthesis. The data mentioned are about the same when measured in terms of acid-insoluble sulfur, arginine, or lysine, showing that bacteria and phage particles contain similar relative amounts of these three substances, any one of which forms a suitable measure of protein content.

Phage particles start to form at 15 min after infection, and accumulate at a diminishing but generally linear rate measuring 2 to 3 per bacterium per minute after the 30th min. The measurement by plaque count and by sulfur content agree satisfactorily, showing that the assays are reproducible, that the phage-equivalent unit is suitably chosen, and that the 15,000 rev/min pellet contains little protein other than phage particles.

Relatively little protein is incorporated into the bacterial debris, and most of this is formed during the first 10 min after infection.

Protein (other than phage particles) precipitable by antiphage serum begins to accumulate about 7 min after infection and measures about 20 phage-equivalent units per bacterium by the 20th min, after which the amount remains constant or slowly increases. This agrees with some preliminary estimates of 15 units (2×10^{-12} μg of sulfur each) based on the unit measured from inferior phage preparations (Hershey, 1956) and is less than that found in some of the experiments of Watanabe (1957).

At all times, somewhat less than half of the specifically precipitable protein other than phage particles sediments at 20,000 rev/min. The sedimenting fraction is probably empty head membranes; the remainder is probably a mixture of these and smaller particles.

The residue of low molecular weight protein not precipitable by antiserum comprises about half the total protein synthesized during the first 10 min. At later times it accumulates at the much slower rate of about 0·67 units per bacterium per minute.

Since the protein synthesized during the first 10 min after infection contains very little phage precursor (Hershey & Melechen, 1957; confirmed by labeling with [^{14}C]-arginine and [^{14}C]-lysine), the ratio between the rates of formation of phage particles and total protein at later times measures the fraction of the total protein being synthesized that is phage-precursor: 62% or 70% according to Figs. 1 and 2. (Previously published estimates of 50% to 60% neglect the appreciable phage content of the 5000 rev/min pellet fraction.) Evidently most of the remainder goes into water-soluble protein not precipitated by antiphage serum and into the bacterial debris.

(b) *The flow of protein through the fraction*

In the second type of experiment, the radioactive substrate is fed to the infected culture for a limited time only, which permits one to detect synthesis of proteins that do not accumulate in the fraction in which they are formed. The first experiment of this type to be discussed is shown in Fig. 3. It is designed to measure the total amount of phage-precursor protein in the cells at 30 min after infection. Radiosulfur is fed from the first to the 30th min, and radioactivity in the fractions is measured as usual. The flow of radiosulfur into phage particles subsequent to the 30th min measures

28 phage-equivalent units and is half completed in about 5 min. The flow of radiosulfur into the other fractions and into protein in general stops abruptly at 30 min. These facts show that the culture contains about 28 phage-equivalent units of phage-precursor protein per bacterium, which has a half-time in the precursor state of about 5 min. (An estimate of the amount of precursor at 20 min, reported as 16 units per bacterium by Hershey & Melechen (1957), becomes 24 units when corrected for phage sedimenting at low speed and for the change in definition of units.)

It is also evident from Fig. 3 that the protein entering phage particles comes from two fractions: protein precipitable by antiphage serum and low molecular weight protein that is not precipitable. This and other features of the data are better seen in the experiments to be described next.

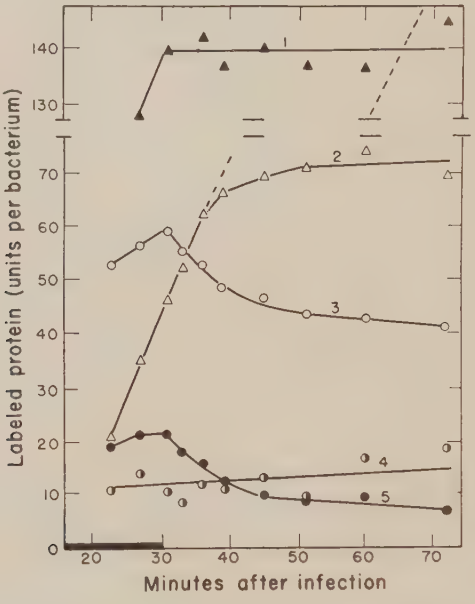

Fig. 3. Incorporation of radiosulfur, fed from the first to the 30th min, into acid-insoluble fractions of infected bacteria. The unit is $1{\cdot}5 \times 10^{-12}$ μg of sulfur assimilated during the labeling period. The broken line indicates yields of phage particles measured by plaque count. Curves numbered as in Fig. 1.

In Figs. 4, 5, and 6 we show the results of similar experiments in which radiosulfur or radioarginine is fed for an interval of 5 or 6 min only, beginning either at 10 min or at 20 min after infection. All the experiments show similar effects and we describe only their common features, referring to Fig. 6 (labeling with radiosulfur between the 20th and 25th min) for numerical illustration. (Certain features peculiar to Fig. 4 are probably due to the early labeling, at a time when the precursor pools are not yet filled.)

First, we note that labeling of protein is concomitant with the period of feeding of radiosulfur, and that radioactivity incorporated into protein does not subsequently leave it. Second, very little radioactivity enters the bacterial debris, and that small amount does not diminish after the end of the labeling period. Third, about 12·2 phage-equivalent units per bacterium of sulfur assimilated during the 5 min labeling period are incorporated into phage particles, representing a rate of synthesis of phage precursors of 2·4 units per bacterium per minute. (This is a slight underestimate,

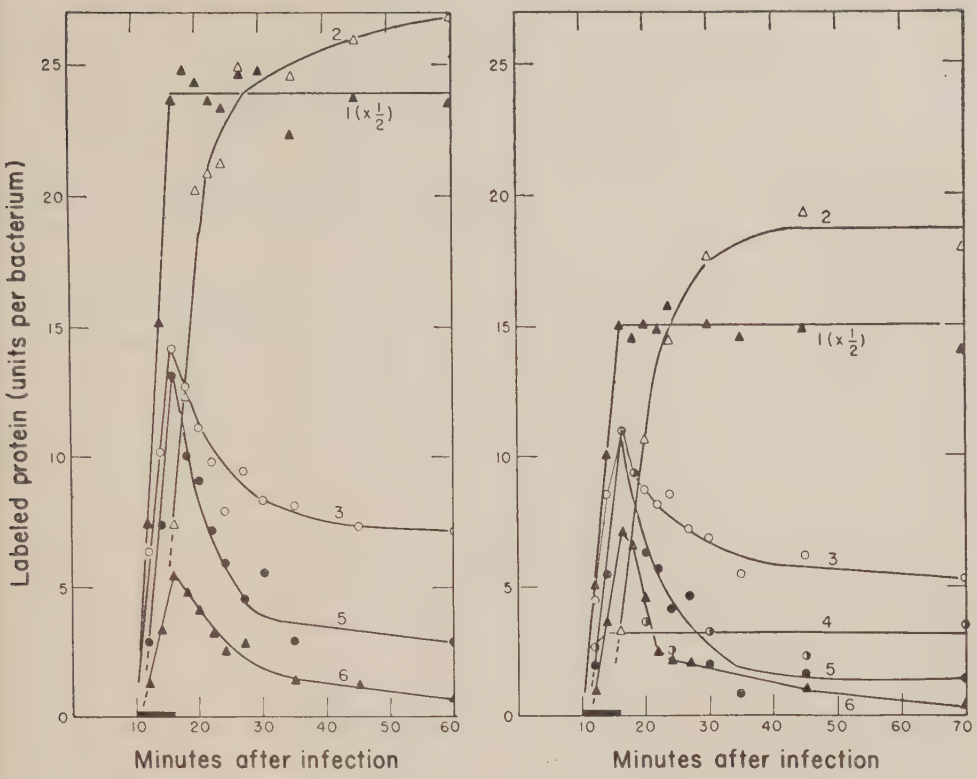

FIG. 4 (left). Incorporation of arginine radiocarbon, fed from the 10th to the 16th min, into several fractions of infected bacteria. The unit is $1{\cdot}3 \times 10^{-11}$ μg of arginine assimilated from the culture medium during the labeling period. Multiply ordinate scale by two to read points on curve 1. Curves numbered as in Fig. 1.

FIG. 5 (right). Incorporation of radiosulfur, fed from the 10th to the 16th min, into several fractions of infected bacteria. The unit is $1{\cdot}5 \times 10^{-12}$ μg of sulfur assimilated during the labeling period. Multiply ordinate scale by two to read points on curve 1. Curves numbered as in Fig. 1.

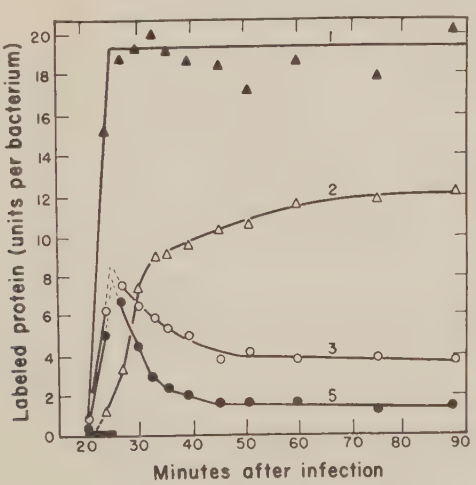

FIG. 6. Incorporation of radiosulfur, fed from the 20th to the 25th min, into several fractions of infected bacteria. The unit is $1{\cdot}5 \times 10^{-12}$ μg of sulfur assimilated during the labeling period. Curves numbered as Fig. 1.

since methionine added at the end of the labeling period prevents some assimilated radiosulfur from entering protein.) Of the 12·2 units of labeled protein per bacterium incorporated into phage particles, 10 units enter after the end of the labeling period, again with a half-time of 5 min. Fourth, at all times subsequent to the labeling period, the sum of the radiosulfur content of three fractions, phage particles, other protein precipitable by antiphage serum, and low molecular weight protein not precipitable, is constant, showing that sulfur incorporated into phage particles is derived exclusively from the other two fractions.

At the end of the labeling period, the two precursor-containing fractions include about eight units each of labeled protein per bacterium, and have so far donated only two units to phage particles. The rates of synthesis of the two fractions are therefore about equal. Not all the protein in the two fractions is phage precursor, however. About 1·5 units per bacterium of labeled specifically precipitable protein and 3·8 units of labeled non-precipitable protein remain at the end of the experiment. The total amount of protein synthesized in each of the two precursor fractions during the labeling period is therefore half of 12·2 + 1·5 + 3·8 or about 8·8 units per bacterium. Of the precipitable protein formed, a fraction 1·5/8·8 or 17% is not phage precursor. Of the non-precipitable protein this fraction is 3·8/8·8 or 43%. The overal efficiency of incorporation of precursor protein into phage particles is at least 12·2/17·5 or 70%; and undoubtedly more since at least one of the fractions must contain proteins that are not potential precursors.

The flow of radiosulfur into and out of the two precursor-containing fractions is virtually simultaneous, suggesting that the fraction which cannot be precipitated by antiphage is not a precursor of the precipitable protein, unless the pool of non-precipitable precursor is very small relative to the total amount of precursors. The data cited above indicate, however, that the rate of synthesis of non-precipitable precursor is about 41% of the total rate of precursor synthesis. This should measure also the fractional size of the corresponding precursor pool if the system is in its steady state. More directly, one sees from Fig. 3 that, out of a total precursor pool of 28 units per bacterium, about half is specifically precipitable protein with precursor status, and half is non-precipitable precursor.

To explain the somewhat faster incorporation of radioisotope into non-precipitable than into precipitable protein, therefore, one has to suppose that the non-precipitable phage-precursor protein consists of two parts, one that is precursor to precipitable protein and one that is not. The time difference between the labeling of precipitable and non-precipitable protein is at most one minute or 22% of the difference between the labeling of protein and labeling of phage particles. Thus, of the 28 units per bacterium of phage precursor protein, not more than 20% or 5·6 units may consist of non-precipitable protein that is precursor to precipitable protein, leaving about 6·4 units of non-precipitable protein that is precursor to phage particles but not to precipitable precursor, and 16 units of precipitable precursor. The 6·4 unit part would then account for the slow loss of radioactivity from non-precipitable precursor subsequent to the end of the labeling period.

The rates of synthesis of non-precursor proteins of the two categories are also directly measurable from Fig. 6. For non-precipitable nonprecursor the rate is 3·8/5 or 0·76 units per bacterium per minute, which may be compared with the measured slope of 0·67 units per bacterium per minute in curve 3 of Fig. 2. For precipitable protein the corresponding rate is 1·5/5 or 0·3 units per bacterium per minute, too small to be reliably measured in Figs. 1 and 2.

Finally, we note that radiosulfur also flows through the 20,000 rev/min pellet fraction (empty head membranes) on its way to phage particles. This precursor fraction is labeled almost simultaneously with, and shows the same percursor status as, specifically precipitable protein in general (Figs. 4 and 5).

To summarize, three independent measurements show that, during the linear phase of phage growth beginning 20 to 30 min after infection, the culture contains a constant amount of phage precursor protein, about 28 phage-equivalent units per bacterium. This is measured (1) as the total amount of labeled protein incorporated into phage particles subsequent to the labeling period when all the precursors are labeled (Fig. 3); (2) from direct measurements showing that the culture contains 20 units per bacterium of a specifically precipitable protein (Figs. 1 and 2) of which about 83% is precursor (Fig. 6) as well as a second protein formed at a similar rate of which about 57% is phage precursor (Fig. 6); and (3) from the half-time of persistence of labeled protein in the precursor pool, which measures 5 min (Figs. 3 and 6) and calls for a pool size (for a randomly sampled pool) of 22 units per bacterium at the observed rate of formation of phage particles (3 per bacterium per minute in Fig. 3). The third estimate is much less accurate than the others.

The proteins in the precursor pool yield, after lysis, three categories of structure: empty head membranes, smaller particles likewise precipitable by antiphage serum, and protein that is not carried down in a phage-antiphage precipitate. None of these three fractions is primarily a precursor of the others; all three enter phage particles simultaneously. A part of the non-precipitable protein, however, is probably a precursor of the protein in the precipitable fraction.

(c) *Time constants of protein synthesis*

Several of the experiments reported in this paper show that the time interval between the assimilation of labeled substrates and their incorporation into intrabacterial protein is short. In the following experiments this interval is measured somewhat more accurately.

Radiosulfate was fed to uninfected bacterial cultures (6×10^8 cells per ml.) for 30 sec only, and samples of the culture were withdrawn for the assay of acid-insoluble radiosulfur at intervals. Results of two experiments are shown in Fig. 7. In one (curve 1), the assimilation of radiosulfur was stopped at the end of the feeding period by adding ammonium sulfate only. In the other (curve 2), both ammonium sulfate and methionine were added. Curve 1 shows that the half-time of the rise subsequent to the labeling period is about 37 sec (in another experiment only 15 sec). Thus the median time spent by sulfur atoms on the intrabacterial route from sulfate to acid-insoluble protein is approximately 30 sec. In curve 2 the rise subsequent to the end of the labeling period is too small to be detected by manual sampling methods, suggesting that most of the time measured in curve 1 is spent *en route* from sulfate to amino acids rather than *en route* from amino acids to protein. In any case it is clear that the pool of intrabacterial precursors of protein is small enough to be neglected in experiments of the type described in this paper.

(d) *Distribution of bacterial proteins among the fractions*

Similar experiments to that described in Fig. 3 were carried out with cultures labeled before infection. The bacteria were allowed to grow for three generations in medium containing radiosulfur and then for 30 min in non-radioactive medium,

before infection and analysis. The distribution of labeled protein among the fractions is shown in Table 2. The data are interesting in several connections. First, it is clear

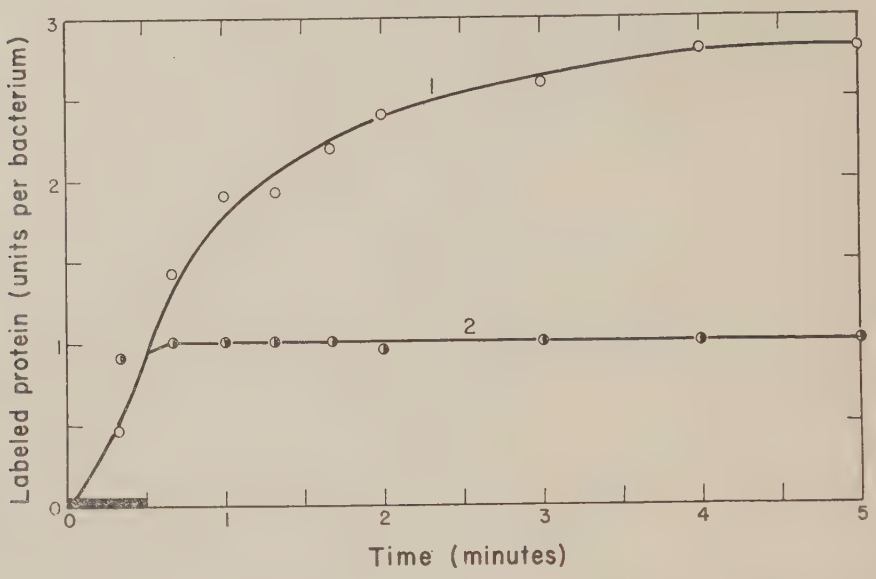

FIG. 7. Incorporation of radiosulfur, fed for 30 sec to an uninfected culture, into bacterial proteins.

Curve 1, labeling period terminated by addition of excess sulfate only.

Curve 2, labeling period terminated by addition of sulfate and methionine.

TABLE 2

Distribution of labeled bacterial protein among fractions of lysates of infected bacteria

Fraction	25-minute lysate		60-minute lysate	
	^{35}S per B	Protease-sensitive %	^{35}S per B	Protease-sensitive %
5,000 rev/min pellet	159	38	169	46
15,000 rev/pellet	43	33	44	38
Antiphage precipitate	29	82	19	72
Remainder	449	69	440	69

Bacteria were labeled for 3 generations, then grown in non-radioactive medium for 0·5 generation, before infection. Samples were lysed at 25 min and at 60 min after infection. Radiosulfur is expressed in phage-equivalent units per bacterium at the specific activity of the labeling medium, and represents about 71% of the total sulfur content at the time of infection. The protease sensitivity is measured as the fraction of the radioactivity rendered acid-soluble by digestion with pancreatin.

that bacterial proteins do not yield up appreciable sulfur to phage precursors, because the radiosulfur content of the 15,000 rev/min pellet does not increase from the 25th to the 60th min, nor is its content of labeled protein more resistant to protease digestion than that of the 5000 rev/min pellet, which is the chief source of contamination

(see also Hershey *et al.*, 1954). Second, the contamination of the 15,000 rev/min pellet with protease-resistant material from the 5000 rev/min pellet is at most 18% of the latter. From the data of Table 1, this would amount to 4·3 phage equivalents per bacterium, representing 5·5% of the radiosulfur attributed to phage particles in that experiment. Third, antiphage serum precipitates only 4 to 6% of the total radioactivity in the 15,000 rev/min supernatant. This would amount to only 4 units or 13% of the radioactivity attributed to specifically precipitatable protein in the measurements described in Table 1. Most of this is mechanical contamination of the (unwashed precipitate, and is digested almost completely by pancreatin. The corresponding material labeled after infection, on the contrary, is resistant to digestion. (The unprecipitated fraction is sensitive to digestion in both cases.) We conclude that typical bacterial constituents, if formed after infection, do not serve as precursors to phage proteins, and do not interfere with the types of analysis employed in our experiments.

(c) *The separation of phage particles from serologically related materials by centrifugation*

Our separation of phage particles from lighter materials (by three centrifugations at 15,000 rev/min) was adopted after numerous trials of which the one shown in Table 3 is representative. It shows that most of the lighter material is separated by

Table 3

Separation of phage particles from other materials precipitable by antiphage

	Phage per B	^{35}S per B	Difference
Supernatant 1, 15,000 rev/min	0·36	14·8	14·4
Supernatant 2, 15,000 rev/min	0·42	3·2	2·8
Supernatant 3, 15,000 rev/min	0·36	1·6	1·2
Supernatant 4, 10,000 rev/min	1·2	2·0	0·8
Final pellet	2·9	4·3	1·4

Centrifugal fractionation of a culture labeled with ^{35}S for 20 min after infection and lysed at that time. Phage titrations were made before and radio-assays were made after precipitation with antiphage. Radioactivity is expressed in phage-equivalent units of sulfur per bacterium. The final pellet only was digested with pancreatin. The excess of radiosulfur over phage particles in this fraction reflects contamination with bacterial debris, measurable when the phage yield is small. The excess in the supernatant fractions shows the distribution of specifically precipitable protein other than phage particles.

two centrifugations, and that centrifugation at lower speed does not reveal any more)

In another experiment a suspension of labeled phage particles, isolated from a 25 min lysate by our standard procedure, was spun again at 10,000 rev/min. This centrifugation yielded two fractions between which phage particles and labeled protein were identically distributed.

(f) *Test for bacterial proteases*

Since our pulse experiments detect all the intrabacterial precursors of phage protein, appreciable action of bacterial proteases in the lysates cannot have occurred. The following facts confirm that the lysates do not contain proteases that might affect

our results. About 60% of the sulfur of boiled, labeled phage ghosts is rendered acid-soluble by digestion with pancreatin. Less than 1% is made acid-soluble by prolonged incubation in lysates of infected bacteria of the kind described in this paper.

4. Discussion

The experiments described in this paper yield information about the synthesis of proteins that make up the membrane of the phage head, which comprise about 90% of the total protein of the phage particle (Van Vanukis, Baker & Brown, 1958; Brenner *et al.*, 1959). We refer to such protein as head protein, and to the more-or-less intact head membranes as membranes. The principal facts may be summarized as follows.

During the first few minutes after infection of bacterial cultures with phage T2, rapid synthesis of protein continues, but very little of the protein synthesized is phage precursor. Synthesis of head protein begins about 7 min after infection, simultaneously with or shortly after the initiation of synthesis of phage precursor nucleic acid, and well in advance of the completion of the first phage particles at 15 min.

Beginning about 20 min after infection, a steady state of phage growth prevails, characterized by linear rates of formation of phage particles, nucleic acid, and protein (Hershey *et al.*, 1954). During this phase, protein of all kinds is formed at a rate of 3 to 5 phage-equivalent units per bacterium per minute and phage particles are formed at a rate of 2 to 3 per bacterium per minute. Of the total protein synthesized, 60% to 70% is phage precursor. This measure is more reproducible than the absolute rates. The cultures contain about 28 phage-equivalent units per bacterium of phage precursor protein, which forms a pool of constant size characterized by 5 min half-time of incorporation into phage particles.

Phage precursor labeled during the linear phase of phage growth is found in two protein fractions after lysis of the cells; namely, protein identifiable as coat protein by precipitation with antiserum and protein not identifiable in this way, which may be referred to as protein that is specifically precipitable or not, respectively. The two fractions are also distinguished by the fact that the precipitable fraction is resistant to proteases whereas the unprecipitable fraction is sensitive. Of the precipitable protein found in the lysates, about 83% is derived from authentic phage precursors and the remainder represents protein that accumulates in the cultures, at least partly as a result of lysis of some of the cells during the course of the experiment. Of the labeled non-precipitable protein found in the lysates, only 57% is derived from phage precursors, evidently because this fraction includes several proteins some of which are not potential phage precursors. Of the 28 units of precursor protein per bacterium present in the cultures, all are recovered after lysis, about 16 units as specifically precipitable protein and 12 units as non-precipitable protein.

The specifically precipitable protein fraction of the lysates is separable by centrifugation into two subfractions representing head membranes and smaller particles, respectively. The coats make up at least one third of the precipitable protein and very likely more, but these subfractions are poorly characterized. The two subfractions are identical with respect to precursor status. We thus recognize three categories of phage precursor protein: larger and smaller particles serologically identifiable as coat protein, and protein (small particles) that is not serologically identifiable by our methods, each representing 20 to 40% of the phage-precursor protein in the lysates.

When a pulse of radiosulfate is fed to an infected culture in the linear phase of phage growth, radiosulfur enters promptly and almost simultaneously into all three

categories of phage-precursor protein last mentioned, and simultaneously leaves all three at the end of the pulse to enter phage particles with a half-time of 5 min. We conclude, therefore, that most of the small particles of precursor protein found in lysates are not precursors of the large ones, that the phage coat is completed up to the stage at which it becomes sedimentable at 30,000 *g* and recognizable microscopically in a time interval of the order of one minute, and that no further major additions of protein to the coat are made during the ensuing 5 min or so. The origin of the small particles, which also represent coat protein with precursor status, will be returned to presently.

The information summarized above can be combined with information from other sources to yield a reasonably specific pattern of events characterizing the growth of T2.

First of all, phage particles do contain one or more proteins, the "internal antigen" described by Levine, Barlow & Van Vanukis (1958) and the "nonsedimentable protein" of Hershey (1955), that begin to form immediately after infection with T2 (Murakami, personal communication; Minagawa, personal communication). The 7 min delay preceding the appearance of coat protein, therefore, presents a special problem related to the sequential character of morphogenetic processes, and is not characteristic of phage-directed protein synthesis in general.

Kellenberger (1959) has summarized work in progress concerning the morphological aspects of phage growth. In ultra-thin sections of infected bacteria, nucleic acid can be recognized microscopically in two forms; namely, an extended, presumably molecularly dispersed form, and a condensed form exhibiting the polyhedral shape characteristic of finished phage particles. Membrane protein cannot be discerned in the sections. In lysates, finished phage particles and empty head membranes can be enumerated. However, the sum of these two counts is considerably less at early times than the number of polyhedral structures seen in sections. Either many of these lack membranes, or the membranes do not survive lysis as visible structures. The empty heads that can be seen may be presumed to have contained nucleic acid at the time of their formation, and to have lost it subsequent to lysis. This supposition is supported by the finding of partially filled heads in freshly fixed lysates (of cultures containing proflavin), which rapidly lose their contents on storage before fixation (Brenner, cited by Kellenberger, 1959).

Some chemical investigations of coat protein are also pertinent here. Van Vanukis *et al.* (1958) find a single subunit structure of molecular weight about 80,000 in the head membrane of T2. Similar conclusions have been reached by preliminary application of the "fingerprint" method to the head protein of T2 (Brenner *et al.*, 1959).

Our finding that small particles of head protein are not mainly precursors of the larger particles is difficult to understand if the several protein fractions recognized by us are distinctive precursors of phage particles. To describe our results on this basis it would be necessary to say that three roughly equal amounts of protein persist separately in the cell for about 5 min and then come together to form a phage particle in about 1 min. On this interpretation the empty phage heads found in lysates should contain only about one-third as much sulfur per particle as the finished phage, whereas the actual measurement (for proflavin lysates) is 75% (DeMars *et al.*, 1953). Moreover, it is difficult to envisage the formation of three distinctive precursors from one subunit protein. We prefer, therefore, the following interpretation of our results.

The membrane of the phage head is formed virtually complete from amino acids in about 1 min, contains most of the protein intended for one phage particle, and thus

represents the principal phage-precursor protein structure. Only about 20% of the total phage-precursor protein in the cells consists of small particles that are intermediates in the formation of this structure. At the time of its formation, the head membrane is filled with nucleic acid but is an unstable structure, breaking down when the cell lyses to yield free nucleic acid and a variety of protein fragments, including more or less intact head membranes and smaller particles, many of them (for reasons not clear) not precipitable by antiphage and sensitive to proteolytic action. For a space of about 5 min, the head structure persists in this unstable state inside the bacterium and then is completed, during an interval of about 1 min and without

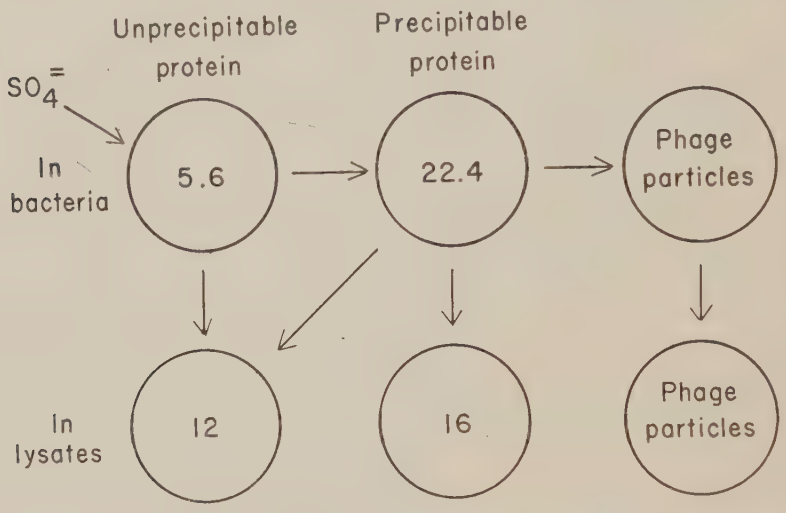

FIG. 8. Phage precursor proteins inside infected bacteria and in lysates. Precipitable means precipitable by antiphage. The numbers express phage-equivalent units of protein per bacterium during the linear phase of phage growth.

major additions of protein, to yield the stable, infective phage particle. It seems therefore that the terminal steps in the formation of a phage particle are not confined to the addition of tail parts, as might be supposed, but call for qualitative changes in the head membrane as well. The quantitative aspects of this model are summarized in Fig. 8 in terms of numbers that are not, of course, to be taken as literally exact.

The interpretation given above raises two related questions. Why is the stability of the unfinished phage particle unchanging during most of its lifetime and what, in fact, is it doing during this time? Some of our results have a certain bearing on these questions. One might ask, for instance, whether the 5 min half-time of a newly formed phage head is spent mainly in waiting for a rapid series of events that converts it into a phage particle, or whether the time is occupied by these events. The first alternative is suggested by our finding that the acquisition of stability is not progressive but seemingly all-or-none. It is suggested more strongly by the finding that the half-time of transfer of radioactivity from the incomplete structures of phage particles is the same whether all of the unfinished structures are labeled (Fig. 3), or only some of the more recently formed individuals (Fig. 6). In fact, if the unfinished phages were ordered, one would expect the descending curves in Fig. 6 to be concave toward the origin. The observed results seem to mean that the decision as to which phage particle

is to be completed next is made by a random choice amongst the majority of still unfinished particles.

Perhaps the most interesting question that might be raised at this time is the following. Are the protein subunits that are to be incorporated into a given phage particle synthesized in the neighbourhood of that particle, or are they formed at large and later transported to the particle? In the latter case the cells would have to contain low molecular weight protein that is precursor to the large particles. Our experiments suggest that there is a small amount of such protein, since in the pulse experiments radioactivity enters protein that is not precipitable by antiserum about 1 min before it appears in precipitable protein. The amount of such protein measures perhaps 20% of the total phage precursor protein, or 5·6 phage equivalent units per bacterium, which would yield a concentration of the order 0·1 g/l. if dissolved in the cell sap. The formation of a head membrane in 1 min by deposition of protein from such a solution may seem unlikely but the mechanism cannot be excluded on this basis.

The status of the phage-precursor nucleic acid is somewhat clarified by the new findings. Nearly all of the nucleic acid formed in infected cells is phage-precursor, synthesized about 10 min in advance of its incorporation into phage particles, and forming a phage-precursor pool containing about 45 phage-equivalent units per bacterium (Hershey & Melechen, 1957). Our present results confirm the suggestions of these authors and of Kellenberger (1959) that the precursor nucleic acid shares two pools, one representing free nucleic acid (which can accumulate in the presence of chloramphenicol), the second representing nucleic acid associated with protein. Moreover, since our experiments show that the individual phage head is completed very quickly, the association between nucleic acid and protein in the cell must be unit for unit, independently of the detailed interpretation of the results. Thus the average cell (in steady state cultures of the kind described in this paper) must contain about 28 phage-equivalent units of nucleic acid already condensed inside unfinished phage membranes, and only 17 units in the free state, presumably replicating and accessible for the matings that produce genetic recombinants. The generation time in our cultures, computed for geometric growth by twos, is 17 divided by 2 to 3 per min, or 6 to 9 min. In nutrient broth cultures the growth is faster and the pool size about double the figures cited (Hershey, 1953). For such cultures estimates by genetic methods suggest a mating pool of 30 to 46 units per bacterium (Levinthal & Visconti, 1953; Hershey, 1958). The agreement between the genetic and chemical estimates, therefore, is now very satisfactory.

We are indebted to Dr. Catherine Roesel and Dr. Lawrence Levine for generous gifts of antiserum.

REFERENCES

Anderson, T. F., Rappaport, C. & Muscatine, N. A. (1953). *Ann. Inst. Pasteur*, **84**, 5.
Brenner, S., Streisinger, G., Horne, R. W., Champe, S. P., Barnett, L. & Benzer, S. (1959). *J. Mol. Biol.* **1**, 281.
DeMars, R. I. (1955). *Virology*, **1**, 83.
DeMars, R. I., Luria, S. E., Fisher, H. & Levinthal, C. (1953). *Ann. Inst. Pasteur*, **84**, 113.
Hershey, A. D. (1953). *J. Gen. Physiol.* **37**, 1.
Hershey, A. D. (1955). *Virology*, **1**, 108.
Hershey, A. D. (1956). *Brookhaven Symp. Biol.* **8**, 6.

Hershey, A. D. (1957). *Virology*, **4**, 237.
Hershey, A. D. (1958). *Cold Spr. Harb. Symp. Quant. Biol.* **23**, 19.
Hershey, A. D., Garen, A., Fraser, D. K. & Hudis, J. D. (1954). *Yearb. Carneg. Instn.* **53**, 210.
Hershey, A. D. & Melechen, N. E. (1957). *Virology*, **3**, 207.
Hogness, D. S., Cohn, M. & Monod. J. (1955). *Biochim. biophys. Acta*, **16**, 99.
Kellenberger, E. (1959). *Symp. Soc. Exp. Biol.* (in press).
Kellenberger, E. & Séchaud, J. (1957). *Virology*, **3**, 256.
Lanni, Y. T. (1954). *J. Bact.* **67**, 640.
Lehman, I. R., Zimmerman, S. B., Adler, J., Bessman, M. J., Simms, E. S. & Kornberg, A. (1958). *Proc. Nat. Acad. Sci., Wash.* **44**, 1191.
Levine, L., Barlow, J. L. & Van Vanukis, H. (1958). *Virology*, **6**, 702.
Levinthal, C. & Fisher, H. (1952). *Biochim. biophys. Acta*, **9**, 419.
Levinthal, C. & Visconti, N. (1953). *Genetics*, **38**, 500.
Maaløe, O. & Symonds, N. (1953). *J. Bact.* **65**, 177.
Meselson, M. & Stahl, F. W. (1958). *Proc. Nat. Acad. Sci., Wash.* **44**, 671.
Tomizawa, J. (1958). *Virology*, **6**, 55.
Van Vanukis, H., Baker, W. H. & Brown, R. K. (1958). *Virology*, **5**, 327.
Watanabe, I. (1957). *J. Gen. Physiol.* **40**, 521.
Watanabe, I., Stent, G. S. & Schachman, H. K. (1954). *Biochim. biophys. Acta*, **15**, 38.
Watson, J. D. & Crick, F. H. C. (1953). *Nature*, **171**, 737.

J. Mol. Biol. (1959) **1**, 277-280

Further Studies on the Electron Microscopy of the *Tipula* Iridescent Virus

Kenneth M. Smith and G. J. Hills

Agricultural Research Council, Virus Research Unit, Huntingdon Road, Cambridge, England

(*Received 23 June 1959*)

In a study on the electron microscopy of the *Tipula* iridescent virus (TIV), a number of staining techniques were employed. The aspects particularly investigated were the empty particles which occur in the early stages of infection, the membranes surrounding the particles and the protein subunits. For this purpose phosphotungstic acid was the most successful stain and its use revealed the apparent presence of two membranes enclosing the virus particle. By using virus from abnormal hosts it was possible to show that the icosahedral faces of the virus particle were made up of numbers of small subunits.

1. Introduction

The *Tipula* Iridescent Virus (TIV) is of comparatively large size, shows great uniformity and is easily available in large quantities (Williams & Smith, 1957, 1958). These properties make the virus a suitable one for electron microscopy and we have used a variety of techniques and stains towards this end.

We wished particularly to investigate the empty particles which occur in considerable numbers in the infected fatbody in the early stages of the disease (Smith, 1958), the membrane surrounding the virus particles (Smith, 1956) and, if possible, the protein subunits which make up the virus icosahedron.

In cross-transmission experiments it has been shown (Smith & Rivers, 1959) that the host range of TIV is very wide, and we have used virus from some unusual insect hosts to investigate possible structural differences which might occur between virus from the normal host, and virus from an abnormal host.

2. Materials and Methods

The virus used was obtained from larvae of the following insects: (Diptera) *Tipula paludosa, T. oleracea, T. livida, Bibio marci* and *Calliphora vomitoria;* (Lepidoptera) *Pieris brassicae;* (Coleoptera) *Tenebrio molitor*. The fatbody of larvae in different stages of the disease was isolated by dissection and fixed for thin sectioning. In addition whole virus particles treated in various ways were examined. The diseased fatbody or centrifuged pellets were fixed in 1% osmic acid buffered at pH 6·8 with citrate buffer. At this stage the material was treated with a stain, dehydrated in alcohols and embedded in methacrylate or araldite (Glauert & Glauert, 1958). To observe early stages of the disease, material was fixed in neutralized formalin or 1% phosphotungstic acid buffered at pH 5·4, with phthalate buffer.

After fixation in osmic acid various stains were used to observe either steps in the multiplication of the virus or detail present in the virus particles. The stains used were 1% phosphotungstic acid at pH 5·4 (Selby, 1955), 1% phosphomolybdic acid buffered at pH 5·4 with phthalate buffer, chrome gallocyanin dye for 24 hr (Bahr, 1953), 0·1 M-ferric chloride for 15 min after washing the material in 0·9% sodium chloride for 15 min (Berstein, 1956), mercuric bromophenol blue for 1 hr (Harris & Mazia, 1959), 0·5% uranium acetate buffered at pH 6·1 with veronal acetate buffer of Michaelis (Kellenberger, Ryter & Séchauld, 1958), 2% lead acetate for 15 min (K. R. Porter, personal communication).

Single virus particles were studied by spraying the particles with 2% phosphotungstic acid adjusted to pH 7·0 with potassium hydroxide (Brenner & Horne, 1959).

The electron microscope was a Siemens Elmiskop I.

3. Results

For study of the earliest stages of the disease, which were selected by electron microscopy, formalin-fixed fatbody was found to give best results. Using this fixation technique early stages in the formation of the icosahedral shell are apparent. Large quantities of hexagonal shells 1,200 to 1,400 Å in diameter are found where an infected area meets an uninfected area of fatbody. As seen from Plate I(a) the shells have the same granulated appearance as the cytoplasmic background, while the appearance of the shell surrounding the mature particle is quite different. A later stage fixed in osmic acid is shown in Plate I(b). Mature virus particles are almost wholly absent but the amount of fat present is decreasing. The fat decreases as the amount of virus increases although only in the larvae of *Tenebrio molitor* have the virus particles been observed inside the fat globules. Early stages of the virus, either fixed in phosphotungstic acid or stained in phosphotungstic acid after osmic fixation, show thread-like material present in the shells which cannot be observed in the mature particle (Plate II(a)). By partially stripping the protein from the tobacco mosaic virus rod Hart (1958) demonstrated the presence of threads of ribonucleic acid. A somewhat similar phenomenon has been shown with the TIV particle. Thin sections of the virus particle stained in phosphotungstic acid or uranium acetate revealed the presence of numerous threads presumably of deoxyribonucleic acid (Plate III (a)). However, since it had been observed that the TIV from *T. livida* seemed to be more fragile than the virus from its natural host, *T. paludosa*, micrographs were made of whole virus particles from *T. livida* negatively stained with phosphotungstic acid. In Plate III (b) are three particles, partially broken down, showing beaded strings or helices of DNA surrounding them.

In sections of the mature particle, observed at a later stage of the disease (Plate II(b)), it appears as two concentric hexagons, the inner hexagon being formed by the stained junction between the contents and the membrane. In sections of empty particles of the TIV stained with phosphotungstic acid at pH 5·4, one membrane of $\sim$ 150 Å thickness is resolved.

Using the negative staining technique with neutralized phosphotungstic acid, empty particles at high resolution appear to have two membranes 40 Å thick separated by a space of 40 Å. The particles and the space between the two membranes are filled with phosphotungstic acid and appear dark (Plate IV (a)). Suggestions have been made that the double membrane appearance may be produced by an optical phenomenon. The TIV from *Bibio marci* seems unstable when added to neutralized phosphotungstic acid and rupture of the membranes takes place, but in some cases part of the outer membrane is removed while the inner one remains intact. This seems to suggest that the second membrane does actually exist.

In thin sections of TIV particles from *Tipula paludosa* stained with phosphotungstic acid, and also in particles negatively stained, it is possible to make out individual units on the surface of the virus particle. High resolution micrographs of virus from *B. marci*, negatively stained do show a regular arrangement of the protein subunits, the icosahedral faces being made up of small subunits (Plate IV (b)). Similar subunits have been observed on virus particles obtained from larvae of the white butterfly, *Pieris brassicae*.

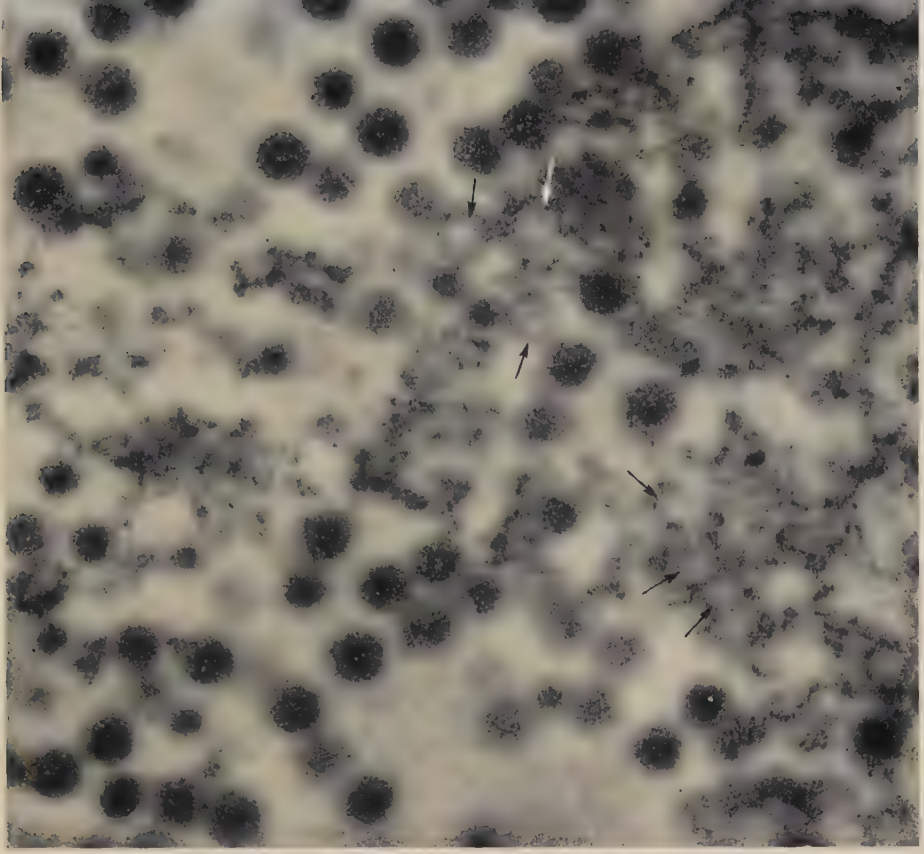

PLATE I(a). Ultrathin section of fatbody, fixed in formalin, from the larva of *Tipula paludosa* in an early stage of infection with TIV; note the apparent development of empty shells. (× 53,000).

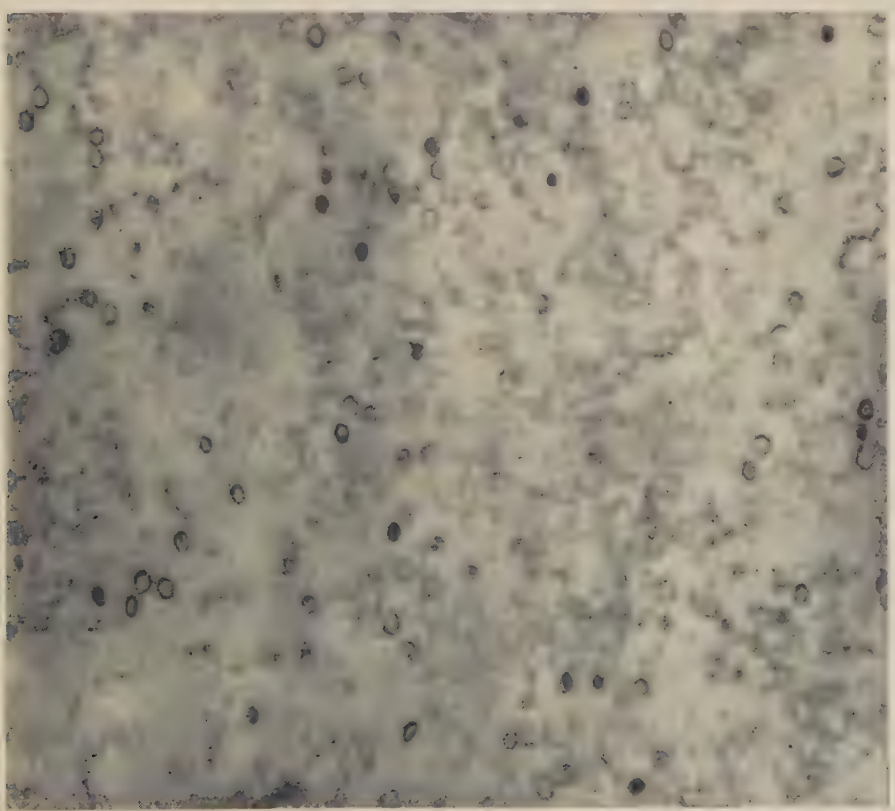

PLATE I(b). Similar to Plate I(a), but fixed in osmic acid; note the large numbers of empty shells and absence of mature virus particles. (× 20,000).

[*To face page* 278.

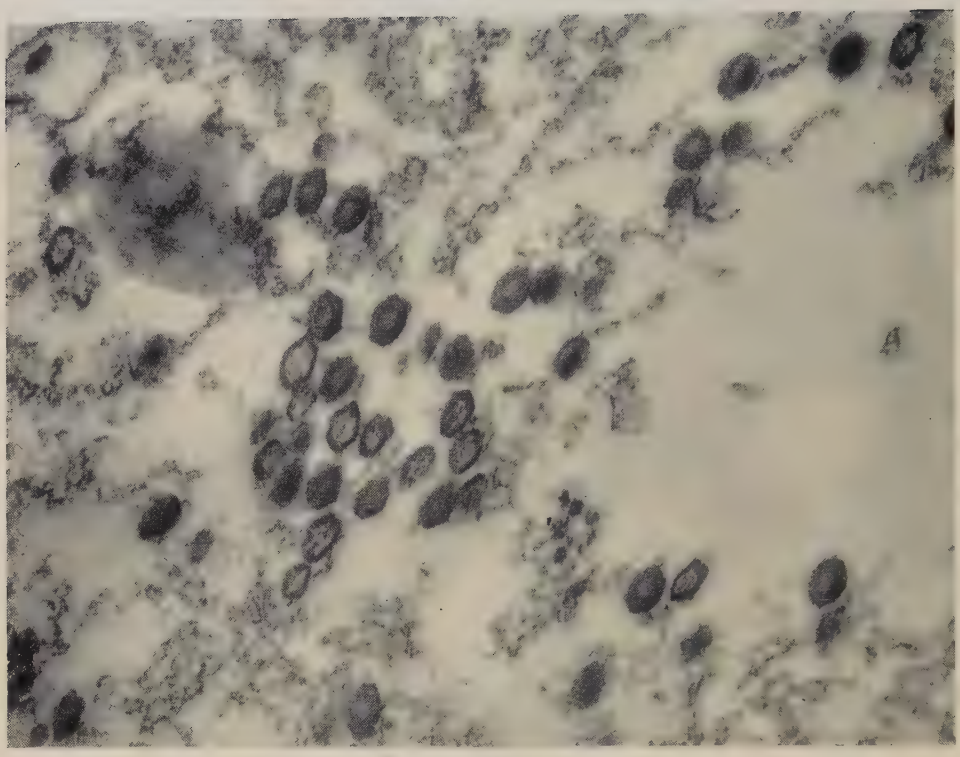

PLATE II(a). Similar to Plate I(b), but fixed in osmic acid and stained with phosphotungstic acid; note the threads in some partially empty particles. ($\times$ 60,000).

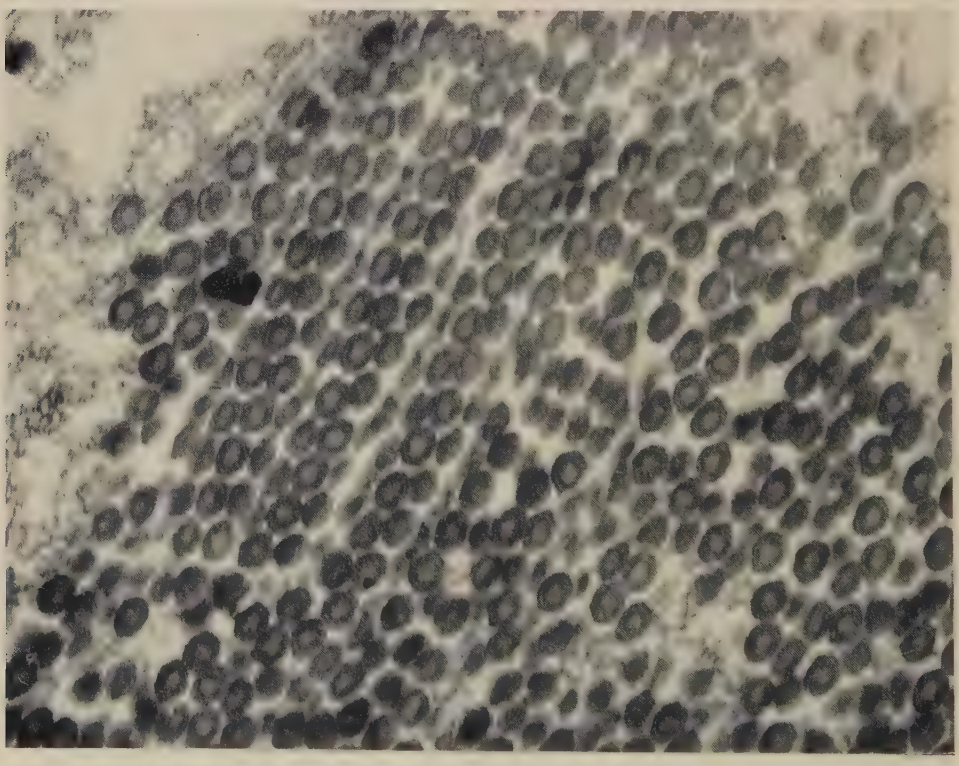

PLATE II(b). Similar to Plate II(a), but at a late stage of the disease; note the absence of empty shells, and that the particles, which appear as concentric hexagons, are becoming orientated. ($\times$ 60,000).

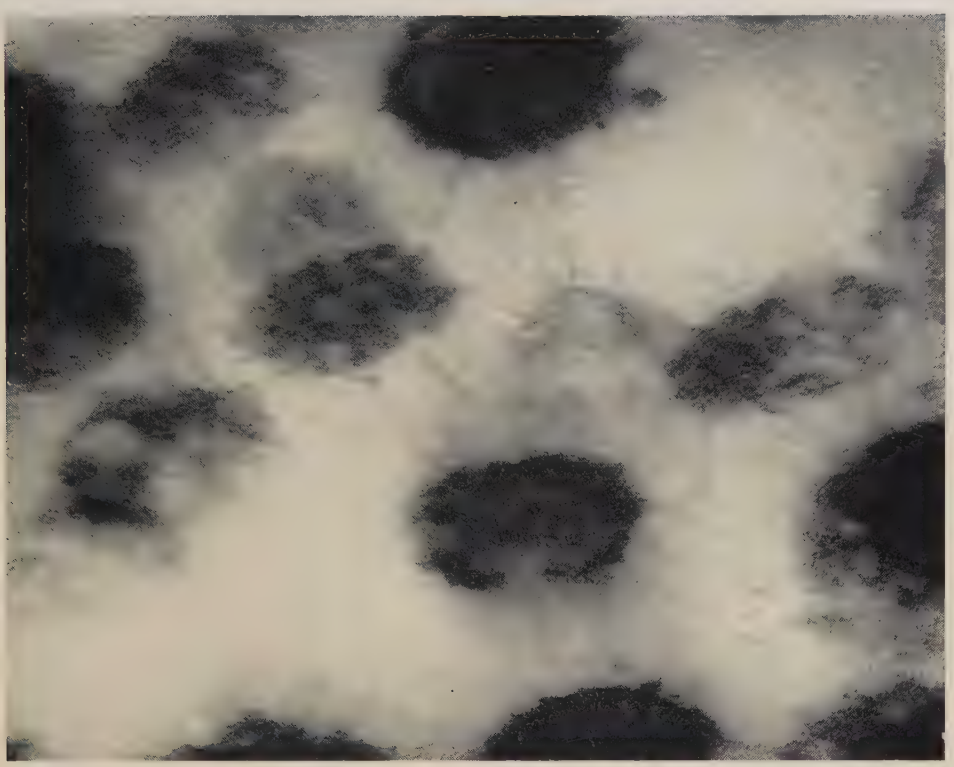

PLATE III(a). Thin sections of TIV particles (ex *Tipula paludosa*) fixed and stained with aqueous phosphotungstic acid; note the numerous threads presumably of deoxyribonucleic acid. ($\times$240,000).

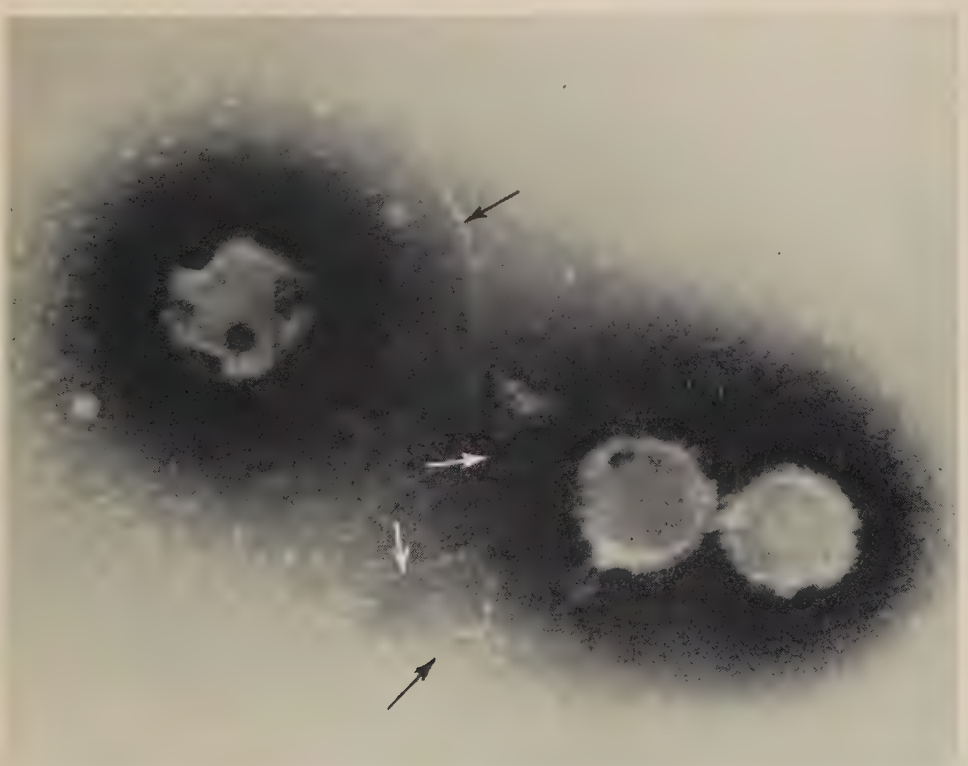

PLATE III(b). Three virus particles from *Tipula livida* negatively stained with phosphotungstic acid; the particles are partly broken down and show beaded strings or helices of deoxyribonucleic acid. ($\times$ 120,000).

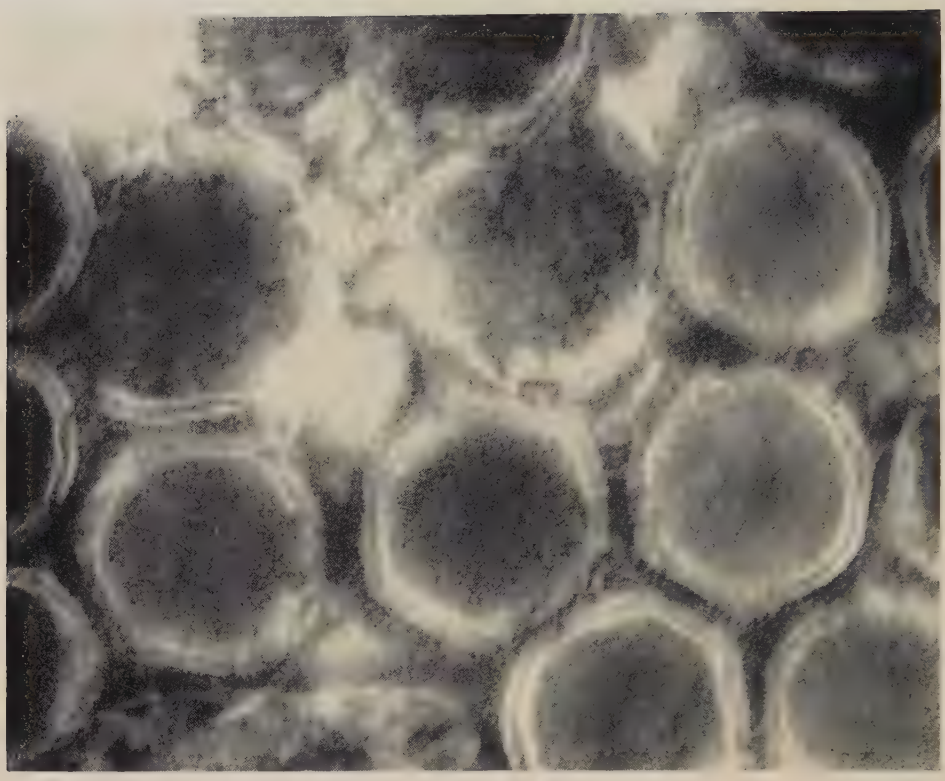

PLATE IV(a). TIV particles negatively stained with phosphotungstic acid; the empty particles are seen to have two membranes 40 Å thick separated by a space of 40 Å. The empty particles and the space between the two membranes are filled with phosphotungstic acid and appear dark. (× 240,000).

PLATE IV(b). High resolution micrograph of virus from the larvae of *Bibio marci*, negatively stained with phosphotungstic acid; note the regular arrangement of the protein subunits. (× 480,000).

4. Discussion

The occurrence of empty shells or incomplete particles is now a well-recognized phenomenon with many viruses, and has been observed with the viruses of influenza (Birch-Andersen & Paucker, 1959), of the Lucké renal adenocarcinoma (Fawcett, 1956), and of the turnip yellow mosaic (Markham & Smith, 1949). It is on the interpretation of the significance of these empty or partially empty shells that opinion is divided. Birch-Anderson & Paucker (1959), working with incomplete particles of influenza virus, say that it is not known "whether they represent intermediates which have been blocked at a more advanced stage in the reproductive process or whether they may be aberrant forms altogether."

Careful study of the empty forms of TIV suggests very strongly that they are stages in the reproduction of the virus. This is borne out by the following facts; first. empty or partially empty shells occur predominantly in the early stages of the disease, In some sections, indeed, practically no mature virus particles are visible but large numbers of empty shells occur (Plate I (b)). Secondly, what appear to be stages in the development of the contents of the particles can be seen. These vary from a few threads (Plate II (a)) to a darkly staining body concentrically placed.

The criticism has been made that it is unlikely that the outer membrane is formed first and the nucleic acid subsequently introduced; this may be a valid criticism, but we have never observed anything suggestive of a primary particle forming first and later enclosed in a membrane. On the contrary, in formalin-fixed material it is possible to see the membranes apparently forming out of the granular substrate of the cytoplasm (Plate I (a)).

The suggestion has also been put forward that the nucleic acid has been expelled from the particles during the preparation of the material for electron microscopy, and further that in the early stages of the disease the virus is likely to be soft and more susceptible to injury. This also seems unlikely, first because of the tough membrane encircling the particle which is highly resistant to changes in pH, and secondly because the central core most probably does not consist of nucleic acid alone but contains protein in addition. There seems no reason to suppose that both these would be expelled in so wholesale a manner.

The cross-transmission of an insect virus between three different orders of insects is, so far as we know, unique and it is interesting to find that the TIV can propagate itself in such different hosts. Superficially the virus particles from the various insects resemble each other, but there are differences. For example, the iridescent colour of the virus pellet varies according to the host source; it is green from *Pieris brassicae*, blue from *Tipula livida* and violet from the natural host *T. paludosa*. This suggests a slight difference in size and in consequence a different degree of packing in the crystal. Moreover, when centrifuged in a sucrose gradient the rate of sedimentation differs when the virus comes from different hosts. We have also noticed that the virus particles in the larvae of *Bibio marci* are slightly less perfect in formation than those from *T. paludosa*, and decidedly more fragile when treated with phosphotungstic acid. The membranes surrounding the particles fracture in a manner never observed with virus from *T. paludosa*, and from this we get some support for the suggestion that the apparent second membrane does in fact exist.

REFERENCES

Bahr, G. F. (1953). *Exp. Cell Res.* **5**, 551.
Bernstein, M. H. (1956). *J. Biophys. Biochem. Cytol.* **2**, 633.
Birch-Andersen, A. & Paucker, K. (1959). *Virology*, **8**, 21.
Brenner, S. & Horne, R. W. (1959). *Biochim. biophys. Acta*, **34**, 103.
Fawcett, D. W. (1956). *J. Biophys. Biochem. Cytol.* **2**, 725.
Glauert, A. M. & Glauert, R. H. (1958). *J. Biophys. Biochem. Cytol.* **4**, 191.
Harris, P. & Mazia, D. (1959). *J. Biophys. Biochem. Cytol.* **5**, 343.
Hart, R. G. (1958). *Biochim. biophys. Acta*, **28**, 457.
Kellenberger, E., Ryter, A. & Séchauld, J. (1958). *J. Biophys. Biochem. Cytol.* **4**, 671.
Markham, R. & Smith, K. M. (1949). *Parasitology*, **39**, 330.
Selby, C. C. (1955). *J. Biophys. Biochem. Cytol.* **1**, 429.
Smith, K. M. (1956). *J. Biophys. Biochem. Cytol.* **2**, 301.
Smith, K. M. (1958). *Parasitology*, **48**, 459.
Smith, K. M. & Rivers, C. F. (1959). *Virology*, **9**, 140.
Wlliams, R. C. & Smith, K. M. (1957). *Nature*, **179**, 119.
Wiilliams, R. C. & Smith, K. M. (1958). *Biochim. biophys. Acta*, **28**, 464.

J. Mol. Biol. (1959) **1**, 281-292

Structural Components of Bacteriophage

S. Brenner†, G. Streisinger†[1], R. W. Horne§, S. P. Champe†[2], L. Barnett†, S. Benzer†[3] and M. W. Rees‖

† *Medical Research Council Unit for Molecular Biology and* § *Electron Microscope Group, Cavendish Laboratory, and* ‖ *Department of Biochemistry, University of Cambridge, Cambridge, England*

(*Received 23 July 1959*)

A procedure is described for the efficient disjoining of the even-numbered T bacteriophages into structural components. Tail fibres and tail sheaths from T2L have been separated and purified, and sheaths can be obtained from the other T-even phages. The components have been characterized by electron microscopy using the phosphotungstate method and by chemical and physical methods. The tail of the bacteriophage consists of a sheath surrounding a core at the base of which are attached tail fibres. The sheath appears to be built of helically arranged subunits which form a hollow cylinder. We have confirmed that the sheath can contract in length, and have shown that the contraction is accompanied by an increase in diameter such that the volume of the sheath is approximately conserved. The core of the tail has been found to be a hollow cylinder with the central hole 25 Å in diameter.

Chemical studies, using fingerprinting, suggest that the sheath is composed of about 200 repeated subunits of approximately 50,000 molecular weight. No N-terminal amino acid could be detected in sheaths. Fingerprints confirm the previous finding that the head membrane of the phage is composed of a large number of repeated subunits with a molecular weight of 80,000. The tail fibres appear to have a subunit with a molecular weight not less than 100,000. These studies show that the proteins composing the head, sheath and tail fibres of the phage have different primary structures.

1. Introduction

Bacteriophages, once regarded as simple nucleoprotein particles, are now known to be amazingly sophisticated in structure. Phages of the T-even group (T2, T4, T6) are tadpole-shaped, the head having the form of a bipyramidal hexagonal prism (Anderson, 1946; Williams & Fraser, 1953), while a cylindrical tail is the organ of attachment of the phage to its host cell (Anderson, 1953; Kellenberger & Arber, 1955; Williams & Fraser, 1956). The demonstration that the head and tail contain distinct antigens suggests that these morphological parts are made of different proteins (Levinthal & Fisher, 1952; Lanni & Lanni, 1953; De Mars, Luria, Levinthal & Fisher, 1953; Anderson, Rappaport & Muscatine, 1953).

Recent work has shown that the tail itself is a complex structure. Kozloff & Henderson (1955), Kellenberger & Arber (1955) and Williams & Fraser (1956) reported structural changes of the tail produced by treatment of the phage with cadmium

[1] Fellow of the National Foundation for Infantile Paralysis on leave of absence from the Department of Genetics, Carnegie Institution of Washington, Cold Spring Harbor, Long Island, N.Y., U.S.A.

[2] Research Fellow of the Purdue Research Foundation on leave of absence from the Department of Biological Sciences, Purdue University, W. Lafayette, Indiana, U.S.A.

[3] Senior Postdoctoral Fellow of the National Science Foundation on leave of absence from the Department of Biological Sciences, Purdue University, W. Lafayette, Indiana, U.S.A.

cyanide, hydrogen peroxide and freezing and thawing respectively. The most striking alteration, as revealed in the electron microscope, is a shortening of the outer layer (the sheath) of the tail, revealing an inner core coaxial with the sheath, which displays at its distal tip a small diffuse structure and a number of outstretched fibres. Apparently some degree of fragmentation of the phage is effected by these treatments, since isolated cores and fibres are also observed.

The proteins of bacteriophage are of particular interest because they might offer favourable material for studying the genetic control of protein structure. The high resolving power of genetic analysis in phage makes it possible to construct maps of the genetic structure on the molecular level, as exemplified by the work of Benzer (1955, 1957) with the r_{II} mutants of bacteriophage T4. The relevant protein in this case has not been found, and does not appear to be an integral part of the phage structure. However, other regions of the genetic structure do affect proteins of the phage particle. The *h* region of T2L controls the serological specificity of the phage with respect to inactivating antiserum, and also its ability to attach to specific bacterial cells (Streisinger, 1956*a*,*b*; Streisinger & Franklin, 1956). It seems likely that this genetic region controls a protein of the tail fibres, since the fibres attach to bacterial hosts with the same specificity as the whole phage particle from which they are derived (Williams & Fraser, 1956). A particular advantage of this protein is the possibility of assaying it by its ability to block inactivating antiserum. Also promising are the *c* mutations of bacteriophage T4, which cause L-tryptophan to be required for attachment of the phage to the bacterium (Anderson, 1945, 1946; Delbruck, 1948; Wollman & Stent, 1950). The *h* and *c* mutations are localized within small and separate regions of the genetic map, each segment forming a functional unit or cistron (Streisinger & Franklin, 1956; Brenner, 1957). It is probable that the protein affected by the *c* mutations is also part of the tail (Ping-Yao Cheng, 1956). We have therefore attempted to isolate and characterize the structural components of the T-even phages in order to assess their suitability for analysis on the chemical, as well as genetical, levels.

In this paper we describe a technique for disjoining the components of the phage particle more effectively than the methods previously described; this has made possible the purification of tail fibres and tail sheaths. A study of the morphological and chemical properties of these and other phage components shows that the protein coat of the bacteriophage is a complex superstructure, built from different kinds of structural elements, each consisting of distinct proteins. In other papers we will deal with the serological and functional properties of the components and their genetic control.

2. Materials and Methods

Phages. T2, strains T2L (Luria) and T2H (Hershey), T4, strain T4B (Benzer), and T6 were used.

Bacteria. Escherichia coli, strain B was used for all assays and *E. coli* strain BB (Berkeley) for growth of phages.

Phage techniques. The methods of handling phages were those described by Adams (1959). Serum blocking power assays were carried out by the procedure described by De Mars (1955).

Hydroxyapatite columns were prepared following the directions of Tiselius, Hjertén & Levin (1956).

Enzymes were the crystalline products of Worthington Biochemical Corporation, Freehold, N.J.

(a) *Growth and purification of large amounts of phage*

Two methods were used to produce phage on a large scale. In the first, 35 l. cultures of *E. Coli* BB grown in M9 medium (Adams, 1959) to a cell count of 3×10^8/ml. were infected with 10^6 phage particles per ml. Aeration was continued for 3 hr, at which time the cells were artificially lysed by the addition of 1 l. of chloroform. Such lysates yielded a phage titre of 1 to 2×10^{11}/ml. Lysates of T2L could be concentrated by the acid precipitation technique described by Herriott & Barlow (1952). However, this technique was not successful with T4 or T6 strains and gave erratic results with T2L. The second and preferred method was to grow the phage in 5 l. batches in a simplified form of the apparatus designed by Fraser (1951). Using the medium 3XD (Fraser & Jerrel, 1953) *E. coli* BB was grown under vigorous aeration to a concentration of 2×10^9 cells/ml. and infected with 10^7 phage per ml. Artificial lysis with chloroform at $3\frac{1}{2}$ to 4 hr after infection yielded extremely viscous lysates containing from 0·6 to $1{\cdot}5 \times 10^{12}$ phage/ml. After reducing the viscosity by the addition of a small amount of deoxyribonuclease (DNase) the phage was purified from the lysate by cycles of low and high speed centrifugation until clean phage pellets were obtained. To avoid ghosting, phage pellets were resuspended slowly in phosphate buffer pH 7·0 in the cold, in a total volume of about 500 ml. Each 5 l. batch generally yielded between $\frac{1}{2}$ and 1 gm of purified phage.

(b) *Electron microscopy*

Samples were prepared for electron microscopy in one of the following ways: (1) Solutions of phage or components in a volatile buffer (1% ammonium acetate or 2% ammonium bicarbonate) were sprayed onto nitrocellulose-coated grids and shadowed with chromium metal at a 60° angle. (2) Phosphotungstate (PTA) "embedded" preparations were made according to the procedure previously described (Brenner & Horne, 1959). The sample, in 1% ammonium acetate, was mixed with an equal volume of a 2% aqueous solution of phosphotungstic acid previously adjusted to pH 7·0 with N-KOH, and the mixture sprayed onto carbon-coated grids. Metal shadow casting (in method (1)) and carbon evaporation (in method (2)) were carried out in an experimental evaporator unit (Cosslett & Horne, 1957) using mercury diffusion pumps and traps to reduce possible oil vapour contamination.

A Siemens Elmiskop was used at instrumental magnifications of 8,000, 40,000 and 80,000. To minimize heating effects which were observed in the droplet patterns of PTA preparations when employing single condenser lens illumination, double condenser illumination was used, and the illuminating beam reduced to 25 to 30 microns in diameter. Through-focal series were taken during the investigation of the components to ensure that the structures observed in the micrographs were not due to electron phase contrast effects.

Ultracentrifugation was performed in a Spinco Model E centrifuge.

Electrophoresis was performed in a Perkin-Elmer Tiselius apparatus after overnight equilibration of the sample with the buffer solution by dialysis.

(c) *Preparation of samples for "fingerprinting"*

Proteins were digested with enzymes in one of two ways. When large amounts were available, the denatured protein, suspended in water, was adjusted to pH 8·0 at 30°C. An amount of enzyme (trypsin or chymotrypsin in 0·001 N-HCl) equal to 1% of the weight of the protein substrate was added, and the course of peptide bond hydrolysis was followed by recording the amount of sodium hydroxide required to maintain the pH at 8·0. Digestions with trypsin were essentially complete in 90 min, but chymotrypsin digestions required some hours. For smaller quantities the denatured protein was digested in 2% ammonium bicarbonate which buffers at pH 8·0. A drop of acetic acid was then added and the volatile salt removed by lyophilization. One-dimensional ionophoretic separation of peptides was carried out on Whatman 3MM paper using pyridine-acetic acid buffer pH 6·4 (Michl, 1951). For two-dimensional separations, or fingerprinting, Ingram's procedure was followed (Ingram, 1958).

3. Experiments and Results

(a) *Purification of tail components*

Kozloff, Lute & Henderson (1957) reported that cadmium cyanide, $Cd(CN_3)^-$, removed the tail fibres from T2, as judged by electron micrographs, and failure to recover all of the serum blocking power (SBP) in high speed pellets of treated phage. In our hands this technique did not yield free fibres from T2L or T2H. After treatment of the phage with 0·0062 M-$Cd(CN_3)^-$, less than 3% of the SBP remained in the supernatant after high speed centrifugation, while controls showed that the reagent inactivated the phage but did not appreciably reduce the total SBP. Electron micrographs of $Cd(CN_3)^-$ treated phage prepared by the PTA method showed that tail fibres remained attached to most of the altered particles. We have made several attempts to disjoin phage by freezing and thawing following the procedure of Williams & Fraser (1956), but very poor yields of free components were obtained. The method which was developed for efficient disjoining of phage T2L and purification of several of its components is as follows (Fig. 1). Purified phage suspensions in 0·1 M-NaCl were added to an equal volume of 0·2 M-glycine-HCl buffer with 0·1 M-NaCl at pH 2, and the pH adjusted to 2 if necessary. A precipitate of DNA and protein is obtained. This precipitate gave a very viscous suspension when reneutralized due to the liberation of DNA from the phage heads. Digestion with DNase reduced the viscosity, but did not solubilize the phage protein, which was collected by low speed centrifugation. The morphology of the altered phage in this precipitate cannot be easily studied with the electron microscope. However, the precipitate can be dispersed by brief treatment with 8 M-urea (5 min at room temperature) followed by dilution and dialysis against 1% ammonium acetate. Plate I is an electron micrograph of this material showing clumps of altered phage particles aggregated by damaged heads. Sheaths, cores, and tail fibres may be seen, indicating that the phage had been disjoined, but attempts to extract the components were unsuccessful at this stage. Digestion of the precipitate with trypsin or chymotrypsin at pH 8·0 (50 μg/ml. in 2% ammonium bicarbonate) results in rapid clearing of the suspension, leaving little insoluble material. Plate II(a) is an electron micrograph of such a digest showing that the damaged heads have been completely dissolved leaving a solution of contracted free sheaths, cores and tail fibres.

Removal and purification of the sheaths, which sediment at 100,000 *g* in 1 hr, was accomplished by differential centrifugation. Resuspension of the sheath pellet, in 1% ammonium acetate pH 6·5, will generally aggregate any non-sheath material, which can then be removed by low speed centrifugation. Recentrifugation of the sheaths yields almost completely translucent pellets.

Chromatographic separation of the tail fibres from the remaining mixture of fibres, cores and head peptides was achieved by chromatography on a hydroxyapatite column. The suspension was dialysed against 0·01 M-phosphate buffer (pH 6·8) and the precipitate discarded. The solution was then absorbed to a hydroxyapatite column, washed exhaustively with 0·01 M-phosphate buffer, and eluted in a stepwise manner with increasing concentrations of phosphate buffer at the same pH. Over 90% of the input protein (head peptides) was removed from the column by the initial washing. The tail fibres, detected by electron microscopy and serum blocking power assays, eluted between 0·08 and 0·12 M buffer concentrations. Alternatively, adsorption and elution can be performed as a batch process, washing the hydroxyapatite by centrifugation. An electron micrograph of purified tail fibres is shown in Plate II(b).

PLATE I. Electron micrograph of pH 2·0 treated T2L phage, dispersed with urea. (Chromium shadowed, × 50,000.)

[*To face page* 284.

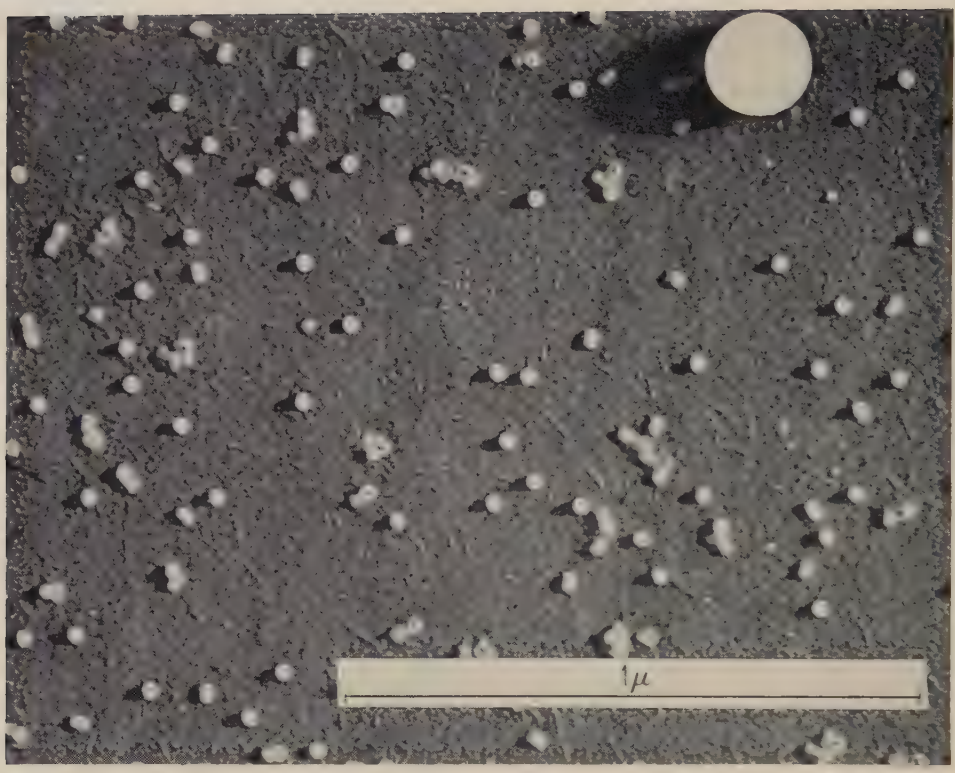

PLATE II(a). Electron micrograph of pH 2·0 treated T2L, digested with chymotrypsin. (Chromium shadowed, · 75,000.)

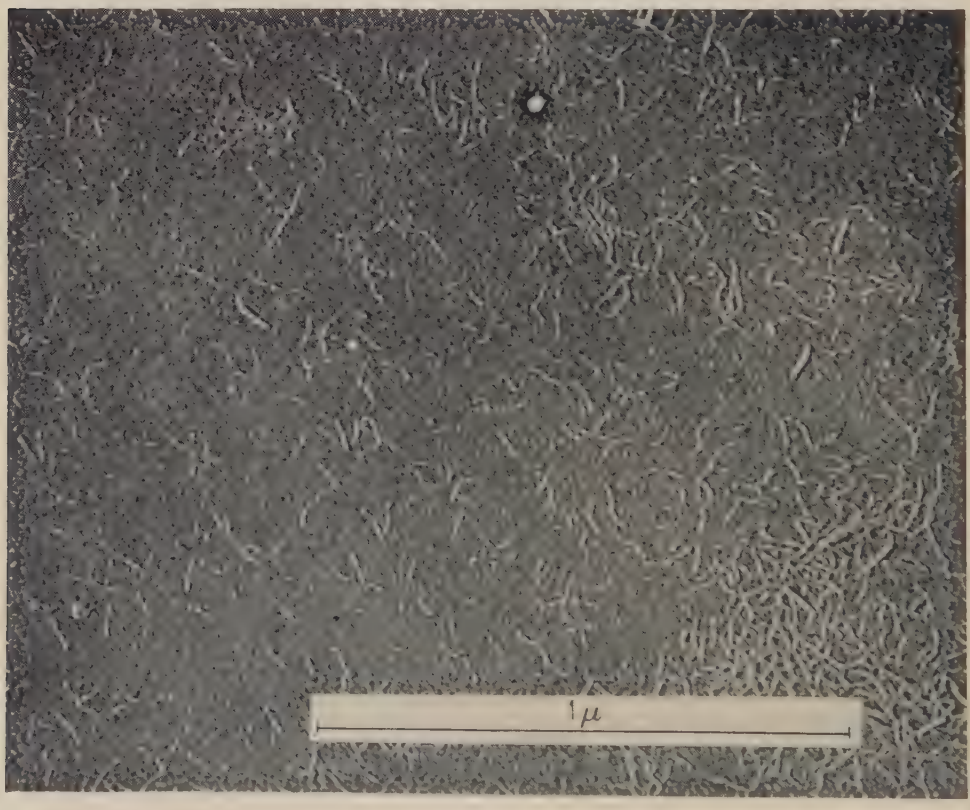

PLATE II(b). Electron micrograph of purified tail fibres. A few cores are also present. (Chromium shadowed, 70,000.)

In the cases of T2H, T4B and T6 we were not able to use the foregoing procedure to obtain fibres because stronger acid was required to denature the heads of these

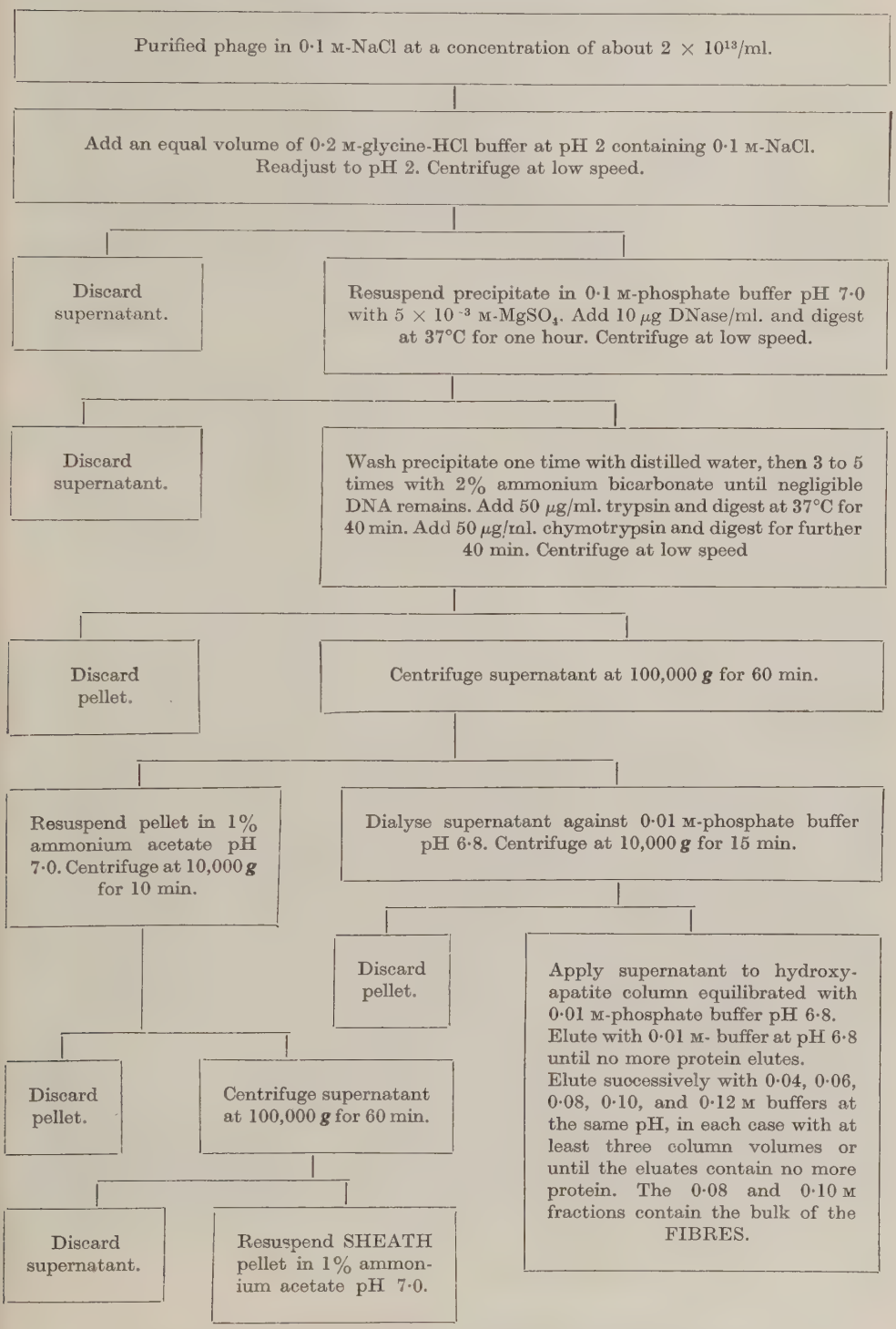
Purified phage in 0·1 M-NaCl at a concentration of about 2 × 10¹³/ml.
Add an equal volume of 0·2 M-glycine-HCl buffer at pH 2 containing 0·1 M-NaCl. Readjust to pH 2. Centrifuge at low speed.
Discard supernatant.
Resuspend precipitate in 0·1 M-phosphate buffer pH 7·0 with 5 × 10⁻³ M-MgSO₄. Add 10 μg DNase/ml. and digest at 37°C for one hour. Centrifuge at low speed.
Discard supernatant.
Wash precipitate one time with distilled water, then 3 to 5 times with 2% ammonium bicarbonate until negligible DNA remains. Add 50 μg/ml. trypsin and digest at 37°C for 40 min. Add 50 μg/ml. chymotrypsin and digest for further 40 min. Centrifuge at low speed
Discard pellet.
Centrifuge supernatant at 100,000 g for 60 min.
Resuspend pellet in 1% ammonium acetate pH 7·0. Centrifuge at 10,000 g for 10 min.
Dialyse supernatant against 0·01 M-phosphate buffer pH 6·8. Centrifuge at 10,000 g for 15 min.
Discard pellet.
Apply supernatant to hydroxyapatite column equilibrated with 0·01 M-phosphate buffer pH 6·8. Elute with 0·01 M- buffer at pH 6·8 until no more protein elutes. Elute successively with 0·04, 0·06, 0·08, 0·10, and 0·12 M buffers at the same pH, in each case with at least three column volumes or until the eluates contain no more protein. The 0·08 and 0·10 M fractions contain the bulk of the FIBRES.
Discard pellet.
Centrifuge supernatant at 100,000 g for 60 min.
Discard supernatant.
Resuspend SHEATH pellet in 1% ammonium acetate pH 7·0.

FIG. 1. Procedure for purifying sheaths and tail fibres from T2L.

strains. However, sheaths may be prepared from these strains, at the sacrifice of tail fibres and cores, by treating a suspension of phage in 0·3 M-NaCl with an equal volume of N-H_2SO_4 followed by DNase and proteolytic enzyme digestion as described for T2L. The acid treatment was usually repeated after removal of the DNA, since the presence of large quantities of DNA can interfere with the effective denaturation of the heads. The only structures which remain undigested are the sheaths, which can be purified by centrifugation.

(b) *Electron microscopy of phage components*

Kellenberger & Arber (1955) described the effects of exposure to hydrogen peroxide on the morphology of the phage. Plate III is an electron micrograph of bacteriophage treated with hydrogen peroxide to 40% survival of infectivity. Both normal and altered particles are present, aggregated into a rosette by their tail fibres. The sheaths in altered particles are contracted, and are shorter and thicker than the normal sheaths. The core is attached to the hexagonal head which is filled with DNA, but the sheaths appear unattached to the head in both normal and altered phages. The relations between the components can be more clearly seen in the isolated particle from the same preparation shown in Plate IV. At the distal end of the core there is a rather diffuse structure† to which are attached the tail fibres.

Electron micrographs of purified contracted sheaths are shown in Plates V and VI. They are hollow cylinders, 350 Å long and 250 Å in diameter, the diameter of the inner hole being 120 Å. The total volume of the contracted sheath is thus $1{\cdot}3 \times 10^7$ Å^3. By comparison, the diameter of the extended sheath is 165 Å in PTA preparations, and its length is probably equal to that of the core (800 Å). If it is assumed that the diameter of the cylindrical hole in the extended sheath is equal to that of the core (70 Å), then the volume of the extended sheath is computed to be $1{\cdot}4 \times 10^7$ Å^3. This suggests that the volume of the sheath is conserved when it contracts. Very often sheaths standing upright display a "cog wheel" appearance, and those lying obliquely show helical grooving (Plate VI) which suggests a helical arrangement of subunits in the sheath. In addition, striations can often be seen across the tail of intact phage as shown in Plate VII(a). The number of striations in the extended sheath is close to 25 and their spacing is estimated to be 30 to 40 Å. We have occasionally found structures of the type shown in Plate VII(b), which appears to be a stretched sheath revealing again its helical character.

Several tail fibres are shown in Plate VIII, where it is seen that they are long slender structures 1300 Å by 20 Å and are characteristically kinked in the middle. This structure is partially obscured when fibres from hydroxyapatite columns are examined (Plate II(b)) since the column appears to fragment them.

Cores, as can be seen from Plate VIII, are hollow cylinders 800 Å long and 70 Å in diameter, the diameter of the central hole being estimated to be 25 Å. No attempt has yet been made to obtain pure cores.

By mild acid treatment (pH 2·0) of T4, followed by DNase and trypsin digestion, preparations can be obtained that show empty heads which retain their hexagonal shape and are clearly constituted of a thin membrane, which is estimated to be about 35 Å thick (Plate IX). If it is assumed that the head to sheath volume ratio is equal to their mass ratio (8·5/1), the thickness of the head membrane should be of the order of 60 Å.

† Recently, it has been possible to characterize this structure more fully. It is a hexagonal plate at the base of the core to which six tail fibres are attached (Brenner & Horne, in preparation).

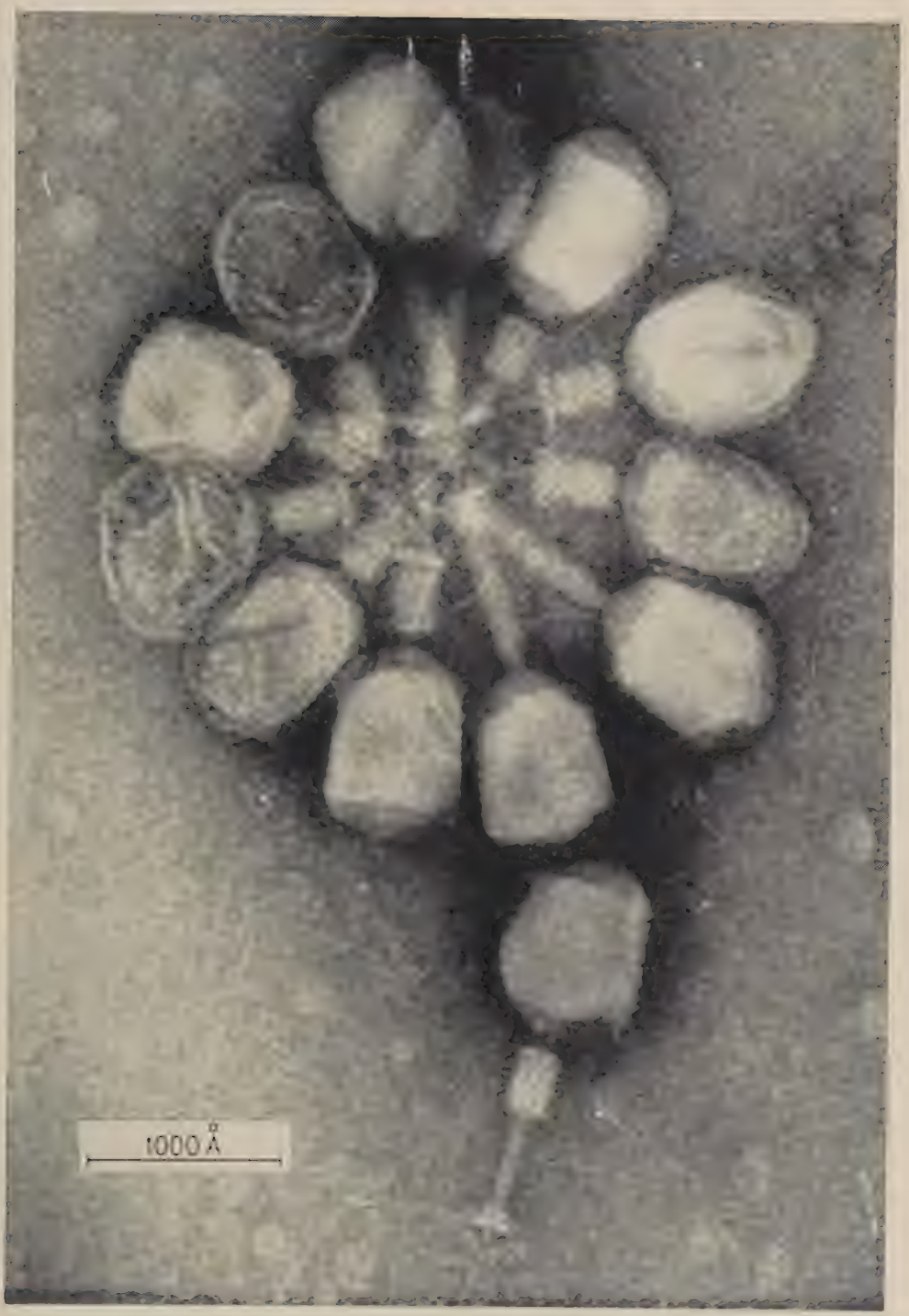

PLATE III. Hydrogen peroxide treated phage particles. Both normal and altered particles with shortened and thickened sheaths are seen in the rosette. (PTA embedded, × 280,000.)

[*To face page* 286.

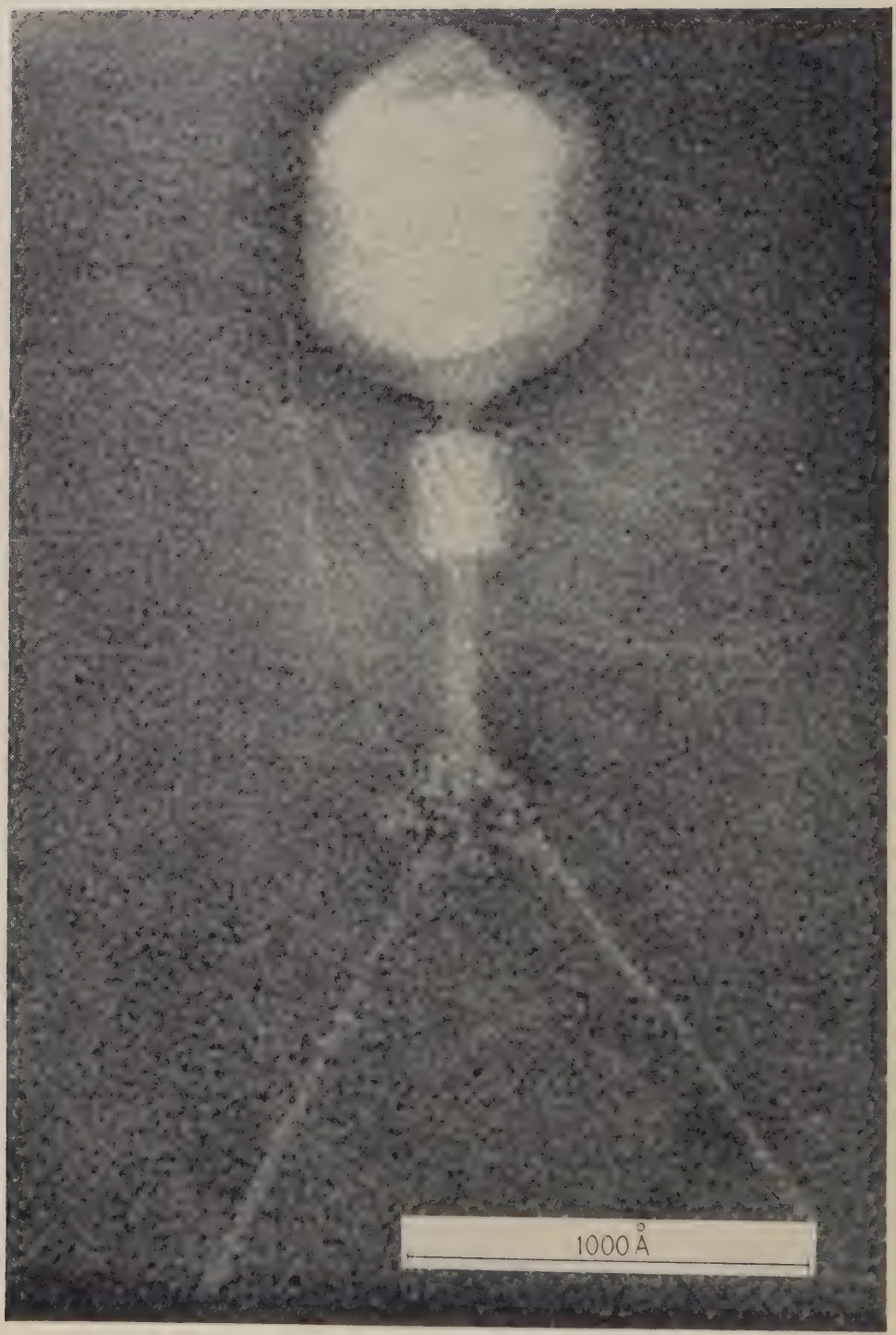

PLATE IV. Isolated hydrogen peroxide treated phage particle, showing the relations of the filled head, contracted sheath, core and tail fibres. (PTA embedded, × 570,000.)

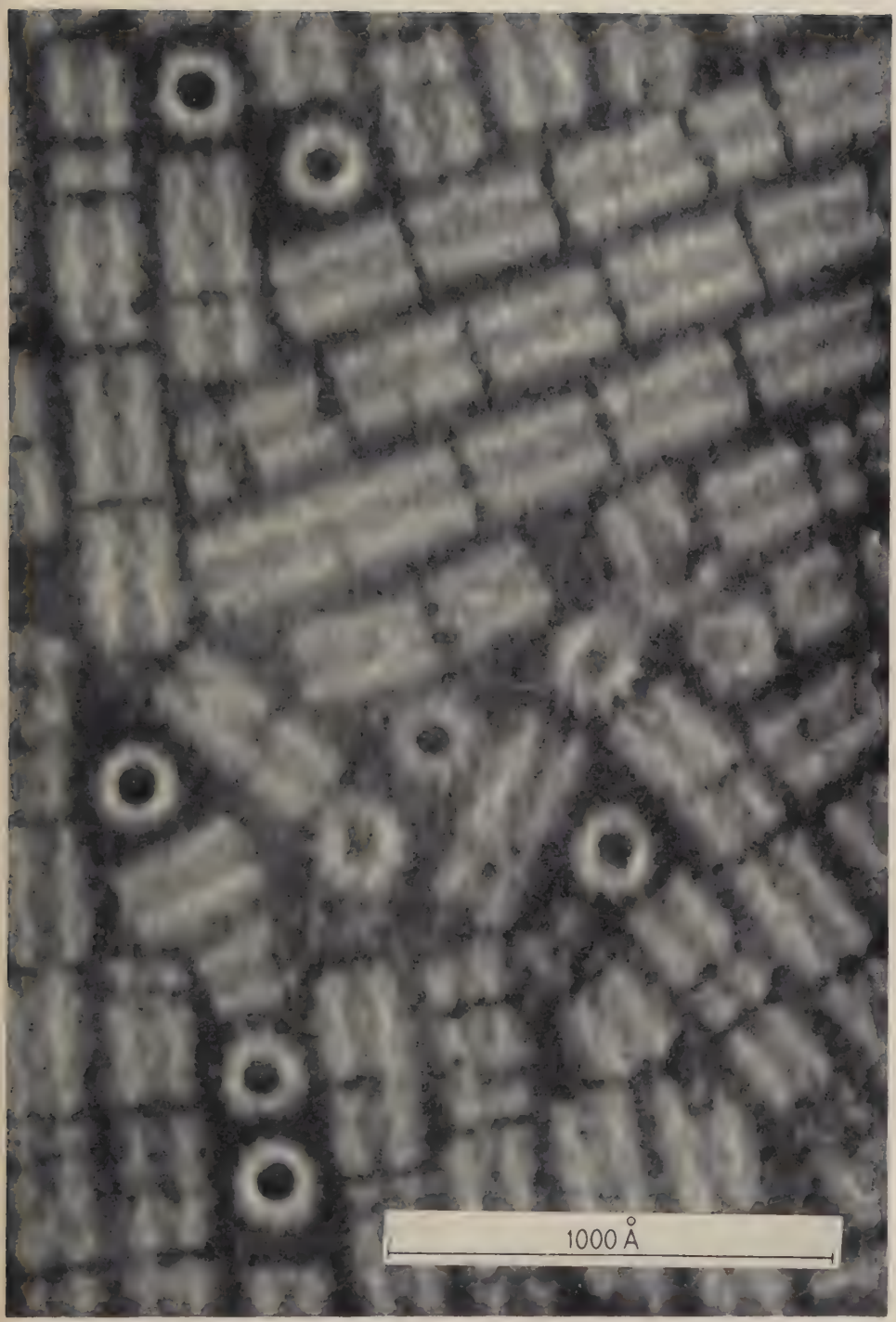

PLATE V. Purified contracted sheaths. A number of sheaths can be seen standing upright revealing the "cog wheel" arrangement of the subunits. (PTA embedded. × 630,000.)

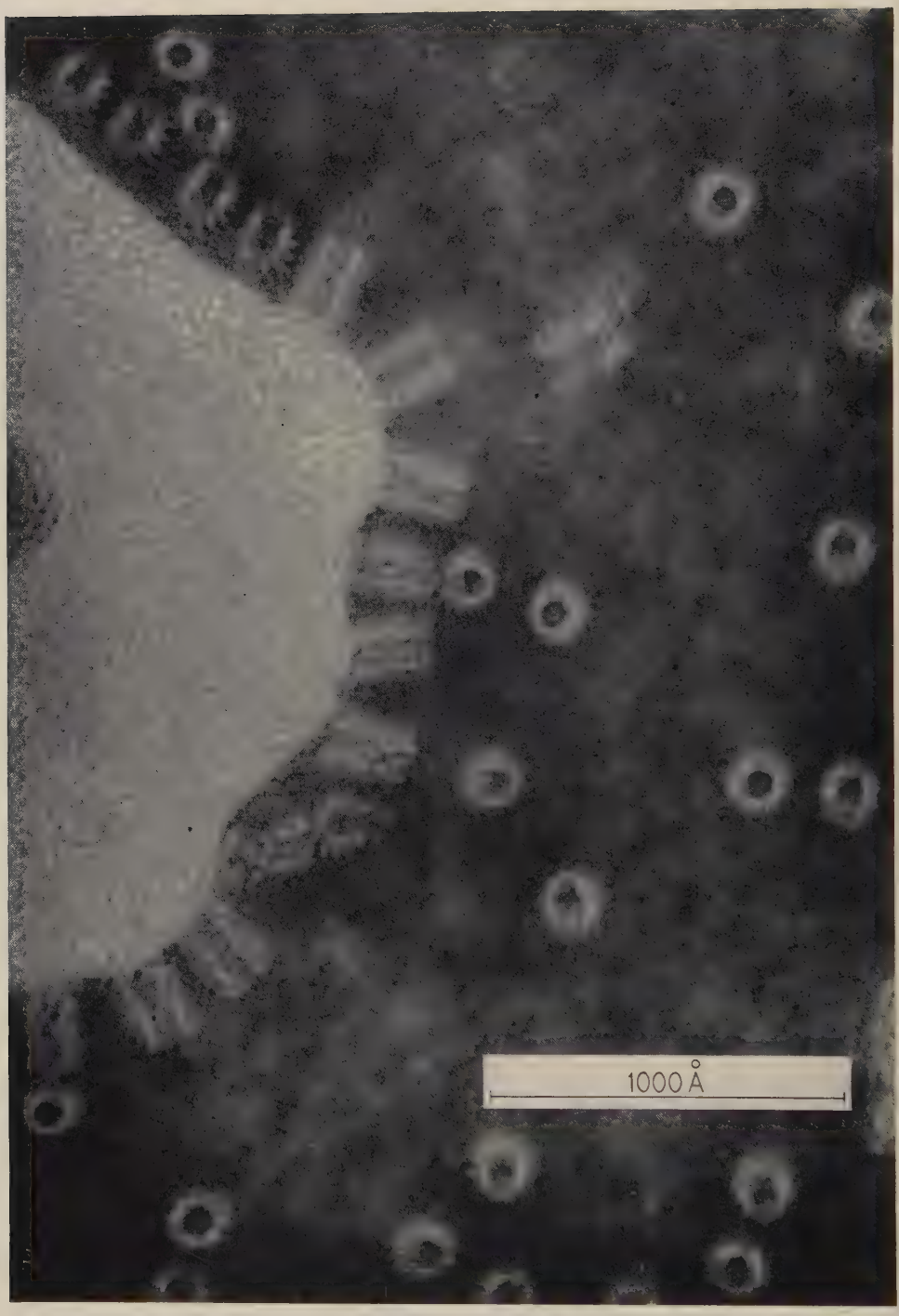

PLATE VI. Purified contracted sheaths. A number of sheaths can be seen standing upright revealing the "cog wheel" arrangement of the subunits (PTA embedded, × 500,000.)

PLATE VII(a). Phage particle showing striations along the length of the tail spaced at approximately 30 Å. (PTA embedded, × 400,000.)

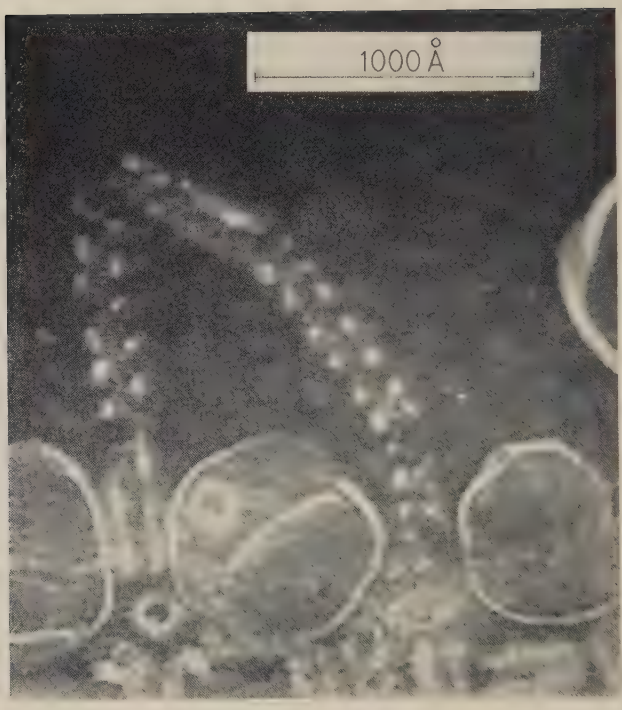

PLATE VII(b). A helical structure which appears to be a stretched sheath. (PTA embedded, × 370,000

PLATE VIII. Tail fibres (F) and hollow cores (C) embedded in a PTA droplet. The full length of the tail fibres can be seen together with the characteristic kinking at the centre. (PTA embedded, × 500,000.)

PLATE IX. Empty T4 head membranes with preserved hexagonal shape. Cores and sheaths are also present (PTA embedded, × 350,000.)

PLATE X. Structures resulting from the treatment of phage with sodium dodecyl sulphate at pH 10·0. These consist of cores surrounded by contracted sheaths. Tail fibres are also present. (PTA embedded, × 400,000.)

PLATE XI(a). Electrophoresis pattern of purified sheaths in 0·1 M-phosphate buffer pH 6·5.

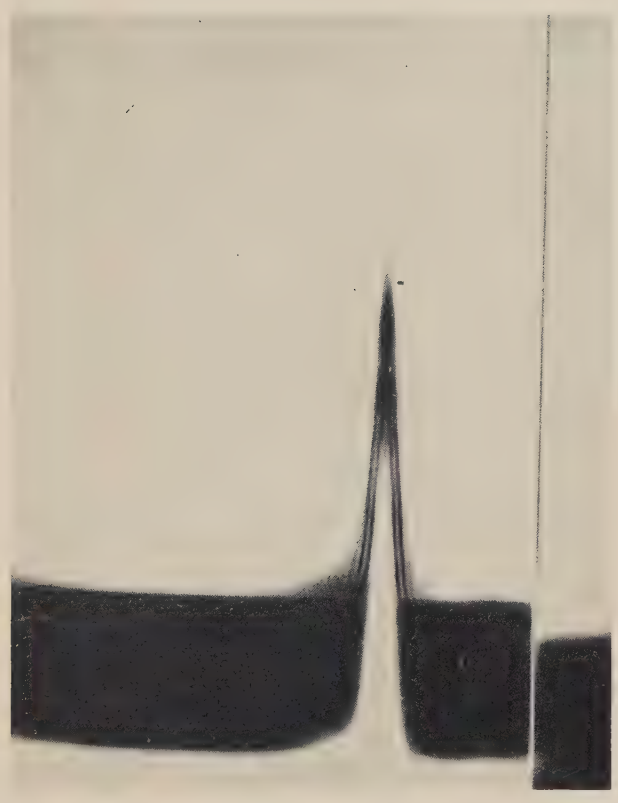

PLATE XI(b). Sedimentation pattern of purified sheaths in 0·1 M-phosphate buffer pH 6·5, 16 min after reaching 20,400 rev/min.

A characteristic structure is produced by treating phage ghosts with sodium dodecyl sulphate at pH 10 following the procedure of Van Vunakis, Baker & Brown (1958). The heads are completely solubilized leaving contracted sheaths surrounding hollow cores (Plate X). Tail fibres may also be seen. This material is presumably identical with the fast-sedimenting component A of Van Vunakis *et al.* which constituted roughly 10% of the structural protein of the phage.

(c) *Physical and chemical properties*

Only sheaths have been isolated in amounts sufficient to investigate by physical techniques. Preparations of sheaths are electrophoretically homogeneous, giving single symmetrical boundaries with a mobility of $7{\cdot}9 \times 10^{-5}$ cm^2/volt sec in 0·1 M-phosphate buffer pH 6·5 (Plate XI(a)). Sheaths give a single symmetrical peak in the ultracentrifuge (Plate XI(b)) with a sedimentation coefficient $S_{20,w} = 114\ S$ when extrapolated to zero concentration. Preliminary light scattering measurements indicate a particle weight of approximately 12,000,000 (Doty, P., personal communication), and a similar value is estimated from the electron microscopic dimensions of the sheath.

Sheaths are remarkably resistant structures, retaining their characteristic appearance after treatment with acid and alkali (N-H_2SO_4 or 0·2 N-NaOH), after boiling for 20 min, or after treatment for 24 hr with 8 M-urea, 8 M-guanidine hydrochloride, or 1% sodium dodecyl sulphate at pH 10·5. However, we have found it possible to

TABLE 1

Amino acid composition of the sheaths

Amino acid	g/100 g protein	Residues per 54,000 molecular weight
½ cystine	0·23	1
methionine	0·81	3
aspartic acid	13·0	52
threonine	7·78	35
serine	5·78	29
glutamic acid	9·94	36
proline	3·1	14
glycine	4·98	35
alanine	7·6	46
valine	6·61	30
*iso*leucine	7·5	31
leucine	7·0	28
tyrosine	6·35	19
phenylalanine	5·0	16
lysine	6·21	23
arginine	5·70	17
histidine	0·55	2
NH_3	1·94	(61)

dissociate the sheaths and sensitize them to enzyme action by the same procedure used by Fraenkel-Conrat (1957) to dissociate the subunits of tobacco mosaic virus (TMV). An aqueous suspension of sheaths, cooled to 0°C and mixed with two volumes of glacial acetic acid just above its freezing point, promptly loses its characteristic

opalescence and becomes extremely viscous. Microscopic observation shows complete disappearance of the organised structure. Dialysis of the solution against distilled water or phosphate buffer pH 6·5 results in precipitation of the protein which cannot be readily redissolved even in 8 M-urea. However, if the acetic acid solution is dialysed directly into 8 M-urea buffered at pH 6·5 by 0·1 M-phosphate, most of the protein remains in solution, although an increased opalescence indicates that some reaggregation occurs. This prevented study of the physical properties of the dissociated sheaths.

Attempts to demonstrate an N-terminal amino acid using the fluorodinitrobenzene technique of Sanger (1945) have been unsuccessful. Dinitrophenylation of dissociated sheaths in 8 M-urea yielded only a trace of DNP-glutamic acid (one residue per 3×10^6 molecular weight), although one ϵ-DNP-lysine residue was recovered per 7,000 molecular weight showing that dinitrophenylation had occurred. It is possible that the N-terminal group is protected as in the subunit of TMV (Narita, 1958).

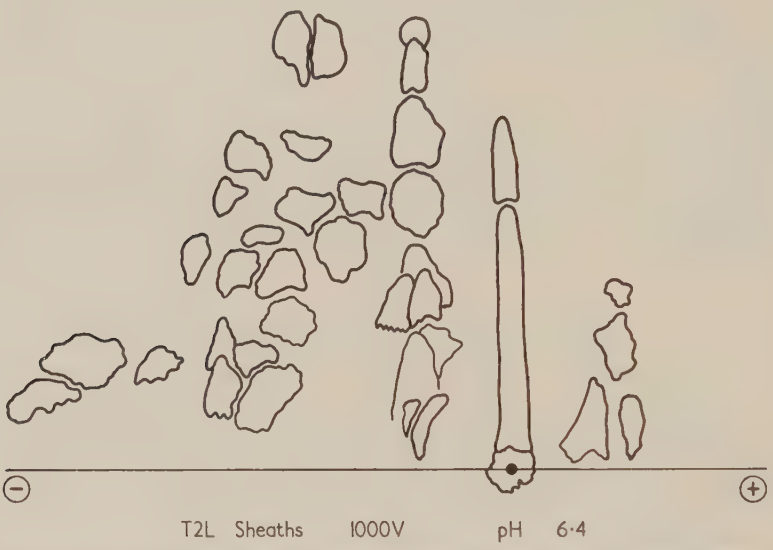

FIG. 2. Fingerprint of trypsin digest of T2L sheaths. Ionophoresis : pH 6·4, 1,000 v, 2½ hours. Chromatography : *n*-butanol, acetic acid, water (3 : 1 : 1), 15 hours ascending.

A quantitative amino acid analysis of sheaths was carried out and the results are given in Table 1. From these data, combined with the results of fingerprinting a tryptic digest of the protein, an estimate of the size of the repeating subunit may be made. Since trypsin cleaves specifically those bonds in which the carbonyl group is contributed by lysine and arginine residues, the fact that fingerprints of sheaths (Fig. 2) display about 37 peptides indicates that the number of lysine and arginine residues in the subunit is of this order. From the proportion of these amino acids to the total, the molecular weight indicated for the subunit would be about 50,000. Based upon the relatively rare histidine residues, the molecular weight should be an integral multiple of 27,000. Only one histidine-containing peptide has been found in the fingerprint, but some material invariably remains at the origin. It is not yet known whether this represents undigested protein or peptides insoluble in the buffer.

We have investigated the head protein of T2L by fingerprinting the tryptic peptides of phage denatured by acid. Since the sheaths remain undigested, contamination from other proteins is only a few per cent. The fingerprint, developed with ninhydrin,

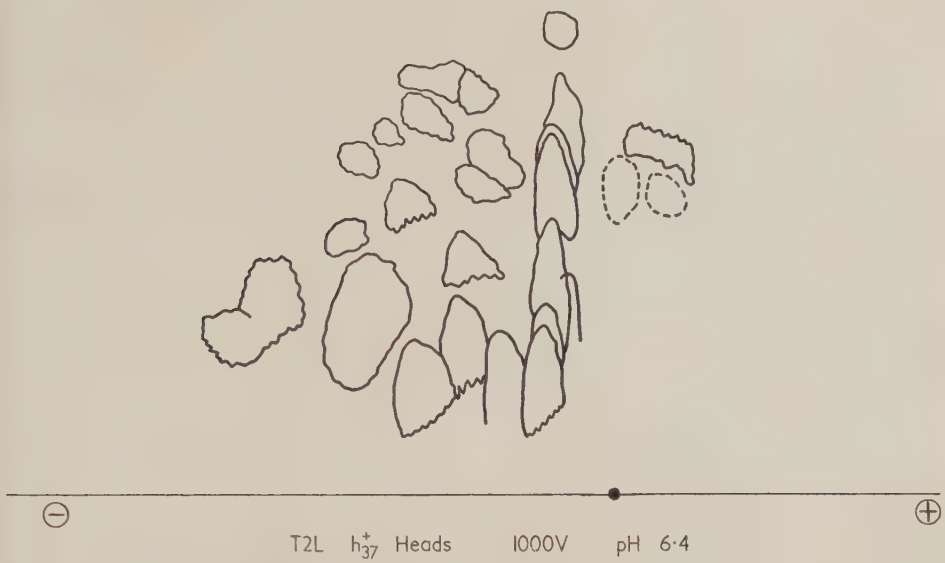

FIG 3. Fingerprint of trypsin digest of T2L head protein. Ionophoresis : pH 6·4, 1000 v, 2½ hours. Chromatography : *n*-butanol, acetic, acid, water (3 : 1 : 1), 15 hours ascending,

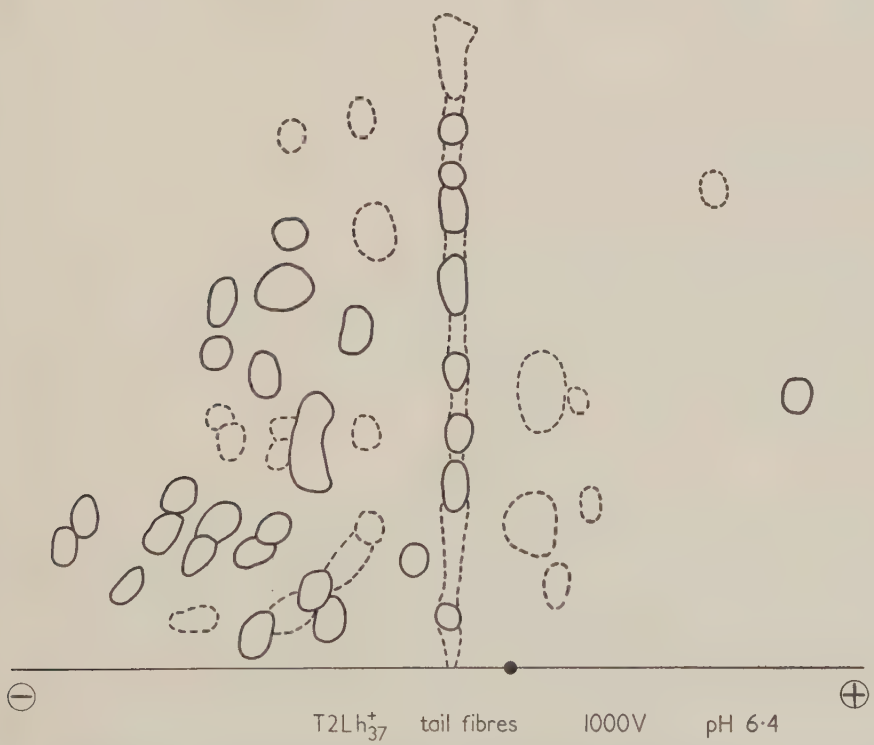

FIG. 4. Fingerprint of trypsin digest of T2L tail fibres. Many of the peptides were faint since only a small quantity of fibres was available. Ionophoresis : pH 6·4, 1,000 v, 2½ hours. Chromatography : *n*-butanol, acetic acid, water (3 : 1 : 1), 15 hours ascending.

resolves approximately 28 peptides (Fig. 3). By applying specific stains for histidine, tyrosine, arginine and tryptophan, a total of some 40 peptides can be distinguished. The head subunit isolated from T2 ghosts by Van Vunakis *et al.* (1958) was reported to have a molecular weight of about 80,000 as judged from its N-terminal alanine content, and physical properties. The amino acid analysis of whole phage (Fraser, 1957) indicates 21 arginine and 32 lysine residues for a subunit of 80,000 molecular weight. Thus 53 tryptic peptides would be expected. Since the number of peptides actually resolved is a minimum value, the fingerprint supports the evidence for a repeating subunit of this molecular weight.

The quantities of tail fibres which have been isolated have been too small to permit precise physicochemical studies. Fingerprints of tail fibres are complex, showing more peptides than in the case of heads or sheaths (Fig. 4). If the fibres have about the same lysine and arginine content as the other components, a molecular weight of the order of 100,000 would be indicated for the repeating subunit. From the dimensions observed in the electron micrographs, the particle weight of an entire fibre is estimated to be of the order of 400,000.

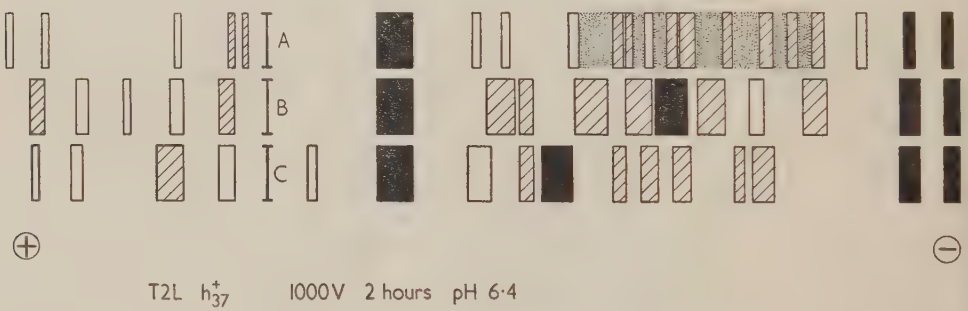

FIG. 5. Ionophoretic comparison of tryptic peptides of T2L tail fibres (A), sheaths (B) and heads (C).

In addition to the fingerprints, a direct comparison of head, sheath and tail fibre proteins was made by separating the tryptic peptides of these proteins side by side, employing paper ionophoresis. Fig. 5 is a tracing of the ionophoretogram after staining with ninhydrin. The radically different patterns demonstrate that each of these morphological components is composed of a protein with primary structure distinct from the others.

4. Discussion

We have isolated two of the components of the protein coat of T-even bacteriophages, the tail sheath and the tail fibres, and have helped to characterise two more, the head and the core. To these components can be added the hexagonal plate at the base of the tail, the structure of which suggests that the number of tail fibres is six (Brenner & Horne, in preparation). Apart from these proteins and the DNA, other components have been found. Hershey (1955) described an internal protein, containing about 3% of the phage sulphur which is released by osmotic shock, while Levine, Barlow & Van Vunakis (1958) have recently shown that this fraction includes a serologically distinct internal protein, representing 4 to 6% of the total protein of the phage. Other internal constituents are the polyamines, putrescine and spermidine, and another minor polypeptide (Hershey, 1957; Ames, Dubin & Rosenthal, 1958). Koch &

Dreyer (1958) isolated a lysozyme from lysates of phage T2, and this enzyme is apparently also part of the phage structure (Koch & Weidel, 1956; Barrington & Kozloff, 1956).

The electron micrographs of the components prepared by the phosphotungstate method show a wealth of structural detail. This procedure not only provides good contrast but also can preserve three-dimensional morphology, as is particularly well demonstrated in the case of the empty head membranes which retain their hexagonal shape. The technique shows the cores to be hollow and has permitted resolution of the helical structure of the sheaths. The dimensions of components measured in the present study differ somewhat from those found by previous authors (Kellenberger & Arber, 1955; Williams & Fraser, 1956) using shadow-cast preparations. The latter procedure is liable to overestimation due to the presence of the metal, while the phosphotungstate method is liable to underestimation because only structure impermeable to the electron dense material is visualized. Thus we do not place much reliance on the measured thickness of the head membrane of 35 Å, since calculation shows that it should be nearer to 60 Å. On the other hand, the diameter of the hole down the core cannot be greater than the measured diameter of 25 Å.

Our results support the findings of Van Vunakis *et al.* (1958) that the phage head is built of a large number of subunits of molecular weight about 80,000. We have also been able to show that the sheath contains a subunit of approximately 50,000 molecular weight, the N-terminal group of which appears to be unavailable to dinitrophenylation. This explains why Van Vunakis *et al.* (1958) found only the N-terminal alanine of the head protein in whole ghosts. From the weight of the intact sheath and that of the subunit we estimate that each sheath contains about 200 subunits. In end-on views of the contracted sheaths, about 15 "cogs" can be seen. If these represent the subunits in one turn of a helix the entire sheath should contain thirteen such turns. It is to be noted that the number of striations observed along the length of extended sheaths is about 25, and these may therefore represent the number of turns of the helix in the *extended structure*. This is consistent with the contraction of the sheaths to about one half of their extended length. The increase in diameter of the sheath accompanying its contraction can be understood for a helical structure if the contraction represents an increase in the number of subunits per turn, the total number then remaining constant. In contracted sheaths, the helical grooves run in the direction of the long axis of the structure. A helical structure built of subunits related by screw symmetry has many sets of grooves and the set which is most emphasized depends on the exact shape of the subunits. Hence the same structure may show different sets of grooves under different conditions.

The characteristic structural feature of the tail fibres is the presence of a central kink. The difficulty of isolating sufficient amounts of tail fibres has limited their characterisation. The complexity of the fingerprint shows that if a single repeating unit exists it has a molecular weight probably not less than 100,000. Conversely, if smaller subunits are present there must be a number of different ones. It is conceivable that the length of the fibre is determined by the length of a single polypeptide chain, the fibre being a bundle of such chains. An α-helix 1,300 Å long would contain about 860 amino acids and have a molecular weight of about 100,000.

The quantity, the ease of isolation, and the molecular weight of the sheath and head proteins makes their analysis possible and prompts efforts to discover their genetic control. The tail fibres, on the other hand, for which a genetic system is available, seem unsuitable for chemical analysis because of their apparently large molecular weight, and the small quantity obtainable.

The complexity of phage as a whole is to be contrasted with the relatively simple structures of plant viruses such as tobacco mosaic virus and turnip yellow mosaic virus. Although the components of phage, like the small viruses, seem to be built on a simple plan, the assembly of the parts would seem to pose a formidable problem.

REFERENCES

Adams, M. H. (1959). *Bacteriophages*. New York: Interscience Publishers.
Ames, B., Dubin, D. T. & Rosenthal, S. M. (1958). *Science*, **127**, 814.
Anderson, T. F. (1945). *J. Cell. Comp. Physiol.* **25**, 17.
Anderson, T. F. (1946). *Cold Spr. Harb. Sym. Quant. Biol.* **11**, 1.
Anderson T. F. (1953). *Cold Spr. Harb. Sym. Quant. Biol.* **18**, 197.
Anderson, T. F., Rappaport, C. & Muscatine, N. A. (1953). *Ann. Inst. Pasteur*, **84**, 5.
Barrington, L. J. & Kozloff, L. M. (1956). *J. Biol. Chem.* **223**, 615.
Benzer, S. (1955). *Proc. Nat. Acad. Sci., Wash.* **41**, 344.
Benzer, S. (1957). *The Chemical Basis of Heredity*, edited by W. D. McElroy & B. Glass. Baltimore: Johns Hopkins Press.
Brenner, S. (1957). *Virology*, **3**, 560.
Brenner, S. & Horne, R. W. (1959). *Biochim. biophys. Acta*, **34**, 103.
Cosslett, V. E. & Horne, R. W. (1957). *Vacuum*, **5**, 109.
Delbrück, M. (1948). *J. Bact.* **56**, 1.
De Mars, R. I. (1955). *Virology*, **1**, 83.
De Mars, R. I., Luria, S. E., Levinthal, C. & Fisher, H. (1953). *Ann. Inst. Pasteur*, **84**, 113.
Fraenkel-Conrat, H. (1957). *Virology*, **4**, 1.
Fraser, D. (1951). *J. Bact.* **61**, 115.
Fraser, D. (1957). *J. Biol. Chem.* **227**, 711.
Fraser, D. & Jerrel, E. A. (1953). *J. Biol. Chem.* **205**, 291.
Herriott, R. M. & Barlow, J. L. (1952). *J. Gen. Physiol.* **36**, 17.
Hershey, A. D. (1955). *Virology*, **1**, 108.
Hershey, A. D. (1957). *Virology*, **4**, 237.
Ingram, V. M. (1958). *Biochim. biophys. Acta*, **28**, 539.
Kellenberger, E. & Arber, E. (1955). *Z. Naturf.* **106**, 698.
Koch, G. & Dreyer, W. J. (1958). *Virology*, **6**, 291.
Koch, G. & Weidel, W. (1956). *Z. Naturf.* **116**, 345.
Kozloff, L. M. & Henderson, K. (1955). *Nature*, **176**, 1169.
Kozloff, L. M., Lute, M. & Henderson, K. (1957). *J. Biol. Chem.* **228**, 511.
Lanni, F. & Lanni, Y. T. (1953). *Cold Spr. Harb. Symp. Quant. Biol.*, **18**, 159.
Levine, L., Barlow, J. L. & Van Vunakis, H. (1958). *Virology*, **6**, 702.
Levinthal, C. & Fisher, H. (1952). *Biochim. biophys. Acta*, **9**, 419.
Michl, H. (1951). *Mh. Chem.* **82**, 489.
Narita, K. (1958). *Biochem. biophys. Acta*, **28**, 184.
Ping-Yao Cheng. (1956). *Biochem. biophys. Acta*, **22**, 433.
Sanger, F. (1945). *Biochem. J.* **39**, 507.
Streisinger, G. (1956*a*). *Virology*, **2**, 377.
Streisinger, G. (1956*b*). *Virology*, **2**, 388.
Streisinger, G. & Franklin, N. C. (1956). *Cold Spr. Harb. Symp. Quant. Biol.* **21**, 103.
Tiselius, A., Hjertén, S. & Levin, Ö. (1956). *Arch. Biochem. Biophys.* **65**, 132.
Van Vunakis, H., Baker, W. & Brown, R. (1958). *Virology*, **5**, 327.
Williams, R. C. & Fraser, D. (1953). *J. Bact.* **66**, 458.
Williams, R. C. & Fraser, D. (1956). *Virology*, **2**, 289.
Wollman, E. L. & Stent, G. S. (1950). *Biochim. biophys. Acta*, **6**, 292.

J. Mol. Biol. (1959) **1**, 293-296.

LETTERS TO THE EDITOR

Carboxyl Group Interactions in Lysozyme†‡

The carboxyl groups of lysozyme which are titratable in KCl solutions are abnormal (Tanford & Wagner, 1954; Donovan, Laskowski & Scheraga, 1958), presumably because of hydrogen bonding or large local electrostatic factors. Evidence summarized here shows that, although these groups titrate normally in mixtures of guanidine hydrochloride (G) and urea (U), three "extra" carboxylate ions also are titrated in these mixtures.

To show the effect of solvent, the pK's of model compounds (at a concentration of 0·02 M), obtained from titration curves at 25°C, are plotted against molarity of G, U and KCl (K) in Fig. 1. Although the variations in pK are large in some cases, the groups still ionize in their normal pH ranges. Since G lowers the pK of acetic acid and U raises it, it is possible to prepare solvents having G/U ratios such that the pK of acetic acid is the same as in 0·15 M-KCl. If acetic acid is a proper model for the protein carboxyl groups, then in the absence of steric, electrostatic and hydrogen bonding interactions, the carboxyl groups should appear normal (pK $\sim$ 4·6) in these solvents. A water solution, 5 M in G and 1·2 M in U, designated GU, was chosen for titration of lysozyme. For the models, $pK_{GU} - pK_{0.15M\text{-}KCl}$ values are as follows: acetic acid, 0; imidazole, + 0·13; phenol, + 0·11; butylamine, — 0·05.

The titration curves of lysozyme in 0·15 M-KCl (K) and in GU are plotted in Fig. 2. This sample (Armour 381–187) has about 1·5 fewer carboxyls than that titrated by Tanford & Wagner (1954) (Armour 003L1), § but three "extra" carboxyls are found in each lot when titrated in GU. If no chloride binding is assumed, the pK of all the side chain carboxyls in GU is $\sim$ 4·6, and the electrostatic factor, w, is 0·05. The very strong interactions concealing the three "extra" carboxyls, and the interactions causing the abnormality of other carboxyls (Tanford & Wagner, 1954; Donovan *et al.*, 1958) in the molecule, thus all appear to have been removed by the GU. When the GU is dialyzed out, and the remaining protein is titrated in 0·15 M-KCl, curve D is obtained. This material seems to have the same number of titratable carboxyls as the "native"‖ lysozyme, and retains its activity¶ towards *M. lysodeikticus*. Titration curves K and GU are reversible from pH 2.

Further evidence for the presence of three "extra" carboxyls was given by the analysis of a water-soluble methylated lysozyme, which showed three more methoxyl groups than the number of carboxyls titratable in the "native" material in KCl, but the same number of amide groups. When the three "extra" carboxyls are included, the total number of amides and free carboxyls in the "native" material agrees with the estimate of the total number of acid residues given by Jolles (private communication). As would be expected, titrations of the methylated derivative showed no more groups in GU than in KCl.

† Supported by Grant G-2461 from the National Science Foundation.

‡ Presented, in part, before the Division of Biological Chemistry at the 131st meeting of the American Chemical Society, Miami, Florida, April 1957.

§ Our titrations of 003L1 in KCl show the same number of carboxyls (within 0·1 group) as has been reported by these authors.

‖ "Native", in this communication, means "this Armour lot, as received."

¶ Léonis (1956) has shown that lysozyme kept in cold 10 M-U shows full activity when the solution is diluted 1/1000 with water after three weeks.

Since an acid solution (pH 2 to 4) of the "native" protein increases in pH when GU is added, indicating an uptake of protons when the interactions concealing the "extra" carboxyls are removed, these carboxyls must be present as carboxylate ions

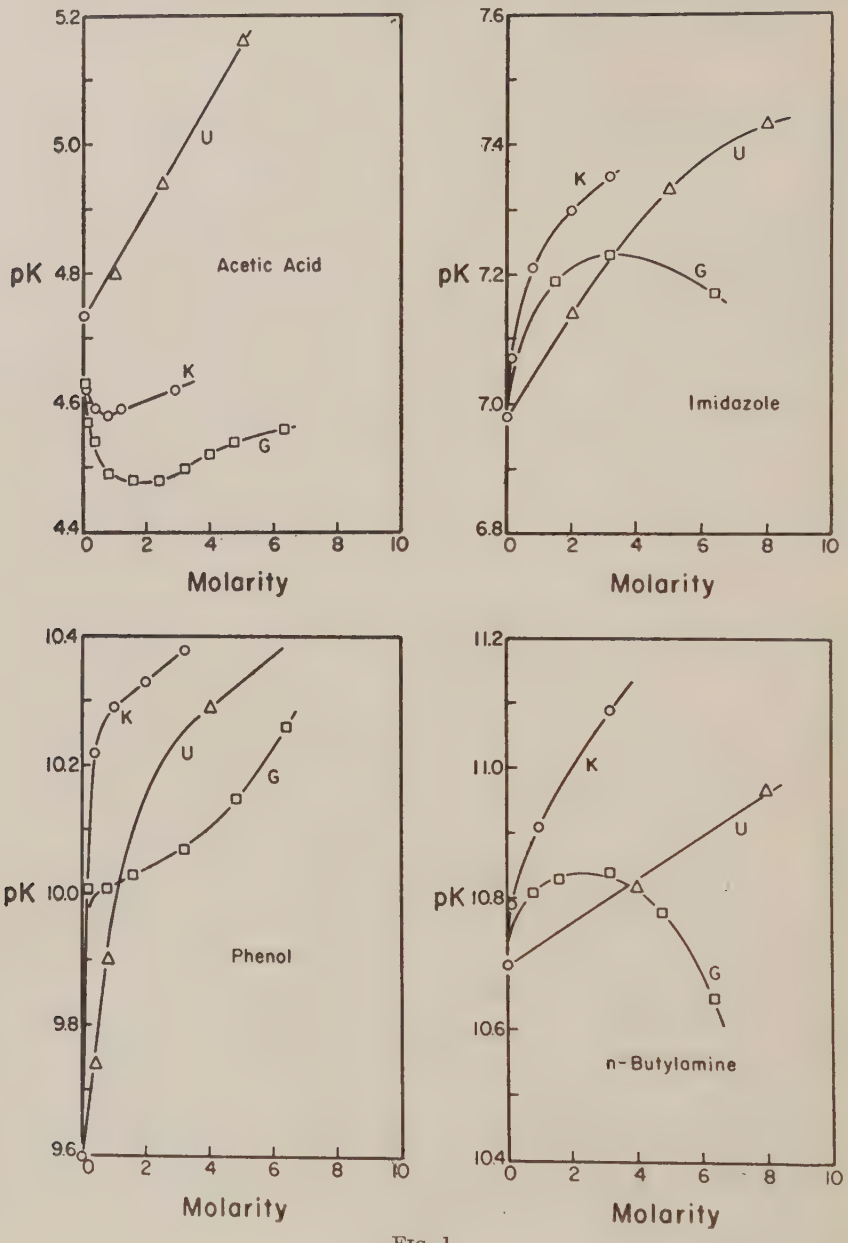

FIG. 1

throughout the titration in KCl. An attempt to convert these carboxylate ions into un-ionized carboxyl groups (by removal of 8 M-G from a pH 2 solution by dialysis against an HCl solution of pH 2) failed, suggesting that the strong interactions that conceal these groups conceal them as carboxylate ions, not un-ionized carboxyl groups.

In an acetylated derivative, the three "extra" carboxyls were titratable in 0·15 M-KCl, and appeared to be indistinguishable from the other carboxyls. However, the

pH dependence of the tyrosyl ionization remained much the same as in the "native" lysozyme, suggesting that the high pK reported for the tyrosyls (Tanford & Wagner, 1954) is not caused by interactions with these three carboxyls. The acetylated derivative showed the same number of carboxyls in GU as in KCl, as did a deaminated derivative. A guanidinated derivative gave a titration curve nearly identical with curve D below pH 8.

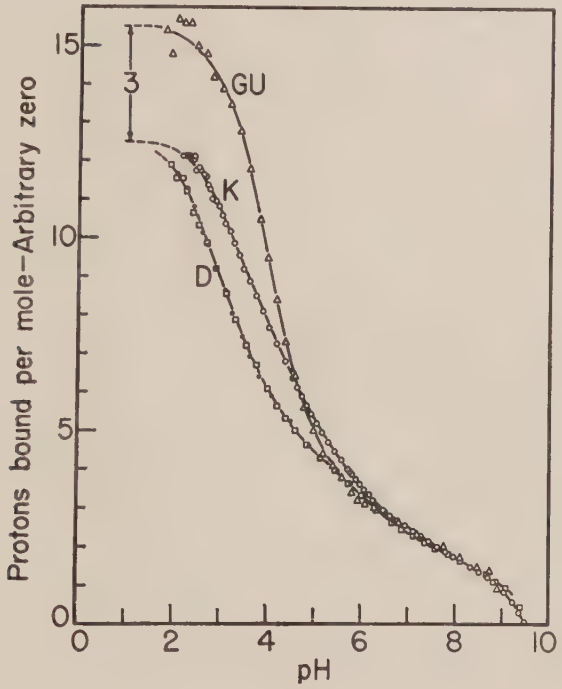

Fig. 2

The simplest explanation of these results is that in the "native" molecule there are either carboxylate ion · · · ϵ-amino hydrogen bonds (carboxylate ion · · · guanidinium hydrogen bonds in the guanidinated derivative), or large local electrostatic effects of ϵ-amino groups (guanidinium groups in the guanidinated derivative) in the neighbourhood of the three carboxylate ions. If Tanford and Wagner's observation (1954) that the ϵ-amino groups in lysozyme have normal pK's is correct, then the carboxylate ion · · · ϵ-amino hydrogen bonds appear to be eliminated as a possibility, since hydrogen bond formation should raise the pK of the ϵ-amino groups. The conclusion that the three "extra" carboxylate ions are concealed by electrostatic effects of ϵ-amino groups should be regarded only as tentative, since quite complex combinations of hydrogen bonding, local electrostatic effects and steric interactions might account for the abnormality of the three "extra" carboxyl groups and the normal pK of the ϵ-amino groups. Details of these and other related experiments will be reported subsequently.

Department of Chemistry
Cornell University
Ithaca, New York, U. S. A.

John W. Donovan,
Michael Laskowski, Jr.
Harold A. Scheraga

Received May 1959

REFERENCES

Donovan, J. W., Laskowski, Jr., M. & Scheraga, H. A. (1958). *Biochim. biophys. Acta*, **29**, 455.
Léonis, J. (1956). *Arch. Biochem. Biophys.* **65**, 182.
Tanford, C. & Wagner, M. L. (1954). *J. Amer. Chem. Soc.* **76**, 3331.

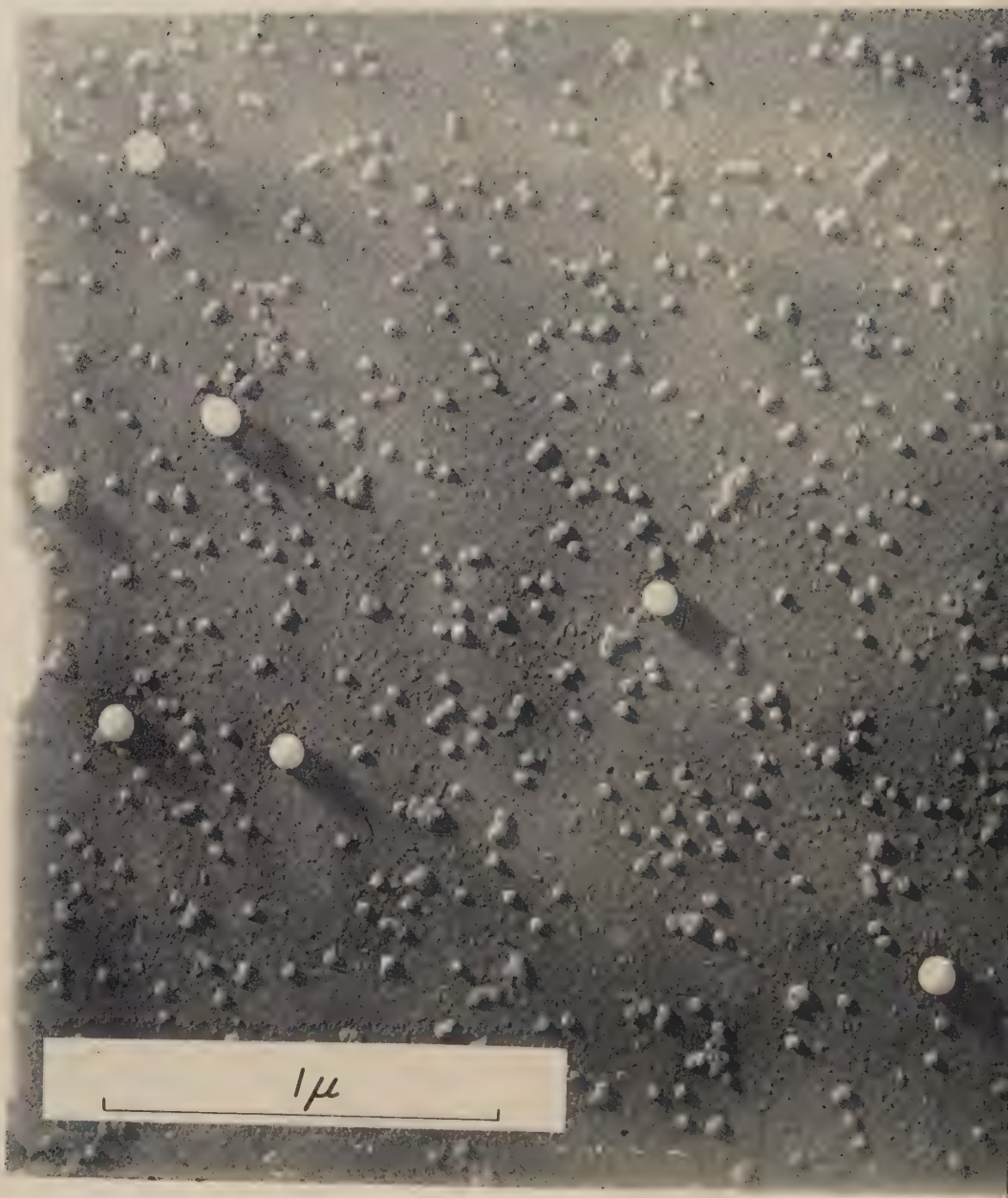

PLATE I. Human serum lipoprotein, S_f^0 6 to 8. Fixed in 1% buffered OsO_4. 880 Å diameter polystyrene latex (PSL) marker molecules. (× 55,000.)

[*To face page* 297.

J. Mol. Biol. (1959), **1**, 297-299.

A Determination of Lipoprotein Molecular Weight by use of the Electron Microscope †

1. Introduction

The physical properties of the serum lipoprotein macromolecules have been studied by a variety of tools including the ultracentrifuge (Lindgren, Nichols & Freeman, 1955; de Lalla, Elliott & Gofman, 1954; Havel, Eder & Bragdon, 1956), electrophoresis (Kunkel & Trautman, 1956), light scattering (Bjorklung & Katz, 1956), and electron microscope (Hayes & Hewitt, 1957). The particles as visualized in the electron microscope agreed in general with the predicted particle size of the centrifugally isolated fractions, but certain anomalies were obvious. Light-scattering data (Bjorkland & Katz, 1956) had indicated a molecular weight of 3×10^6 molecular weight units and the shape of a prolate ellipsoid with axial ratio 2 : 1 and dimensions of 350 Å by 160 Å. These values agreed very well with ultracentrifugal data. The particles as visualized in the electron microscope (Hayes & Hewitt, 1957) appeared to be oblate ellipsoids, with a diameter of 350 Å, flattened to a height of about 175 Å (see Plate I). From volume and density measurements the molecular weight was estimated to be about 6×10^6. One explanation of these results was that the particle seen in the electron microscope was a dimer of the molecule studied by light scattering and the ultracentrifuge.‡

A method for determining macromolecular weights by direct particle counting was first developed by Williams & Backus (1949), and has been used extensively for quantitative electron microscopy (Bachrach & Schwerdt, 1954; Williams, 1957). This work was an attempt to apply this method to the serum lipoprotein macromolecules.

2. Methods

The low-density serum lipoproteins consist of a whole spectrum of closely similar and related macromolecules. It would be desirable, therefore, in any molecular weight determination of certain of the low-density lipoproteins by electron microscope, to obtain as homogeneous a preparation as possible.

For this purpose, a method of isolation yielding a very narrow S_f^0 6 to 8 lipoprotein band utilizing a sedimentation equilibrium salt gradient has been employed. First, the broad class of low-density lipoproteins was isolated from a single serum specimen by preparative flotation in a medium of density 1·046 g/ml.§ This density was achieved by adding solid anhydrous NaBr to the serum. Following preparative ultracentrifugation in the Spinco 40.3 rotor at 40,000 rev/min and 18°C for 24 hr, a top fraction of background density 1·042 g/ml. was collected which contained most of the S_f^0 6 and higher S_f^0 serum lipoproteins originally present in the serum. This drop in density

† Work done under the auspices of the U.S. Atomic Energy Commission.

‡ Nichols, A. V., Freeman, N. K., Lindgren, F. T., Hayes, T. L. & Gofman, J. W. *Structure and Function of Serum Lipoproteins*, Amer. Chem. Soc., 132nd meeting, Abstract no. 169.

§ Densities are given for 20°C.

from 1·046 to 1·042 in the resulting top fraction reflects the shift toward equilibrium of the salts (mostly NaBr) present in the initial serum mixture. Approximately half of this top fraction was diluted with mock serum (NaCl solution of density 1·006 g/ml.) to a final small-molecule density (exclusive of lipoproteins) of 1·031 g/ml. Three ml. aliquots of this 1·031 g/ml. fraction were placed in 6 ml. preparative tubes, and 3 ml. of the more dense 1·042 g/ml. fraction was layered in the bottom of each of the preparative tubes with a syringe and a blunted spinal needle. Following ultracentrifugation for 63 hr, sedimentation equilibrium of both the salts present, as well as of the lipoprotein macromolecules, had been closely approached. Initially, by layering and slight agitation, a salt gradient approximating the equilibrium salt gradient was established in the middle region of the preparative tube before the ultracentrifuge was started. After the conclusion of the 63 hr run, successive fractions were pipetted from each of the preparative tubes. The fraction used for this study was the third milliliter (from the top), which corresponded to a density region on the equilibrium salt gradient of from approximately 1·033 g/ml. to 1·035 g/ml. Thus, the isolated lipoprotein fraction represented a narrow band of physically similar lipoproteins of hydrated density closely approximating this narrow density range. Lipoproteins in the broad band of S_f^0 2 to 20 exhibit a range of estimated hydrated density of from 1·050 g/ml. to 1·006 g/ml. By comparison, ultracentrifugal analysis of this narrow lipoprotein band revealed that it consisted of S_f^0 6 to 8 class lipoproteins (see Plate II).

The lipoprotein macromolecules were fixed by adding 0·1 ml. of the lipoprotein solution to 0·9 ml. of buffered (pH 7·3) 1% osmium tetroxide and allowed to stand at room temperature for 1/2 hr. The stained material was then diluted 1 : 1000 in distilled water. The solution that was sprayed contained human serum albumin (0·1%), 2640 Å diameter polystyrene latex ($3{\cdot}4 \times 10^{10}$ particles per ml.), and stained lipoprotein (approximately 2×10^{-6} g/ml.). Spraying was done with a DeVilbiss hand nebulizer, onto screens coated with Parlodion or Formvar, which were then shadowed with uranium or platinum-palladium-gold alloy. Entire drops were photographed in an RCA-2 electron microscope, and the number of polystyrene and lipoprotein particles in each drop was determined. The concentration of lipoprotein in the original solution was determined by ultracentrifugal analysis. The number of latex particles per ml. was determined by knowing the volume of the latex spheres, the density of the latex and the dry weight of the latex particles in a known volume of suspension (Williams & Backus, 1949). Both measurements are accurate to better than 5%.

To determine the lipoprotein molecular weight, the volume of a drop is calculated by counting the number of polystyrene latex spheres (PSL) present in the drop. This volume is used to determine the weight of lipoprotein present in the drop from the known lipoprotein w/v concentration. The weight of lipoprotein present is then divided by the number of lipoprotein particles present to give the weight per particle, and this is converted to molecular weight units.

3. Results and Discussion

A typical drop pattern is shown in Plate III along with an enlarged inset. The large polystyrene particles and the smaller lipoprotein macromolecules can be seen. The edge of the drop is outlined by the human serum albumin that was included in the sprayed mixture.

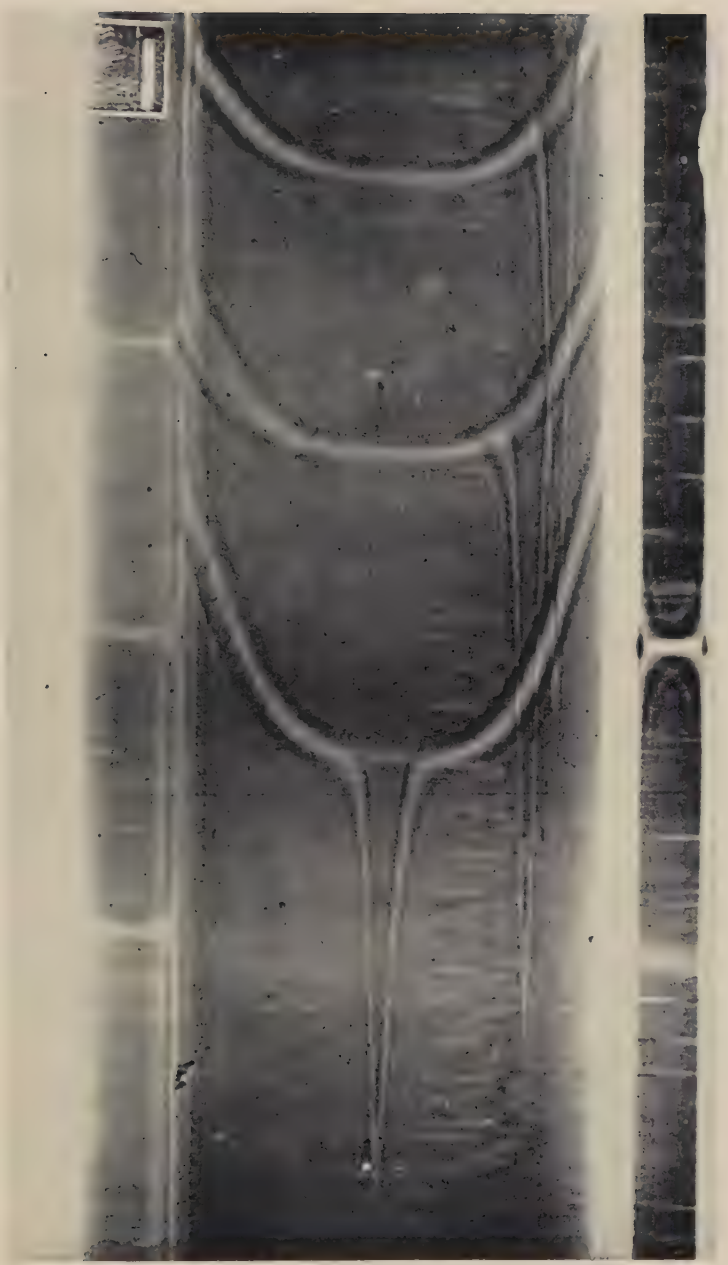

PLATE II. Analytic flotation of S_f^0 6 to 8 low-density serum lipoproteins. Schlieren patterns were obtained at 14 min after rotor reached full speed (52,640 rev/min) in a Spinco Model E ultracentrifuge. Flotation proceeds from right to left and occurs here in 0·195 M-NaCl solutions to which has been added solid NaBr to yield resultant solution densities (26°C) of 1·057 g/ml., 1·077 g/ml. and 1·192 g/ml. for the top, middle and bottom patterns, respectively.

[*To face page* 298.

PLATE III. Spray drop pattern. S_f 6 to 8 human serum lipoprotein. 2640 Å diameter polystyrene latex marker molecules. ($\times$ 6,700. Enlarged inset $\times$ 11,600.)

Table 1 is a compilation of the particle counts obtained. The average value for the molecular weight is $6{\cdot}9 \times 10^6$. This value would tend to support the hypothesis that the particle seen in the electron microscope is a dimer or higher-multiple unit of the macromolecule observed in the ultracentrifuge and by light scattering.

TABLE 1

Particle counts obtained

S_f^0 6 to 8 (g/ml.)	2640Å PSL particles per ml.	Number of drops counted	Total PSL counted	Total S_f^0 6 to 8 counted	Molecular weight
$2{\cdot}21 \times 10^{-6}$	$3{\cdot}4 \times 10^{10}$	16	577	3501	$6{\cdot}5 \times 10^6$
$2{\cdot}88 \times 10^{-6}$	$3{\cdot}4 \times 10^{10}$	8	572	3146	$8{\cdot}3 \times 10^6$
$2{\cdot}88 \times 10^{-6}$	$4{\cdot}0 \times 10^{10}$	5	198	1372	$6{\cdot}0 \times 10^6$

The reason for this apparent dimerization is not known, but it seems probable that it takes place either during fixation or during drying of the specimen for the electron microscope. Similar instances of specific aggregation prior to viewing in the electron microscope have been noted in other macromolecules (Polson & Wyckoff, 1947). Research is in progress to determine the properties of this aggregation and its relationship to lipoprotein structure.

THOMAS L. HAYES
JACK C. MURCHIO †
FRANK T. LINDGREN
ALEX. V. NICHOLS

Donner Laboratory of Biophysics
& Medical Physics,
University of California,
Berkeley, California, U.S.A.

Received 4 June 1959

† Cutter Laboratories, Berkeley.

REFERENCES

Bachrach, H. L. & Schwerdt, C. E. (1954). *J. Immunol.* **72**, 30.
Bjorklund, R. & Katz, S. (1956). *J. Amer. Chem. Soc.* **78**, 2122.
deLalla, O. F., Elliott, H. A. & Gofman, J. W. (1954). *Amer. J. Physiol.* **179**, 333.
Havel, R. J., Eder, H. A. & Bragdon, J. H. (1956). *J. Clin. Invest.* **35**, 1025.
Hayes, T. L. & Hewitt, J. E. (1957). *J. Appl. Physiol.* **2**, 425.
Kunkel, H. G. & Trautman, R. (1956). *J. Clin. Invest.* **35**, 641.
Lindgren, F. T., Nichols, A. V. & Freeman, N. K. (1955). *J. Phys. Chem.* **59**, 930.
Polson, A. & Wyckoff, R. W. G. (1947). *Nature*, **160**, 153.
Williams, R. C. (1957). *Int. Rev. Cytol.* **6**, 130.
Williams, R. C. & Backus, R. C. (1949). *J. Amer. Chem. Soc.* **71**, 4052.

INSTRUCTIONS TO AUTHORS

1. The *Journal of Molecular Biology* will publish papers on the nature, production and replication of biological structure at the molecular level, and its relation to function. Suitable subjects are sub-cellular organization: molecular genetics: structure and replication of viruses: molecular structure of muscle, nerve and other tissues: structure of proteins, nucleic acids, carbohydrates, lipids, etc., and their synthetic analogues, as investigated by X-rays, light absorption and other methods: problems of inter- and intra-molecular energy transfer.

2. The Journal will also publish Letters to the Editor (averaging 1000 words), and occasional review articles dealing with a more restricted or immediately topical field than those in review journals. (The Editor should be consulted in advance by anyone who considers submitting such a review.)

3. Communications will often describe results obtained by specialized techniques (for example, those of X-ray crystallography and of genetics), and it is most important that technical terms should be avoided or be clearly defined; in any event the actual results obtained and their implications should be described in a way which does not demand from the reader specialized knowledge of a particular technique.

Papers should contain the maximum density of information compatible with clarity, and every sentence should be scrutinized to ensure that its presence is essential. Authors should include enough experimental details to enable others to repeat the work (these may be printed in small type). Careful preparation of manuscript will aid prompt publication; carelessness will cause delay.

4. *Submission of Manuscripts.* Manuscripts should be sent to Dr. J. C. Kendrew, Peterhouse, Cambridge, England, or to any member of the Editorial Board. The submission of manuscript will be taken to imply that the material is original, and that no similar paper has been or will be submitted for publication elsewhere.

Papers will normally be published in English. Manuscripts in French or German will also be accepted, though the use of these languages may cause delay in publication.

5. *Copy.* Papers should be typewritten in double spacing *throughout* (including tables, legends and footnotes), on one side of quarto paper, with a margin of 1 inch all round. The position of tables and illustrations should be indicated in the text; tables and legends for illustrations should be typed separately at the end of the manuscript. All pages should be numbered serially and securely fastened together. Two copies of each manuscript should be submitted, together with three copies of the summary (see §6) and four copies of the abstract (see §9).

A short running title of not more than 40 characters (including spaces), suitable for page headings, should be indicated if the full title is longer than this.

The name of the laboratory where the work has been done should be indicated on the title page. All typescript (including the references) should be carefully checked for errors.

6. *Summary.* A summary will be printed at the head of all papers (excluding Letters to the Editor); this should generally not exceed 300 words, and should be intelligible to the general reader without reference to the main text. Abbreviations should be avoided. Summaries of papers to be printed in French or German will be in English, and should be longer (up to 1000 words) for the benefit of readers not familiar with these languages.

7. *Conventions.* The conventions used in current issues of the Journal for headings, references, etc., should be followed in preparing manuscripts. References should be listed alphabetically at the end of the paper, and abbreviated according to the *World List of Scientific Periodicals*, except that for periodicals with English names capital initial letters should be used throughout. Citations in the text should read thus: Smith, Brown & Robinson (1957), or (Smith, Brown & Robinson, 1957). When a citation has more than two authors, the names of all of them should be given at the first citation (except for more than five authors), and on subsequent citations thus: (Smith *et al.*, 1957). The conventions (Brown, 1957*a*), (Brown, 1957*b*) should be used where more than one paper by the same author(s) has appeared in one year. Volume number should be indicated in the typescript thus: **35.**

Footnotes should be avoided whenever possible. Essential footnotes should be indicated by superscript figures in the text and collected on a single page placed at the end of the manuscript.

Customary abbreviations will be used; authors may refer to *Chemical Abstracts*, to the *Biochemical Journal*, **66**, 8 (1957), and to *Notes on the preparation of papers to be communicated to the Royal Society* (1951). Certain non-standard abbreviations of chemical substances are convenient, and those listed in the *Journal of Biological Chemistry* may be used without further definition (e.g. DNA, ATP). Any other abbreviations of this kind should be used sparingly, and must be defined in a footnote at the point in each manuscript where the first such abbreviation occurs.

8. *Illustrations.* It is often convenient to make a *drawing* two or three times larger than it will appear in the Journal, but very large drawings should be avoided and it will be helpful if drawings and illustrations are submitted on quarto (or 8½ by 11 inch) sheets. Drawings should be made in

Indian ink on tracing linen, Bristol board, or faintly blue-lined graph paper; the originals should always be submitted with the manuscript, since photo-prints of drawings often cannot be reproduced satisfactorily. Explanations should, as far as possible, be placed in the legend; the drawing itself should contain a minimum of lettering, and this should be inserted lightly in *blue pencil*, in lower case except for proper names, when a capital should be used. It should be remembered that drawings will be reduced to a size not exceeding 8 by 5 inches, and that the final thickness of the lines should be 0·25 to 0·3 mm. If a curve is given merely for illustrative purposes no cross-lines are needed, but the axes should be graduated at intervals, and the diagram should be boxed in. Where possible, related diagrams should be grouped to form a single figure, and should be prepared uniformly and *on the same scale*. Where appropriate and possible a scale should be included in the illustration itself; the magnification may be noted in the legend and adjusted after reduction by the blockmaker.

Whenever possible *photographs* should be supplied the same size as they are to appear in the Journal. The page area available for a plate is 5 by 7 inches or, at the most, 6 by 8 inches.

Line drawings will be referred to as Figure 1, Figure 2, etc., and half-tone blocks as Plate I, Plate II, etc. The name(s) of the author(s) and the number should be written on all illustrations, together with the indication "Top" if necessary. Besides the original illustrations *one* duplicate set must accompany the second copy of the manuscript; these may be photo-prints, and need not be of the same quality as the originals but must be clear and legible. If *oversize* original drawings are submitted (bigger than 8½ by 11 inches) they must be accompanied by *two* sets of small photo-prints.

9. *Abstracts*. Authors should send with their manuscripts *four copies* (typewritten in double spacing) of an abstract, in about 100 words, suitable for inclusion in biological abstracting journals. This abstract will not appear in the *Journal of Molecular Biology* but will be scrutinized by the Editors before being passed for publication. The abstract should outline as briefly as possible the results and definitive conclusions of the work. Details of methods are generally not required.

The abstract should be headed as follows: title of paper; name(s) of author(s); *J. Mol. Biol.*, followed by space for the year, volume and page references; abbreviated postal address (including country of origin) to which applications for reprints may be sent. For example: The isolation and properties of deoxyribonucleoprotein particles containing single nucleic acid molecules. G. Zubay & P. Doty. J. Mol. Biol. . . . . (Dept. of Chem., Harvard Univ., Cambridge, Mass., U.S.A.). —text of abstract follows.

10. *Reprints*. Fifty reprints of each paper will be supplied free of charge; additional copies may be purchased.

Advances in

Biological and Medical Physics

EDITED BY J. H. LAWRENCE AND C. A. TOBIAS

University of California, Berkeley, California

VOLUME VI. February 1959, 640 pp., illus., 118s. net

CONTENTS:

RICHARD P. DURBIN, PETER F. CURRAN, and A. K. SOLOMON, Ion and Water Transport in Stomach and Intestine

ERIK ZEUTHEN, Artificial and Induced Periodicity in Living Cells

HERBERT MARCOVICH and RAYMOND LATARJET, Radiobiological Aspects of the Induction of Lysogenic Bacteria to Produce Phage with X-Ray, Gamma Ray, and Ultraviolet Radiations

BO THORELL, Cell Studies with Microspectrography

O. C. A. SCOTT, Some Aspects of the Effect of Ionizing Radiation on Tumors in Experimental Animals

CHARLES L. DUNHAM, Fallout from Nuclear Weapons Tests

B. JACOBSON and R. STUART MACKAY, Radiological Contrast Enhancing Methods

W. H. FREYGANG, JR. and LOUIS SOKOLOFF, Quantitative Measurement of Regional Circulation in the Central Nervous System by the Use of Radioactive Inert Gas

WILLIAM J. FRY, Intense Ultrasound in Investigations of the Central Nervous System

SOLOMON A. BERSON and ROSALYN S. YALOW, Isotopic Tracers in the Study of Diabetes

E. PETER GEIDUSCHEK and ALFRED HOLTZER, Application of Light Scattering to Biological Systems: Deoxyribonucleic Acid and the Muscle Proteins

PAUL HOWARD-FLANDERS, Physical and Chemical Mechanisms in the Injury of Cells by Ionizing Radiations

AUTHOR INDEX—SUBJECT INDEX.

PREVIOUSLY PUBLISHED

Vol. I, 1948, 484 pp., illus., 86s. net
Vol. II, 1951, 348 pp., illus., 80s. net
Vol. III, 1953, 368 pp., illus., 80s. net
Vol. IV, 1956, 356 pp., illus., 80s. net
Vol. V, 1957, 488 pp., illus., 86s. net

REVIEW (Volume IV):

"... The eight contributions to this issue are authoritative and well produced and this volume joins the remainder of the series as an invaluable addition to the library of the biophysicist and the biophysics department." —*Science Progress*

Detailed literature on previously published volumes available upon request

ACADEMIC PRESS INC.

111 Fifth Avenue, New York 3, New York, U.S.A.

British Office: Academic Books Ltd., 17 Old Queen Street, London, S.W.1

Phone: WHItehall 6631

FILED IN STACKS

CONTENTS

BORENFREUND, ELLEN, ROSENKRANZ, HERBERT S. and BENDICH, AARON, Studies on Deoxyribonucleic Acid after Exposure to Tritium Gas 195

NOMURA, MASAYASU and WATSON, J. D., Ribonucleoprotein Particles within Chloromycetin-Inhibited *Escherichia coli* 204

SINSHEIMER, ROBERT L., Is the Nucleic Acid Message in a Two-Symbol Code? 218

TISSIÈRES, A., WATSON, J. D., SCHLESSINGER, D. and HOLLINGWORTH, B. R., Ribonucleoprotein Particles from *Escherichia coli* . 221

HORNE, R. W., RUSSELL, G. E. and TRIM, A. R., High Resolution Electron Miscroscopy of Beet Yellows Virus Filaments 234

SPAHR, P. F. and TISSIÈRES, A., Nucleotide Composition of Ribonucleoprotein Particles from *Escherichia coli* 237

GRUNBERG-MANAGO, MARIANNE, Phosphorolyse et Configuration Macromoléculaire des Polyribonucléotides Biosynthétiques et des Acides Ribonucléiques 240

KOCH, GEBHARD and HERSHEY, A. D., Synthesis of Phage-Precursor Protein in Bacteria Infected with T2 260

SMITH, KENNETH M. and HILLS, G. J., Further Studies on the Electron Microscopy of the *Tipula* Iridescent Virus 277

BRENNER, S., STREISINGER, G., HORNE, R. W., CHAMPE, S. P., BARNETT, L., BENZER, S. and REES, M. W., Structural Components of Bacteriophage 281

Letters to the Editor—

Carboxyl Group Interactions in Lysozyme, JOHN W. DONOVAN, MICHAEL LASKOWSKI, JR. and HAROLD A. SCHERAGA . . 293

A Determination of Lipoprotein Molecular Weight by use of the Electron Microscope, THOMAS L. HAYES, JACK C. MURCHIO, FRANK T. LINDGREN and ALEX. V. NICHOLS 297

Printed in Great Britain at the Aberdeen University Press